

Journal Pre-proof

Spectroscopic study of terrestrial analogues to support rover missions to Mars – a Raman-centred review

Fernando Rull, Marco Veneranda, Jose Antonio Manrique-Martinez, Aurelio Sanz-Arranz, Jesus Saiz, Jesús Medina, Andoni Moral, Carlos Perez, Laura Seoane, Emmanuel Lalla, Elena Charro, Jose Manuel Lopez, Luis Miguel Nieto, Guillermo Lopez-Reyes



PII: S0003-2670(21)00829-1

DOI: <https://doi.org/10.1016/j.aca.2021.339003>

Reference: ACA 339003

To appear in: *Analytica Chimica Acta*

Received Date: 12 May 2021

Revised Date: 25 August 2021

Accepted Date: 25 August 2021

Please cite this article as: F. Rull, M. Veneranda, J.A. Manrique-Martinez, A. Sanz-Arranz, J. Saiz, J. Medina, A. Moral, C. Perez, L. Seoane, E. Lalla, E. Charro, J.M. Lopez, L.M. Nieto, G. Lopez-Reyes, Spectroscopic study of terrestrial analogues to support rover missions to Mars – a Raman-centred review, *Analytica Chimica Acta*, <https://doi.org/10.1016/j.aca.2021.339003>.

This is a PDF file of an article that has undergone enhancements after acceptance, such as the addition of a cover page and metadata, and formatting for readability, but it is not yet the definitive version of record. This version will undergo additional copyediting, typesetting and review before it is published in its final form, but we are providing this version to give early visibility of the article. Please note that, during the production process, errors may be discovered which could affect the content, and all legal disclaimers that apply to the journal pertain.

© 2021 The Author(s). Published by Elsevier B.V.

Terrestrial analogues

This review provides an overview of the most representative terrestrial analogue sites and materials characterized by the ERICA research group in the framework of planetary exploration.

Mission simulations

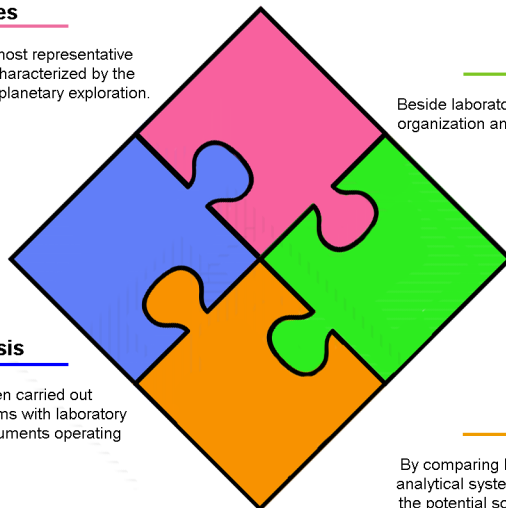
Beside laboratory and in-situ studies, the lesson learnt from the organization and development of mission simulations (AMASE, ExoFIT) are also provided.

Spectroscopic analysis

In-situ and laboratory analysis have been carried out combining commercial spectroscopic systems with laboratory prototypes that simulate the analytical instruments operating on Mars.

Data interpretation

By comparing Raman results with the data gathered by further analytical systems already operating on Mars, inferences about the potential scientific outcome of this technique on Mars have been extrapolated.



Journal Pre-proof

1 Spectroscopic study of terrestrial analogues to support rover missions to 2 Mars – a Raman-centred review

3
4 Fernando Rull¹, Marco Veneranda¹, Jose Antonio Manrique-Martinez¹, Aurelio Sanz-Arranz¹,
5 Jesus Saiz¹, Jesús Medina¹, Andoni Moral², Carlos Perez², Laura Seoane², Emmanuel Lalla³,
6 Elena Charro¹, Jose Manuel Lopez¹, Luis Miguel Nieto¹, Guillermo Lopez-Reyes¹

7
8 ¹ University of Valladolid, Spain. Ave. Francisco Vallés. 8, Boecillo 47151, Spain.

9 ² National Institute for Aerospace Technology (INTA), Torrejón de Ardoz, Spain.

10 ³ Systems Engineering for the Defence of Spain, S. A. (ISDEFE), Madrid, Spain.

11 ⁴ York University, Centre for Research in Earth and Space Science, Toronto, Canada.

12 13 Abstract

14 The 2020s could be called, with little doubt, the "Mars decade". No other period in space
15 exploration history has experienced such interest in placing orbiters, rovers and landers on the
16 Red Planet. In 2021 alone, the Emirates' first Mars Mission (the Hope orbiter), the Chinese
17 Tianwen-1 mission (orbiter, lander and rover), and NASA's Mars 2020 Perseverance rover
18 reached Mars. The ExoMars mission Rosalind Franklin rover is scheduled for launch in 2022.
19 Beyond that, several other missions are proposed or under development. Among these, MMX
20 to Phobos and the very important Mars Sample Return can be cited. One of the key mission
21 objectives of the Mars 2020 and ExoMars 2022 missions is the detection of traces of potential
22 past or present life. This detection relies to a great extent on the analytical results provided by
23 complementary spectroscopic techniques. The development of these novel instruments has
24 been carried out in step with the analytical study of terrestrial analogue sites and materials,
25 which serve to test the scientific capabilities of spectroscopic prototypes while providing
26 crucial information to better understand the geological processes that could have occurred on
27 Mars. Being directly involved in the development of three of the first Raman spectrometers to
28 be validated for space exploration missions (Mars 2020/SuperCam, ExoMars/RLS and
29 RAX/MMX), the present review summarizes some of the most relevant spectroscopy-based
30 analyses of terrestrial analogues carried out over the past two decades. Therefore, the present
31 work describes the analytical results gathered from the study of some of the most distinctive
32 terrestrial analogues of Martian geological contexts, as well as the lessons learned mainly from
33 ExoMars mission simulations conducted at representative analogue sites. Learning from the
34 experience gained in the described studies, a general overview of the scientific outcome
35 expected from the spectroscopic system developed for current and forthcoming planetary
36 missions is provided.

37 INDEX

38	1. Introduction	2
39	2. Terrestrial analogue sites	4
40	2.1. Jaroso Hydrothermal System (JHS, Spain)	4
41	2.2. Rio Tinto (Spain)	6
42	2.3. Barberton (South Africa)	8
43	2.4. Tenerife (Spain)	10
44	2.5. Leka Ophiolite Complex (Norway)	12

1	2.6. <i>Chesapeake Bay Impact Crater (CBIS, USA)</i>	13
2	2.7. <i>El Soplao Cave (Spain)</i>	15
3	3. Planetary mission simulations	17
4	3.1. <i>Arctic Mars Analogue Svalbard Expedition, AMASE (Svalbard, Norway)</i>	18
5	3.2. <i>ExoMars-like Field Testing, ExoFiT (Tabernas, Spain)</i>	20
6	3.3. <i>ExoMars-like Field Testing, ExoFiT (Atacama Desert, Chile)</i>	22
7	4. Discussion	25

9 1. Introduction

10 Spectroscopic analytical techniques are acquiring increasing importance in the field of Mars
 11 exploration. Strictly focusing on ground instruments, elemental data have been successfully
 12 collected by alpha proton X-ray spectrometers (APXS) onboard the Pathfinder [1], Spirit [2],
 13 Opportunity [3] and Curiosity [4] rovers. With respect to the Mars Science Laboratory (MSL)
 14 mission, complementary elemental data were additionally collected by laser-induced
 15 breakdown spectroscopy (LIBS, ChemCam [5]) and X-ray fluorescence instruments (CheMin
 16 [6]) onboard the rover. Regarding mineralogical data, Mössbauer systems onboard Spirit [7]
 17 and Opportunity [8] rovers helped to shed light on the mineral phases composing Martian
 18 primary rocks and their alteration products.

19 Looking ahead, the Mars 2020 and ExoMars rover missions incorporate, among other
 20 spectroscopic techniques, the first Raman instruments to be validated for space exploration.
 21 On the one hand, the main objective of the ExoMars mission is to identify traces of life on
 22 Mars. To do so, the subsurface observations performed by the WISDOM (Water Ice and
 23 Subsurface Deposit Observation on Mars [9]) ground-penetrating radar will guide the drill of
 24 the Rosalind Franklin rover in the collection of geological samples down to a depth of 2 metres.
 25 The Sample and Preparation and Distribution System (SPDS [10]) will crush the geological
 26 materials and will deliver them to the Analytical Laboratory Drawer (ALD) located inside the
 27 body of the rover. Here, the molecular analysis performed by the Raman laser spectrometer
 28 (RLS [11,12]) will serve, together with complementary MicroOmega NIR data [13], to select the
 29 optimal targets to be characterized by the Mars Organic Molecule Analyser (MOMA) system
 30 [14].

31 On the other hand, the main objective of the Mars 2020 mission is to gather astrobiologically
 32 relevant samples and store them in tubes that will be sent back to Earth through the so-called
 33 Mars Sample Return mission [15]. In detail, the Perseverance rover will select the samples
 34 according to the spectroscopic data returned by a combination of remote and proximity
 35 science systems [16]. To do so, the SuperCam multi-suite instrument [17–19] performs remote
 36 Raman, LIBS, VISIR and fluorescence of Martian rocks and soils. Targets of high scientific
 37 interest are then further characterized by proximity instruments mounted on the robotic arm
 38 of the rover. In this case, the elemental data provided by PIXL (Planetary Instrument for X-ray
 39 Lithochemistry [20]) are complemented by the Raman spectra collected by Sherloc [21], a UV
 40 spectrometer whose design has been optimized for the detection of organics.

1 In addition, Raman spectrometers will be used on exploration missions that are currently
2 under development (as is the case of the Raman spectrometer (RAX) onboard the JAXA-
3 Martian Moons eXploration (MMX) rover that is scheduled to land on Phobos in 2025 [22–24])
4 and planning (Raman spectroscopy has been selected among the techniques necessary to
5 meet the science goals outlined for the Europa Lander mission [25–27]).

6 In light of the increasing importance spectroscopic techniques (especially Raman) are acquiring
7 in the field of space exploration, the analytical study of terrestrial analogue sites and materials
8 using these techniques has become an essential tool to estimate the potential scientific
9 outcome derived from their operation on Mars [28–30]. Furthermore, bearing strong analogies
10 with Martian mineralogical/environmental contexts, the analysis of terrestrial analogues also
11 helps to extrapolate important inferences about the geological and environmental evolution of
12 the planet [31] and its past habitability [32].

13 Being involved at different levels in the development of SuperCam (Mars 2020 mission), RLS
14 (ExoMars mission), and RAX (MMX mission) Raman spectrometers, the ERICA group (Raman
15 and Infrared Spectroscopy applied to Cosmogeochemistry and Astrobiology) works in very
16 close collaboration with INTA-CAB (National Institute for Aerospace Technology – Astrobiology
17 Center) and several other laboratories in Spain and abroad to support the required
18 technological advancements with the analytical study of representative terrestrial analogue
19 sites and materials.

20 The spectroscopic-based analytical procedure used for these studies combines in situ analysis
21 of the analogue site with the laboratory investigation of selected samples. In this framework,
22 the analytical study of terrestrial analogue materials is generally carried out using a
23 combination of commercial instruments and analytical prototypes simulating the scientific
24 outcome of planetary instrumentation. In regard to Mars-related investigations, RLS-Sim, RAD-
25 1 and SimulCam have been widely used to simulate RLS-FM and SuperCam operations. As
26 described elsewhere [33,34], RLS-Sim is a laboratory simulator providing Raman spectra
27 qualitatively comparable to the RLS-FM (flight model). Similar to RLS-Sim, RAD-1 is a portable
28 RLS simulator that has been frequently used for the in situ investigation of terrestrial
29 analogues [35]. In addition, SimulCam is a hybrid Raman-LIBS system that, similar to the
30 Mars2020/SuperCam suite, is capable of performing complementary elemental and molecular
31 analysis of remote targets [36]. In addition to representative prototypes, qualification (EQM)
32 and spare (FS) models of the RLS system have also been used during ExoMars mission
33 simulations [12]. Aiming to summarize and contextualize the numerous studies carried out in
34 this field of research, the present review is organized as follows: first, the analytical results
35 gathered from the most distinctive terrestrial analogues of Martian geological contexts are
36 described. Then, the lessons learned from ExoMars mission simulations carried out at
37 terrestrial analogue sites are described. This last aspect also covers the data treatment and
38 database generation and management, which are essential tools to optimize the scientific
39 information derived from Martian spectra. Finally, the potential scientific outcome that could
40 derive from the forthcoming application of novel spectroscopic systems (especially Raman) in
41 planetary missions is evaluated by comparison with complementary analytical instruments
42 used in previous and current missions.

43

1 2. Terrestrial analogue sites

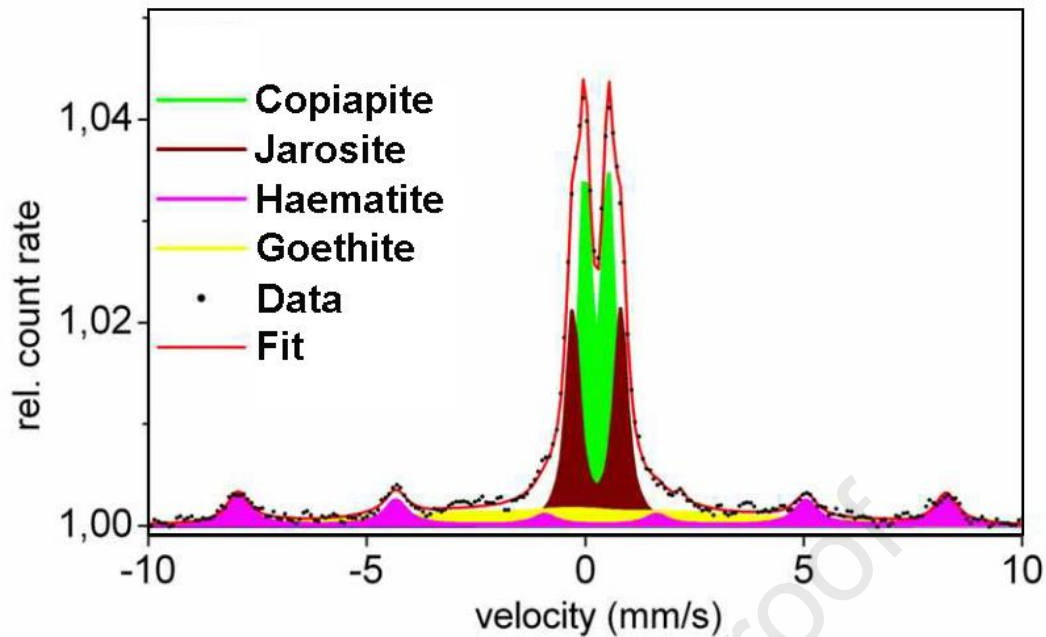
2 Scientific instruments for planetary exploration missions are the results of years of cutting-
3 edge technological developments. Representative field trials are therefore needed to evaluate
4 and optimize their analytical performances. Therefore, an increasing number of field trials are
5 organized to gather insights about the potential scientific outcome of the scientific
6 instruments that will serve, for example, to define the necessary hardware or software
7 updates.

8 In light of the role the ERICA research group and its collaborators are playing in the
9 development of spectroscopic tools onboard Mars 2020, ExoMars and MMX planetary
10 missions, many field trips have been carried out to test the capabilities of analytical prototypes
11 and compare their results with those provided by commercial instruments and complementary
12 space-derived systems. Below, an overview of the research work carried out by the group at
13 some of the most relevant terrestrial analogue sites is provided.

14

15 2.1. Jaroso Hydrothermal System (JHS, Spain)

16 One of the most interesting mineralogical discoveries achieved through the in situ exploration
17 of Mars is the detection of iron oxyhydroxide and hydrated sulfate (alunite group)
18 assemblages, with their crystallization associated with the past occurrence of large-scale
19 hydrothermal systems [37–40]. Since the 1990s, an increasing number of researchers have
20 analysed the mineralogy and tectonics of Jaroso Ravine (type locality for the mineral jarosite)
21 to define the multiple mineralizing stages associated with both hypogenic and supergenic
22 hydrothermal processes [41–44]. According to these studies, the Jaroso Hydrothermal System
23 (JHS) outcrop is an important emplacement where 1) the detection capabilities of analytical
24 instruments for space exploration missions can be tested and 2) constraints on hydrothermal
25 processes that occurred on early Mars can be inferred from [41]. In this framework, a set of
26 complementary in situ and laboratory studies of hydrothermal alteration deposits was carried
27 out between 2004 and 2010 by an interdisciplinary scientific team that involved several
28 members of both ERICA and INTA-CAB groups. Considering that the Mössbauer instrument
29 onboard the Opportunity rover was the first instrument to detect jarosite ($\text{KFe}^{3+}_3(\text{SO}_4)_2(\text{OH})_6$)
30 on Mars [45], this technique was used in combination with Raman spectroscopy to
31 characterize the sulfate deposits found at the JHS. For that, a portable version of the
32 Mössbauer flight instrument (MIMOS II) was used [46]. As detailed in multiple manuscripts
33 [47–49], in addition to successfully identifying jarosite (see Figure 1), the Mössbauer system
34 detected additional sulfates, such as copiapite ($\text{Fe}^{2+}\text{Fe}^{3+}_4(\text{SO}_4)(\text{OH})_2 \cdot 20\text{H}_2\text{O}$) and rozenite (Fe_5O_4
35 $4\text{H}_2\text{O}$), together with minor amounts of iron oxides (goethite $\alpha\text{-FeO}(\text{OH})$ and haematite Fe_2O_3)
36 [47]. This association of minerals is very similar to those detected by the Opportunity rover at
37 the Meridiani Planum [45], which underlines the strong analogy between this terrestrial
38 analogue site and Martian geological contexts.

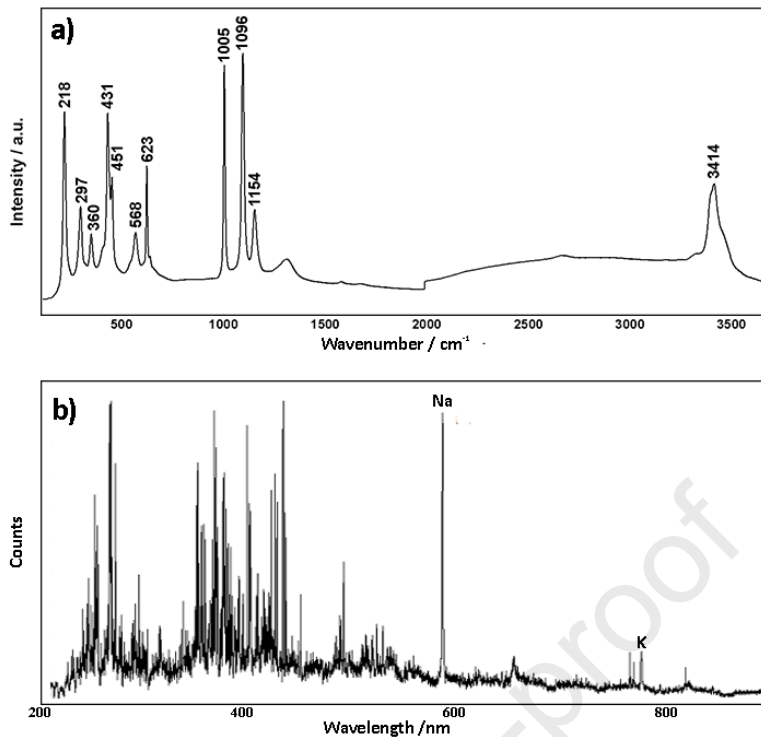


1

2 *Figure 1: Mössbauer spectra from JHS sulfate deposits, detecting the presence of jarosite,*
 3 *copiapite, haematite and goethite (from F. Rull et al. 2008 [47]).*

4 As happens on Earth, jarosite on Mars may have precipitated from hydrothermal acidic (pH <4)
 5 solutions rich in heavy metals [50]. Despite low pH conditions, many chemolithoautotrophic
 6 and thermophilic microorganisms colonize these habitats [51]. In addition, jarosite shelters
 7 organic molecules from UV radiation, thus favouring the preservation of organic molecules
 8 [52]. For these reasons, jarosite deposits are among the most promising scientific targets for
 9 searching for signs of life on Mars.

10 As both ExoMars and Mars 2020 rovers are meant to select geological samples of high
 11 astrobiological relevance according to their mineralogical and geochemical composition,
 12 complementary Raman and LIBS analyses were additionally carried out. Analytical data
 13 gathered in situ and in the laboratory by means of Raman prototypes enabled the precise
 14 detection of jarosite with different cationic compositions (a characteristic Raman-LIBS
 15 spectrum is displayed in Figure 2), copiapite, haematite and goethite, thus confirming the
 16 Mössbauer results. Furthermore, additional hydrothermal alteration products were also
 17 detected, including coquimbite ($\text{Fe}_2(\text{SO}_4)_3 \cdot 9\text{H}_2\text{O}$), halotrichite ($\text{Fe}^{2+}\text{Al}_2(\text{SO}_4)_4 \cdot 22\text{H}_2\text{O}$), gypsum
 18 ($\text{CaSO}_4 \cdot \text{H}_2\text{O}$), barite (BaSO_4) and siderite (FeCO_3) [47,53,54]. These results successfully
 19 demonstrated the potential scientific outcome that could derive from the application of
 20 Raman spectroscopy during Martian exploration missions.

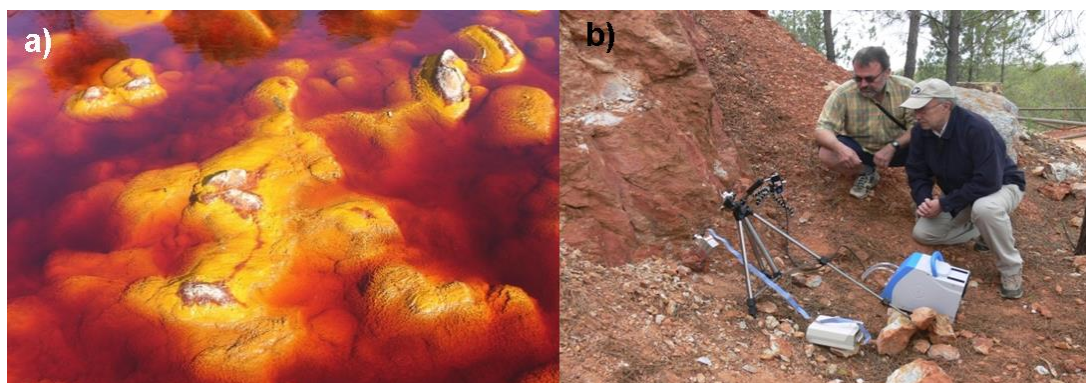


1
2 *Figure 2: Raman spectrum (a) and LIBS spectrum (b) of jarosite collected at the JHS and*
3 *obtained in the laboratory. It is important to note the complementarity between the two*
4 *techniques. From Raman, the mineral phase is precisely identified, and from LIBS, the precise*
5 *cationic chemical composition is deduced.*

6 The campaign of analysis carried out at the JHS also offered the opportunity to test, at a
7 representative analogue site, the advantages provided by the combined use of Raman and LIBS
8 systems. In this sense, by acquiring elemental and molecular data from the same spot of
9 interest, it was possible to establish correlations between variations in the characteristic
10 parameters of Raman peaks (position, width and intensity) and the elemental composition of
11 the target. Thus, by means of the combined Raman-LIBS analysis of alunite deposits, jarosite
12 (rich in K) and natrojarosite (rich in Na) phases [55] were correctly discriminated. As presented
13 in Figure 2, the characteristic emission lines of sodium and potassium have often been
14 detected in the same spot of interest, thus suggesting the presence of jarosite phases whose
15 elemental composition falls within the K-Na solid solution. In this case, peak shifting detected
16 by Raman analysis confirmed the presence of K-Na intermediate mineral phases, while the
17 LIBS-based semiquantitative estimation provided detailed information regarding its
18 geochemistry. As the LIBS spectra collected on Mars by the ChemCam instrument have been
19 effectively used to estimate the elemental abundances of the analysed targets [56], this work
20 suggests that the combined Raman-LIBS analysis performed by SuperCam could be used to
21 extrapolate precise mineralogical and geochemical information about Martian rocks and soils.
22 Additional analytical results, gathered from the use of complementary techniques (XRD, SEM
23 and FTIR, among others) at the JHS, are presented elsewhere [54,57–59].

24
25 **2.2. Rio Tinto (Spain)**

1 As explained in Section 2.1, the iron-rich sulfate precipitation found on Mars is a very
 2 interesting scientific target to look for traces of past and/or present life. Therefore, the Rio
 3 Tinto Basin is widely considered the optimal terrestrial analogue site to test the capability of
 4 space-derived instrumentation to potentially detect biomarkers from extremophilic organisms.
 5 Rio Tinto is a 100 km-long river located in the Iberian Pyrite Belt, which is considered one of
 6 the largest sulfidic deposits in the world (mostly iron and copper sulfides). Partially as a
 7 consequence of mining activities, the red waters of the river (see Figure 3) are characterized by
 8 highly acidic values (mean pH below 2.5) and a remarkable concentration of heavy metals
 9 (mostly Fe, Cu, Zn and As) [60,61].



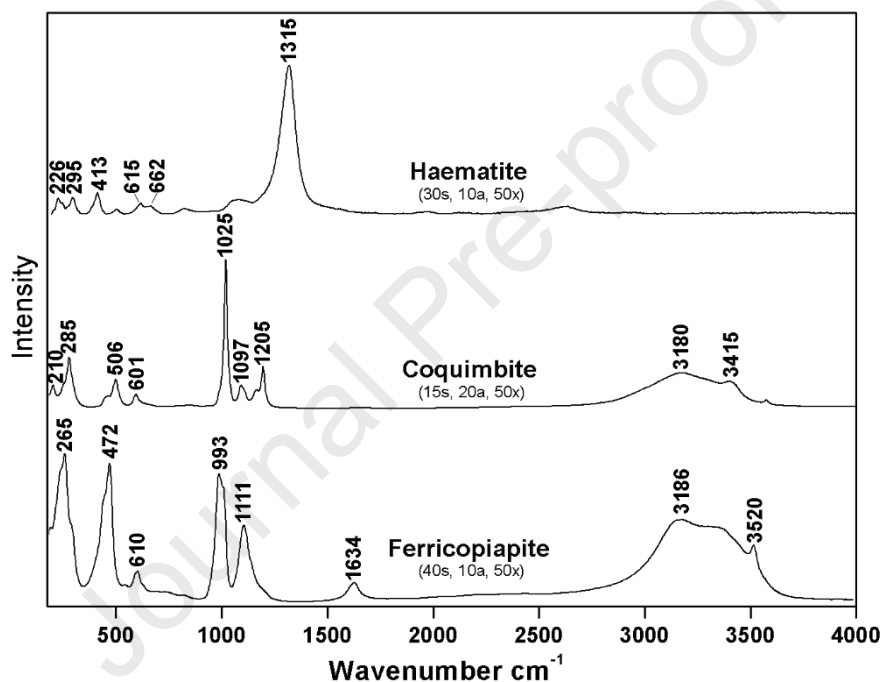
10

11 *Figure 3: a) Picture of Rio Tinto water and associated sulphate-rich precipitation. b) The*
 12 *Mössbauer MIMOS II instrument working in collaboration with a portable Raman system*
 13 *analysing Fe-bearing minerals at an outcrop.*

14 Despite these extremophilic conditions, Rio Tinto presents high levels of microbial diversity.
 15 Among them, chemolithotrophic organisms such as *Thiobacillus ferrooxidans* are partially
 16 responsible for sulfur compound reduction and ferrous iron oxidation [61,62], thus affecting
 17 the composition of the characteristic iron- and sulfate-bearing precipitates of Rio Tinto. Most
 18 recently, bio-mediated processes were also proven to occur in anaerobic conditions [63]. Due
 19 to the astrobiological relevance of this discovery, many research studies are currently focused
 20 on the analytical characterization of sulfate-rich precipitates by means of space-derived
 21 instruments [47,64]. As in the case of the JHS, the Mössbauer analysis of Rio Tinto samples has
 22 been complemented by Raman investigations. The results gathered from Raman prototypes
 23 confirmed Mössbauer results while effectively detecting additional compounds, such as
 24 gypsum, jarosite and pyrite (FeS_2) [65,66] In the work of Sobron et al. (2014) [67], Raman
 25 results gathered from the study of Rio Tinto precipitates were compared with those provided
 26 by instruments employed in further exploration missions, such as the Terra X-ray
 27 diffractometer (commercial version of the XRD system onboard the Curiosity rover) and the
 28 FieldSpecProFR VNIR reflectance spectrometer (emulating the MicrOmega [13] system
 29 onboard the Rosalind Franklin rover). Compared with diffractometric results, the mineralogical
 30 heterogeneity of complex precipitate mixtures can be more effectively disclosed by combining
 31 Raman and VNIR analysis, which is the analytical strategy planned for the ExoMars mission.
 32 Nevertheless, the combination of these complementary techniques shows real potential for
 33 investigating precipitation sequences. Indeed, unlike Raman and VNIR instruments, whose
 34 excitation sources only probe the surface of the target, the gamma radiation used for
 35 Mössbauer spectroscopy penetrates deeper into the sample, thus enabling an in-depth
 36 mineralogical investigation. In this sense, the combination of complementary spectroscopic

1 techniques delivers a level of depth-sensitive information, which could be used to extrapolate
2 reliable inferences about the precipitation sequence.

3 Rio Tinto waters were sampled and used for laboratory experiments to better comprehend the
4 precipitation sequence occurring at this analogue site. After measuring pH, conductivity and
5 elemental composition [68], waters were poured into an evaporation chamber and used to
6 reproduce the precipitation sequence occurring at Rio Tinto riverbanks [69,70]. The
7 representative Raman spectra of some of the precipitated mineral phases are presented in
8 Figure 4. Similarly, microscale experiments were performed by analysing the Raman emissions
9 proceeding from Rio Tinto water droplets during drying [69]. As presented by Rull et al. [71], a
10 set of iron-rich mineral phases progressively formed by following a precipitation sequence that
11 can be summarized as follows: ferricopiapite → coquimbite → copiapite → magnesiocopiapite
12 → haematite → rozenite → szomolnokite → rhomboclase → metavoltine.



13

14 *Figure 4: Raman spectra of ferricopiapite, coquimbite and haematite phases precipitated*
15 *during laboratory macroscale experiments after 1, 3 and 13 days. The experimental conditions*
16 *(acquisition time, number of accumulations, and objective) set for each spectrum are provided*
17 *between parentheses.*

18 Beyond mineralogical studies, Raman spectroscopy was effectively employed to identify the
19 potential presence of biomarkers. As presented by Edwards et al. (2007) [72], from the Raman
20 characterization of mineral deposits collected at the edge of Rio Tinto water pools, organic
21 compounds such as carotenoids, scytonemin and amino acids were detected, some of which
22 could be related to the biological colonization of sulfate-rich precipitation materials.

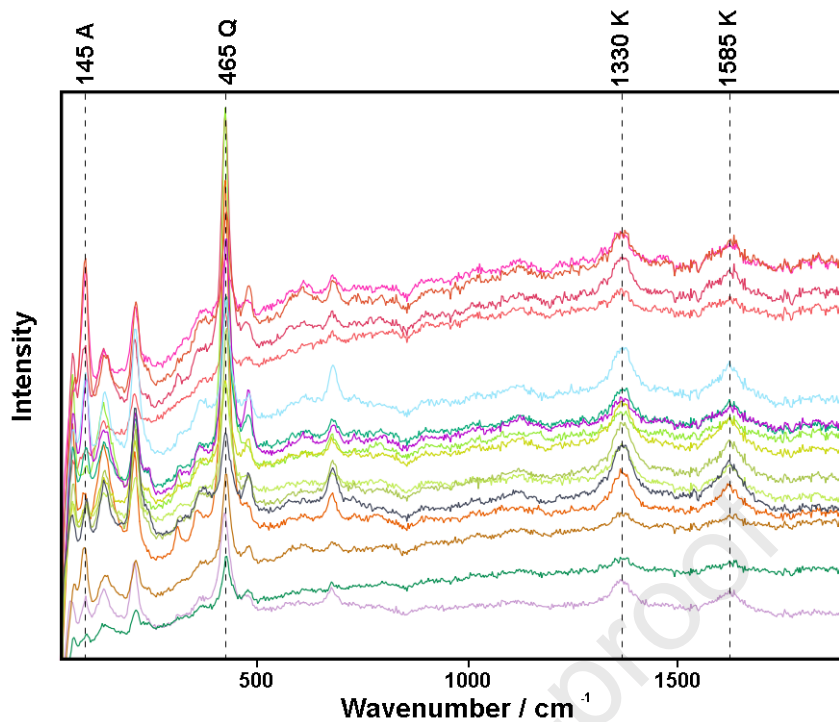
23 2.3. Barberton (South Africa)

24 Recording a geological history of approximately 500 million years, Barberton stratigraphy has
25 been deeply analysed to extrapolate crucial information about the geological and
26 environmental evolution of Earth during the Archean period [73–75]. In recent years, an

1 increasing number of studies have presented Barberton as a potential analogue site of
2 geological contexts that can be found on Mars [76] and other extraterrestrial bodies [77].
3 Within this field, two types of geological materials have attracted the interest of researchers.

4 On the one hand, komatiites from the Barberton Greenstone Belt are ultramafic rocks whose
5 texture (spineliferous) [78,79] and elemental composition (enriched in Mg) [76,80,81] make them
6 surprisingly similar to Martian basalts. As geological materials of high interest for both
7 geological and astrobiological studies, komatiite samples were collected from Barberton and
8 used by the ExoMars team to assess the potential analytical capabilities of the spectroscopic
9 systems onboard the Rosalind Franklin rover [82]. In addition to effectively identifying the
10 main primary phases (olivine and amphiboles), water alteration products were also detected
11 by Raman spectroscopy, including serpentine. It is well known that serpentinization generates
12 hydrogen (H₂) and methane (CH₄, through the Fischer-Tropsch reaction of H₂ with CO₂),
13 which are energy sources that can fuel the metabolism of chemolithotrophic organisms
14 [28,83,84]. Therefore, this work highlights the capability of this technique to detect secondary
15 phases of high astrobiological interest.

16 On the other hand, the black and white banded chert found at Barberton is a silicified volcanic
17 sediment of great astrobiological interest. Indeed, even though black and white layers share
18 the same mineralogical composition (microquartz SiO₂), dark layers mainly differ by the high
19 content of organic matter and carbonaceous material, whose deposition process has been
20 described elsewhere [85]. As one of the oldest pieces of evidence for life on Earth (3.4 billion
21 years ago), Westall and coworkers presented numerous studies in which layered chert samples
22 from Barberton were employed as terrestrial analogue material for astrobiological studies [86–
23 91]. Within this field of research, the ERICA research group carried out a set of studies mainly
24 focused on the use of Raman spectrometers. While correctly characterizing the geological
25 matrix (mainly quartz with trace amounts of anatase TiO₂ and dolomite CaMg(CO₃)₂ phases),
26 the RLS-Sim was capable of clearly detecting the vibrational features of kerogen (Figure 5),
27 which is the organic matter preserved in black veins [92–94]. The detailed analysis of the D and
28 G Raman bands of amorphous carbon allowed us to investigate the structural characteristics of
29 kerogen, which are related to the “maturity process” undergone by the samples under the
30 different geological processes. Nevertheless, these modified characteristics are not sufficient
31 to determine the possible biogenic origin of the kerogen, which is an important challenge for
32 Raman spectroscopy in investigating possible traces of life in these materials.



1
2 *Figure 5: Set of Raman spectra of a chert sample collected by means of the RLS-Sim in*
3 *automatic mode (nominal RLS analytical cycle composed of 20 spectra gathered from different*
4 *spots of interest). Kerogen (K) doublets at 1330 and 1585 cm^{-1} and quartz (Q) at 465 cm^{-1} are*
5 *easily identified. Additional signatures from anatase (A, main peak at 145 cm^{-1}) are also*
6 *detected.*

7 In light of the forthcoming missions to Mars, Barberton chert samples have been widely used
8 to assess the capability of the RLS system to detect organic compounds in ancient geological
9 matrices [11,33,95] and to evaluate how grain-size distribution affects the quality of Raman
10 results [94].

11 12 2.4. Tenerife (Spain)

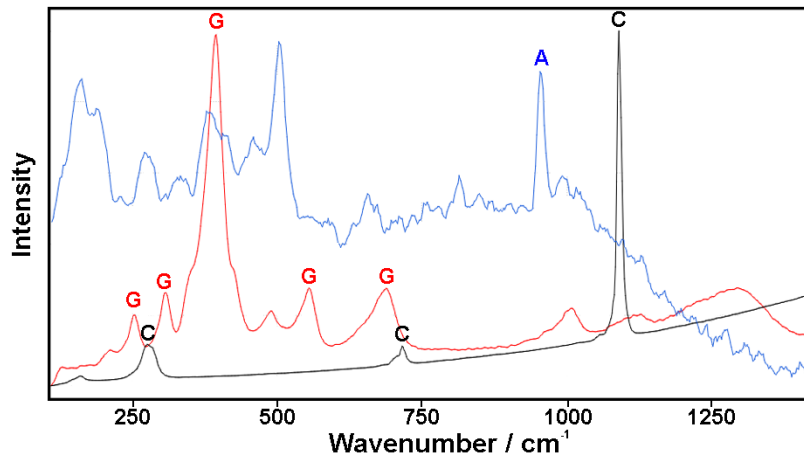
13 The volcanic complex of Tenerife (Spain) is also considered a mineralogical analogue of Mars.
14 Located in the Atlantic Ocean, Tenerife is part of the Canary archipelago, which is composed of
15 7 main volcanic islands. Similar to other young volcanoes (e.g., those on the Hawaii and
16 Galapagos islands), the volcanic complex of Tenerife presents many morphological features
17 with strong similarities with the volcanoes observed on Mars [96–98]. Beyond morphological
18 similarities, the mineralogical and geochemical composition of the basaltic rocks found at
19 Tenerife and their alteration products are analogous to the Martian volcanic materials
20 analysed by orbiters, landers and rovers [99]. Therefore, Tenerife has often been selected as
21 an analogue site to explore the scientific capabilities of analytical techniques involved in
22 planetary missions and to understand geological/biological processes that may have occurred
23 on Mars. Within this field of research, the first investigations carried out by the ERICA group
24 were mainly focused on the mineralogical and geochemical characterization of the geological
25 units composing Tenerife's volcanic complex. Complementary in situ and laboratory results

1 obtained by Raman, XRD, Mössbauer and FTIR systems helped to understand the multiple
2 similarities between the geology of this site and Martian geological contexts [99,100].

3 In addition to analysing the composition of primary rocks, the same analytical procedure was
4 also applied to the study of degradation products [101] by giving particular attention to the
5 investigation of alteration processes related to the interaction with water. Thus, the volcanic
6 complex of Tenerife displayed a great variety of water-related weathering, hydrothermal
7 interactions and underwater alteration processes. As detailed in previous studies, these are
8 some of the geological processes that could have favoured the potential proliferation of life
9 forms on early Mars, when volcanic activity of the planet coexisted with the presence of liquid
10 water on the surface [102,103]. In this framework, mineralogical studies have been recently
11 performed by Lalla et al. (2015) at the Caldera de las Cañadas, an area displaying collapses and
12 depressions whose geomorphology has many similarities with some of the volcanoes detected
13 on Mars [104]. Beyond the mineralogical characterization of primary minerals, XRD,
14 Mössbauer, XRF and Raman instruments were used to study the alteration products produced
15 by the interaction of volcanic rocks with hydrothermal fluids. The effective detection of
16 hydrothermal products (calcite CaCO_3 , hydrotalcite $\text{Mg}_6\text{Al}_2(\text{CO}_3)(\text{OH})_{16}\cdot 4(\text{H}_2\text{O})$ and apatite
17 $\text{Ca}_5(\text{PO}_4)_3(\text{F},\text{Cl},\text{OH})$, among others) proves the capability of spectroscopic instruments to
18 provide the mineralogical information necessary to optimize the selection of soil and rock
19 samples to be analysed by the MOMA instrument onboard the ExoMars rover [14], or to be
20 stored by the Mars 2020/Perseverance rover for the future Sample Return Mission [15,105].

21 Similarly, “Los Azulejos” is a colourful outcrop presenting bluish to greenish hydrothermal
22 alteration layers. Thanks to spectroscopic (Raman and FTIR) and diffractometric (XRD) analyses
23 carried out in situ and in the laboratory, the characteristic colours of this outcrop were proven
24 to be provided by a combination of hydrothermal-mediated minerals such as analcime
25 ($\text{Na}(\text{Si}_2\text{Al})\text{O}_6\cdot\text{H}_2\text{O}$), smectite, sulfates and illite [99,106], most of which have been detected in
26 putative hydrothermal systems on Mars [107].

27 In addition to in situ and laboratory analyses performed by commercial instruments, altered
28 volcanic rocks were also studied in the laboratory by means of spectroscopic prototype
29 systems. While detecting the main primary minerals (pyroxene and feldspar phases), the RLS-
30 Sim was also capable of characterizing the main products of their alteration, including iron
31 oxides, phosphates and carbonates (the most relevant spectra are provided in Figure 6). This
32 investigation indirectly proved the capability of the RLS system onboard the Rosalind Franklin
33 rover to identify mineralogical clues that could help fulfil the objectives of the ExoMars mission
34 [108].



1

2 *Figure 6: Representative Raman spectra of calcite (C), goethite (G) and apatite (A) detected by*
 3 *means of RLS-Sim during the analysis of altered rocks sampled from the Los Azulejos outcrop.*

4

5 2.5. Leka Ophiolite Complex (Norway)

6 By closely resembling the mineralogical and geochemical composition of mafic and ultramafic
 7 rocks detected on Mars by orbiters [109–112] and rovers [113–115], terrestrial ophiolites are
 8 widely considered optimal terrestrial analogue sites to investigate the water alteration of
 9 Martian igneous rocks [116–119]. Indeed, as is the case for terrestrial ophiolites, large areas of
 10 Mars present phyllosilicate features that are concordant with the putative water alteration of
 11 olivine-bearing rocks into serpentine phases [102,120].

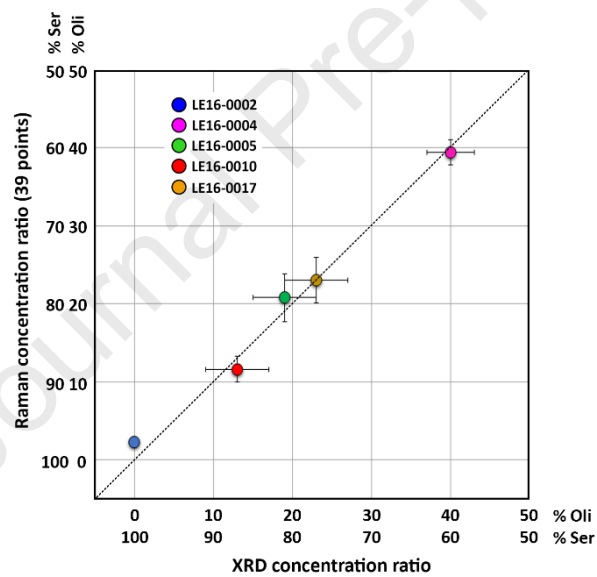
12 As olivine-bearing rocks have been detected at both the ExoMars and Mars 2020 landing sites,
 13 it is important to assess to what degree the analytical tools onboard the Perseverance and
 14 Rosalind Franklin rovers can identify their potential serpentinization. Within this field of
 15 research, the Leka ophiolite complex (LOC) was selected as a very interesting analogue site to
 16 investigate the scientific outcome that could derive from the use of spectroscopic systems in
 17 similar Martian scenarios. Located in Norway, the LOC is the result of the uplift of the ancient
 18 ocean crust that occurred 497 Ma during Caledonian–Appalachian mountain belt formation
 19 [121]. Previous investigations confirmed that the LOC presents multiple altered and
 20 serpentinized peridotite (dunite and harzburgite) units [122–124], some of which have
 21 undergone severe serpentinization and carbonatation reactions [125].

22 Considering the astrobiological relevance that serpentinized ultramafic rocks could play in
 23 sustaining life proliferation on Mars [84], several terrestrial analogue samples were collected
 24 from the LOC to be analysed by instruments relevant for planetary missions. In detail,
 25 ultramafic rock fragments showing different degrees of serpentinization were characterized by
 26 Raman, NIR and LIBS systems. The obtained results were then compared with those provided
 27 by complementary diffractometric analysis.

28 In light of the forthcoming landing of the ExoMars rover at Oxia Planum, the combination of
 29 NIR and Raman analysis proved to be a promising analytical strategy for the mineralogical
 30 characterization of altered rocks on Mars. Indeed, as described in a dedicated manuscript,

1 Raman investigations allowed the identification of main mineralogical phases and the
 2 discrimination between serpentine mineral phases, while NIR results provided complementary
 3 information about the nature of additional alteration products [30]. Furthermore, LIBS and
 4 Raman data collected from the same spot of interest proved that a deeper understanding of
 5 the detected mineral phases can be achieved by joining molecular and elemental information.
 6 In detail, knowing that the wavelength position of the main Raman double peak of olivine
 7 minerals shifts according to the iron/magnesium ratio of the crystal under study (forsterite (Fo,
 8 Mg_2SiO_4) and fayalite (Fa, Fe_2SiO_4), the end-members of the olivine solid solution [126]), an
 9 average composition between Fo87Fa13 and Fo92Fa08 was estimated by taking into
 10 consideration both the Raman peak position and the intensity ratio of LIBS Mg-Fe lines.

11 Focusing on Raman analysis, further studies were carried out to determine whether the
 12 serpentinization degree of the samples could be reliably estimated through univariate analysis
 13 of ExoMars-like Raman datasets (39 spectra collected from the same powdered sample). As
 14 represented in Figure 7, external calibration curves were used to estimate the relative content
 15 of olivine and serpentine in the samples, obtaining concentration ratios that fit very well with
 16 XRD estimations. Therefore, the performed study suggested that the RLS could be used to
 17 perform a semiquantitative analysis of mineralogically heterogeneous targets on Mars.



18

19 *Figure 7: Scatter plot comparing the concentration ratio of olivine and serpentine of Leka*
 20 *samples, calculated from the interpretation of XRD diffractograms and Raman datasets. The*
 21 *error bars show the quantification uncertainties for both techniques (from Veneranda et al.*
 22 *[83]).*

23

24 2.6. Chesapeake Bay Impact Crater (CBIS, USA)

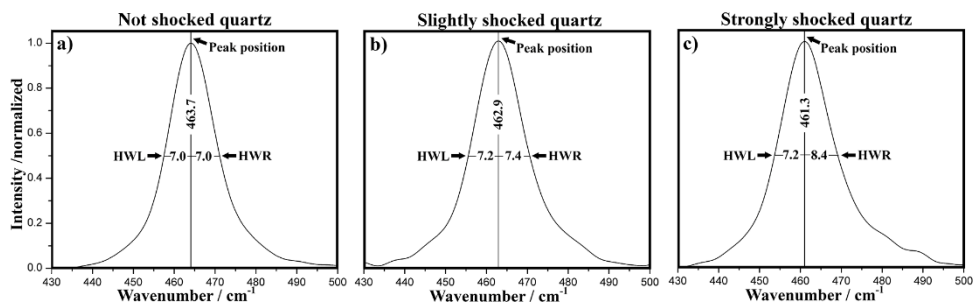
25 Among the different typologies of terrestrial analogue sites, impact craters are particularly
 26 important, as they offer the opportunity to carry out important geological and astrobiological
 27 studies [127–129]. Indeed, impact craters have been selected as landing sites for many
 28 missions to Mars. This is the case for Spirit (Gusev crater [130]), Curiosity (Gale crater [131]),

1 and Perseverance (Jezero crater [132]) exploration rovers. It is believed that impact craters on
 2 Mars and other celestial bodies could have offered the conditions for life proliferation. Indeed,
 3 the high temperatures generated by the impact of a bolide can last for thousands or even
 4 millions of years [133,134]. When the targeted surface contains water, these temperatures
 5 generate hydrothermal systems that provide the basic ingredients necessary to create and
 6 sustain biological activity. Furthermore, one of the oldest life forms found on Earth are
 7 putative fossilized microorganisms recently found in ancient hydrothermal vents, which can be
 8 dated to 3.77–4.28 billion years ago [135].

9 Thanks to the analysis of terrestrial craters, a series of morphological features have been
 10 identified that could be used to distinguish craters produced by a bolide impacting a wet
 11 surface from those produced in dry environments. As presented elsewhere [133], through the
 12 analysis of the high-resolution images gathered by the Mars Orbiter Camera wide-angle (MOC
 13 WA), several impact structures were identified whose morphology has strong similarities with
 14 the CBIS [136]. Knowing the repercussion that the scientific investigation of putative wet target
 15 impact craters on Mars and other planets could have in the potential identification of early
 16 forms of life, impact breccia samples selected from the ICDP-USGS Eyreville core [137] drilled
 17 at the centre of the CBIS were investigated in the laboratory to evaluate the scientific
 18 capabilities of Raman spectrometers to discriminate shock-induced metamorphism suffered by
 19 impact breccia minerals, as well as to detect hydrothermal alteration products.

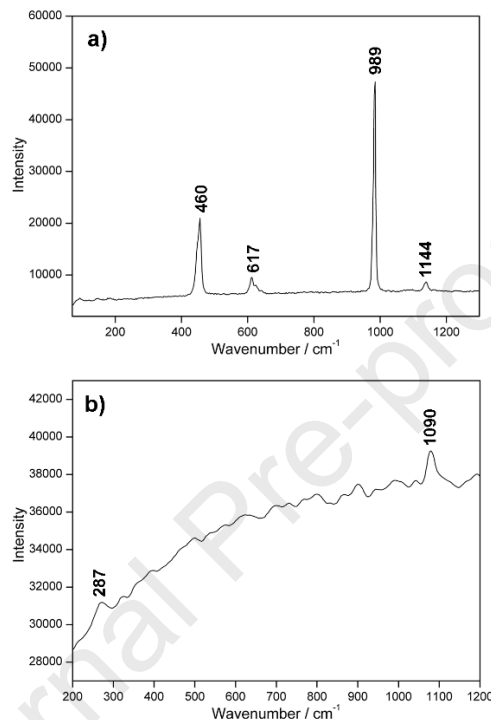
20 As detailed in a dedicated paper [29], Raman investigations were carried out by combining
 21 commercial instruments with the RLS-Sim. Raman results were then compared with those
 22 provided by NIR and XRD systems. RLS-Sim effectively detected the main mineral phases
 23 observed by complementary analytical techniques and described in previous studies [137],
 24 including quartz, cristobalite (SiO_2), illite and feldspars ($(\text{K,Na,Ca})(\text{Si,Al})_4\text{O}_8$). In addition,
 25 additional minor compounds were also found (including haematite, coesite (SiO_2), ilmenite
 26 ($\text{Fe}^{2+}\text{Ti}^{4+}\text{O}_3$), barite and siderite), thus revealing a higher mineralogical complexity.

27 On the one hand, the discrimination of shocked quartz has a high scientific relevance for the
 28 forthcoming ExoMars mission, as it proves that the RLS could be able to identify the
 29 mineralogical evidence necessary to confirm the impact origin of a crater. As shown in Figure
 30 8, impact-induced shocked quartz was recognizable by the shifting of the main peak towards
 31 lower wavelengths [138]. The analysed quartz crystals presented different degrees of
 32 metamorphism: by increasing the shift of the main peak of quartz, the main Raman band
 33 became broader and asymmetrical.



34
 35 *Figure 8: Calculation of the main band parameter from characteristic spectra of a) not shocked,*
 36 *b) slightly shocked, and c) strongly shocked quartz (from Veneranda et al 2019 [29]).*

1 On the other hand, barite (main peaks at 460, 617, 989 and 1144 cm^{-1}) and siderite (main
 2 peaks at 287 and 1090 cm^{-1}) were detected as minor phases (Figure 9). Knowing that the
 3 formation of these mineral phases can occur under hydrothermal conditions [134,139], their
 4 detection can be seen as a mineralogical clue that could be used to detect potential
 5 postimpact hydrothermal systems. The identification of similar alteration features on Martian
 6 rocks would have a strong astrobiological relevance, as hydrothermal systems provide the
 7 chemical energy needed to sustain the metabolism of microbial forms of life [140].



8

9 *Figure 9: Characteristic Raman spectra of barite (a) and siderite (b) collected from CBIS breccia*
 10 *samples using RLS-Sim.*

11 On the whole, the analytical study of the CBIS as a terrestrial analogue site clearly
 12 demonstrates that Raman spectroscopy could play a key role in forthcoming planetary
 13 exploration missions, suggesting that the RLS ExoMars system could potentially be able to
 14 identify the mineralogical clues necessary to confirm the presence of wet-target impact craters
 15 on Mars.

16

17 2.7. El Soplao Cave (Spain)

18 Based on the detailed analysis of high-resolution images collected from orbit, recent studies
 19 have indicated the presence of basaltic caves and lava tubes beneath the surface of Mars
 20 [141,142]. This discovery increased the interest of the scientific community in the analysis of
 21 terrestrial caves as potential analogue sites for astrobiological studies. Indeed, caves ensure
 22 thermal stability and protection from UV radiation. This, together with the potential
 23 preservation of high humidity levels, makes Martian caves an optimal site to look for microbial
 24 forms of life [142]. Although the exploration of caves has not been defined as a scientific

1 objective of Mars 2020 and ExoMars rovers, the analytical study of terrestrial analogues is
2 necessary to develop and optimize analytical procedures to implement for future exploration
3 missions (in particular those paving the way for human exploration). In this sense, an
4 increasing number of scientific articles can be found in the literature on this topic [143,144].

5 Among the terrestrial sites considered very interesting analogues for potential extraterrestrial
6 contexts, El Soplao Cave (Cantabria, Spain) stands out for having critical relevance for
7 astrobiological studies [145,146].



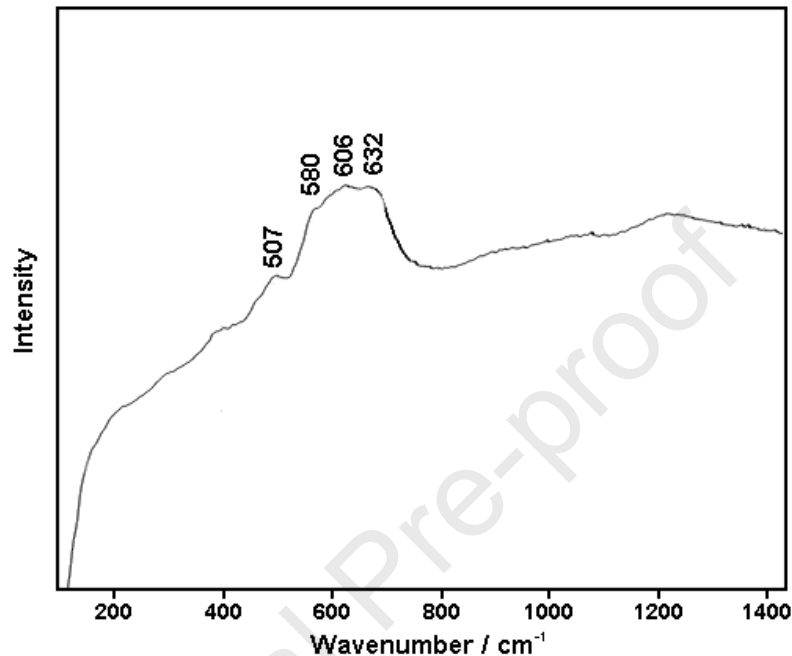
8

9 *Figure 10: In situ Raman characterization of speleothems found at El Soplao Cave.*

10 In situ spectroscopic and diffractometric analyses (Figure 10), combined with complementary
11 laboratory studies of selected samples, were carried out to determine the ancient climate of
12 the cave and to determine its evolution over time. For example, the formation of the
13 characteristic Mg-Fe crusts found in El Soplao Cave has been interpreted as the result of dry
14 precipitation of metallic ions lixiviated from detrital material accumulated during prior
15 turbulent flooding events [145]. Further information regarding speleothem genesis and the
16 climate evolution of this cave is provided elsewhere [146,147].

17 Beyond paleoclimatic studies, the high astrobiological relevance of El Soplao Cave is driven by
18 the recent discovery of stromatolite formations [148]. Stromatolites are laminated
19 sedimentary structures whose formation is mediated by microbial activity and represent some
20 of the most ancient evidence of life on Earth [149,150]. Composed of alternating layers of
21 sediments and organic matter, the analytical study of potential stromatolite formations on
22 Mars has been established as a scientific target of primary importance for the identification of
23 life traces. Therefore, numerous studies have recently focused on the study of terrestrial
24 stromatolites by means of analytical instruments relevant for space exploration [151–154].
25 Compared with other terrestrial analogue sites, El Soplao Cave provides the first reported case
26 of stromatolite formation occurring in the total absence of light, thus mediated by the biogenic
27 activity of chemolithotrophic bacteria [155,156]. Considering the astrobiological relevance of
28 this discovery, spectroscopic analysis of stromatolite samples was carried out to disclose their
29 mineralogical composition [157,158]. In situ and laboratory Raman investigations helped
30 detect Mn-oxide minerals, such as birnessite ($\text{Mn}_2\text{O}_4 \cdot 1.5 \text{H}_2\text{O}$), superposing broad bands

1 between 550 and 650 cm^{-1} [159] (Figure 11) and hausmannite (Mn_3O_4 , main peak at 659 cm^{-1}
 2 together with weak signals between 290 and 380 cm^{-1} [160]), as major components of these
 3 biogenic structures, together with additional minor phases [155]. Thus, spectroscopic analysis
 4 of El Soplao helped to deepen the knowledge regarding biogeochemical processes occurring in
 5 caves and underlined the importance of including Raman spectroscopy in the development of
 6 astrobiologically relevant exploration strategies.



7

8 *Figure 11: Raman spectrum of birnessite ($\text{Mn}_2\text{O}_4 \cdot 1.5 \text{H}_2\text{O}$), collected by means of a laboratory*
 9 *system from a stromatolite sample collected at El Soplao Cave. Compared with reference*
 10 *standards [159,161], the Raman spectrum displays a stronger contribution of the deconvoluted*
 11 *band located at 606 cm^{-1} .*

12

13 3. Planetary mission simulations

14 Analytical campaigns carried out at terrestrial analogue sites offer the opportunity to reliably
 15 evaluate the potential outcome of scientific instruments developed in the framework of
 16 planetary exploration. However, real space missions present additional challenges that need to
 17 be faced. For example, one of the biggest concerns is coordinating the navigation of the rover
 18 by relying only on remotely collected data and adapting its route to unanticipated events that
 19 could endanger its safety. In addition, it is necessary to refine the coordinated work of the
 20 different teams controlling the analytical instruments onboard the rover, thus maximizing the
 21 science return of the mission. Knowing that mistakes during real planetary missions can be
 22 very costly, the involved personnel need to be trained in the coordinated management of
 23 navigation and scientific instruments. In the case of analytical systems, it is also necessary to
 24 develop and test tailored protocols and tools that could help minimize human intervention.
 25 Therefore, instrument development occurs together with the realization of mission trials
 26 where team members can train on how to face the abovementioned challenges. In this

1 framework, the ERICA research group joined multiple mission simulations, the most important
2 of which are described in the following section.

3

4 3.1. *Arctic Mars Analogue Svalbard Expedition, AMASE (Svalbard, Norway)*

5 Svalbard is an archipelago of small islands located 1000 km from the North Pole. The
6 mineralogical variability of the islands, combined with the extreme environmental conditions
7 they present, make this an ideal area where to test instruments for planetary exploration
8 [162]. Since the beginning of 2000, Svalbard periodically hosts crews of researchers from
9 different disciplines to collaborate to carry out mission simulations named the Arctic Mars
10 Analogue Svalbard Expedition (AMASE) [163]. As explained elsewhere, AMASE expeditions are
11 meant to 1) test the hardware robustness and analytical performance of prototype
12 instruments for space exploration under extreme cold conditions [164,165], 2) conduct
13 astrobiological-relevant experiments [166], and 3) refine analytical procedures and sample
14 collection protocols [167].

15 As part of the AMASE team, from 2007 to 2011, the ERICA group carried out Martian-like
16 analytical experiments by combining in situ analysis with the detailed study of samples in the
17 laboratory. The research activities were aimed at pursuing the two objectives summarized
18 below.

19 • *Testing cutting-edge spectroscopic technologies*

20 The first expeditions gave the opportunity to operate, in a representative Martian analogue
21 site, novel spectroscopic prototypes for their potential use in surface planetary missions. In
22 detail, from 2007 to 2009, the ERICA group joined the AMASE scientist crews (including
23 researchers from the University of Leeds, Cornell University, Caltech, NASA and ESA, among
24 others) to test laboratory-assembled remote Raman and Raman-LIBS systems. As the results of
25 conceptual and technological developments started in 2004, these instruments were used for
26 the elemental and molecular characterization of remote targets.

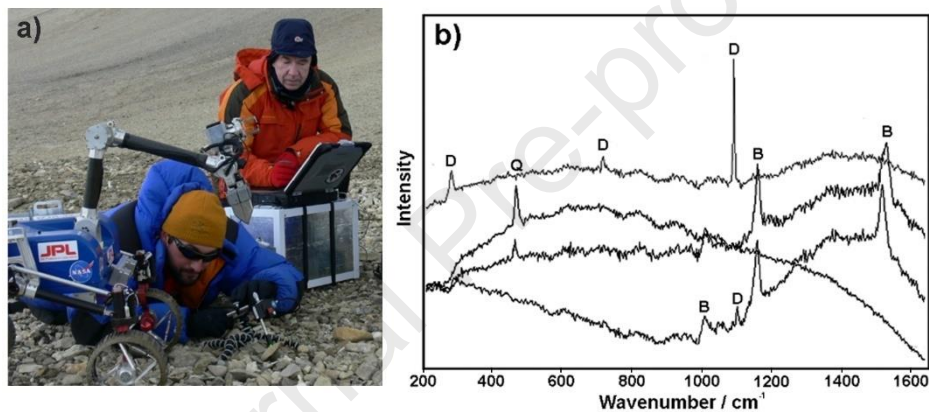
27 Beyond confirming the suitability of remote LIBS analysis, AMASE trials helped prove the
28 feasibility of remote Raman detection of molecular compounds from up to 150 metres of
29 distance [168]. Together with the technological advances presented by other research groups
30 [169], the results achieved in these trials contributed to settling the conceptual knowledge
31 necessary for the design and development of remote Raman-LIBS instruments for space
32 exploration, as is the case of the SuperCam instrument onboard the NASA/Perseverance rover
33 [170].

34 • *Performing research of high astrobiological relevance*

35 Belonging to the Svalbard Archipelago, Spitsbergen Island presents carbonate precipitation on
36 basaltic rocks that has been related to hydrothermal processes that occurred during the
37 Pleistocene when the Sverrefjell Volcano erupted through a layer of ice [171]. Considering that
38 1) the coexistence of liquid water and warm temperature favour the proliferation of microbial
39 life [172] and 2) the carbonate deposits found at Gusev Crater by the Mars Exploration Rover
40 Spirit [173] were interpreted as the result of hydrothermal processes having strong analogies

1 with the one described above [174], the AMASE expeditions served to carry out analytical
2 experiments of high astrobiological relevance.

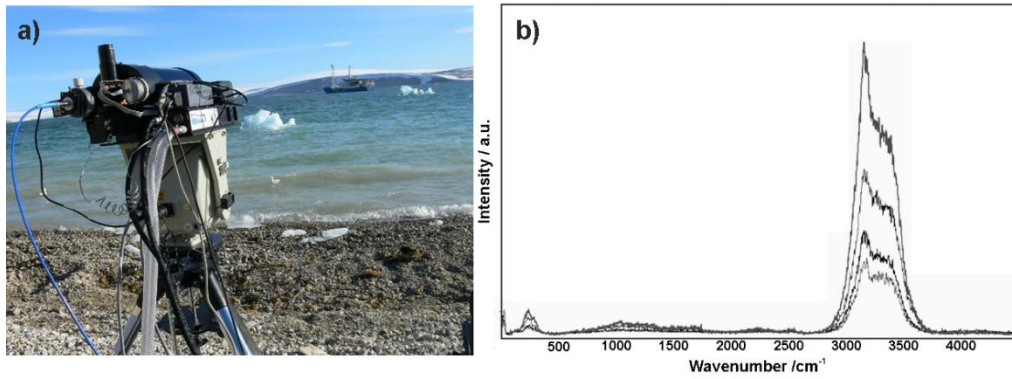
3 As presented by Rull et al. (2011) [168], a combined Raman-LIBS system was successfully used
4 to investigate basaltic rocks and carbonate precipitation from a distance of 15 metres.
5 Focusing on molecular results, Raman spectra successfully identified the main mineral phases
6 of the volcanic targets (pyroxene and feldspars, among others) and detected mixtures of
7 carbonate minerals (calcite, dolomite and magnesite MgCO_3). Based on in situ analysis,
8 geological samples were also collected for analysis in the laboratory. Here, XRD data were
9 compared with the results gathered from the use of Raman simulators that were assembled to
10 provide spectra qualitatively comparable to those expected by the RLS system onboard the
11 ExoMars mission. In addition to detecting the main mineral phases, in situ Raman analysis of
12 altered rocks from Svalbard enabled us to identify the vibrational features of beta-carotene
13 (Figure 12), thus further confirming that the RLS system could potentially detect organic
14 compounds on Mars.



15

16 *Figure 12: a) In situ Raman investigation of altered carbonates found on Svalbard in*
17 *collaboration with the microimager located on the JPL rover prototype. b) Raman spectra*
18 *obtained during in situ analysis (D=dolomite, Q=quartz, and B=beta-carotene). (Picture credits*
19 *JPL-UVA-FR).*

20 Beyond Mars-related studies, natural ice icebergs were also studied to assess the potentiality
21 of remote Raman spectrometers for the in situ exploration of icy extraterrestrial bodies, as is
22 the case of the Europa Lander mission proposed by NASA (according to the updated Europa
23 Lander concept, Raman spectroscopy was selected as one of the techniques necessary to meet
24 the science goals outlined for the mission [25]). In this context, the results presented by Rull et
25 al. (2011) [175] proved that Raman remote systems can be used to analyse icy targets,
26 allowing the detection of spectral changes that can be related to structural modifications
27 induced by the condition of ice formation (e.g., temperature and pressure). Indeed, as shown
28 in Figure 13, the intensity of the Raman spectra proved to be affected by the transparency of
29 the targeted ice [175].



1

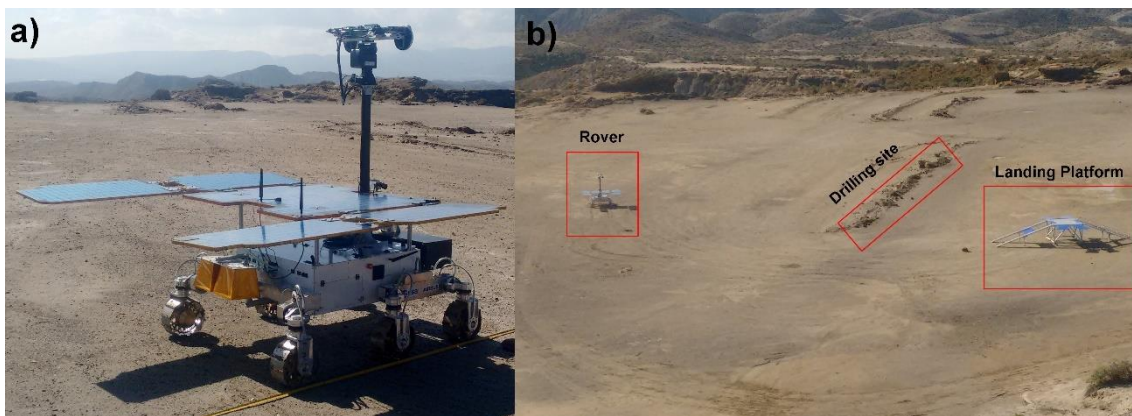
2 *Figure 13: a) Remote Raman analysis of icebergs. b) Raman spectra of translucent (high*
 3 *intensity) and opaque (low intensity) ice targets collected at a 40 m distance (from Rull et al.*
 4 *[175]).*

5 3.2. ExoMars-like Field Testing, ExoFiT (Tabernas, Spain)

6 The ExoMars-like Field Testing (ExoFiT) trials [176] were organized by AIRBUS and ESA to train
 7 the ExoMars operation team to manage the engineering and scientific challenges arising from
 8 the remote control of the Rosalind Franklin rover soon to be operating at Oxia Planum. The
 9 first trial, carried out in 2018, consisted of manoeuvring an emulator of the Rosalind Franklin
 10 rover in the Taberna Desert (Spain) by following the instructions provided by the Remote
 11 Control Centre (RCC) team that operated the simulation (from UK) by only relying on the data
 12 returned by its panoramic instruments.

13 During 9 Martian sols, a broad range of rover activities were simulated. In detail, panoramic
 14 cameras were used to investigate the surroundings. After descending the landing platform, the
 15 rover emulator was driven towards areas of high scientific interest. A combination of surface
 16 (CLUPI [177]) and subsurface (WISDOM radar [9]) investigations was then performed to
 17 identify the optimal drilling sites. After drilling, subsoil samples were crushed and analysed by
 18 the RLS team, which was represented by researchers and technical personnel from the
 19 University of Valladolid (UVa) and INTA.

20 As seen in Figure 14, the location selected for the trial was a flat area covered by sand-silt
 21 deposits with sporadic boulders and an elongated multilayered ridge outcropping at the centre
 22 of the plain.



23

1 *Figure 14: a) Close-up image of the Rosalind Franklin rover's emulator (Charlie) used during*
2 *ExoFit trials. b) Panoramic view of the area selected for the mission simulation.*

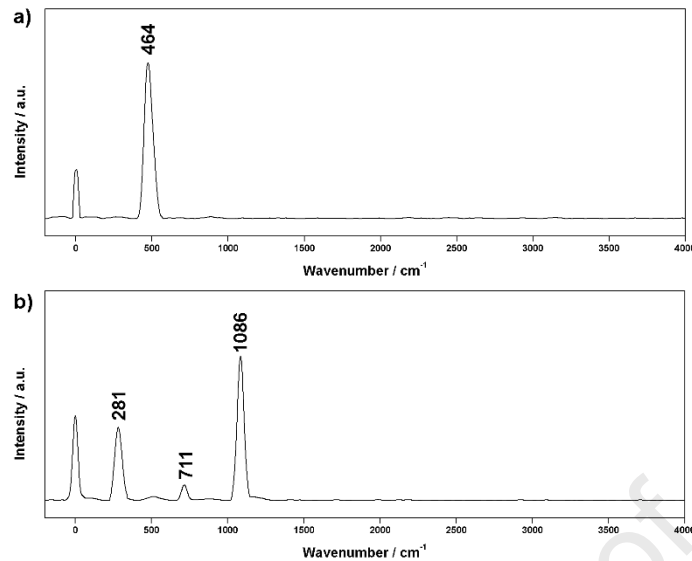
3 In addition to presenting a landscape very similar to what Rosalind Franklin is expected to find
4 at the landing site, two additional characteristics made the selected area a perfect analogue
5 site where to test the analytical tools of the rover. Similar to the fine-clay deposit covering 80%
6 of the landing ellipse, the particle size distribution of the regolith ground found in the Tabernas
7 Desert is dominated by silt-clay particles [178–180]. Knowing that the analysis of fine-grained
8 samples causes an increase in the background level and peak width, together with a decrease
9 in the signal-to-noise ratio (SNR) [94], this trial served to evaluate to what extent sample
10 granulometry could affect the quality of RLS spectra. Furthermore, previous studies
11 demonstrated that despite the arid environment, the surface of the Tabernas Desert is
12 characterized by the proliferation of microorganisms [179], which makes it the perfect site
13 where to test the ability of Raman spectrometers to detect the presence of biomarkers.

14 As explained in the introduction section, the fulfilment of the ExoMars main objective (to find
15 potential biosignatures on Mars) will strongly rely on spectroscopic investigations of geological
16 samples performed by MicrOmega and RLS spectroscopic systems. To simulate RLS operations
17 at the analogue site, Raman analysis was carried out by means of the RAD-1 system (Raman
18 Demonstrator), which is a portable spectrometer that follows the same geometrical concept
19 and spectral characteristics of the RLS-FM. Additional in situ analyses were performed using
20 the RLS qualification model (EQM-2), a replicate of the RLS-FM that has been assembled to
21 demonstrate the ability of the instrument to fulfil the scientific capabilities required by the
22 mission [12]. RAD-1 and EQM-2 data were then complemented by additional laboratory
23 analysis. In this sense, the RLS-Sim was used to replicate the complete analytical cycle (39
24 spectra per sample) established for RLS during nominal operation on Mars. The entire set of
25 Raman data was finally compared with the mineralogical results gathered from the
26 diffractometric analysis of powdered samples, which was carried out through Terra (from
27 Olympus), an XRD system that made use of the same technology developed by NASA for the
28 MSL/Curiosity rover mission (CheMin instrument) [181].

29 • Raman analysis of drilled cores

30 During the mission simulation operation cycle, two cores were drilled (TDC1 and TDC2). Prior
31 to analysis, geological samples were crushed and sieved to replicate the granulometry of the
32 powdered material produced by the ExoMars crusher. After flattening, the RAD-1 and EQM-2
33 systems were used to analyse between 6 and 8 spots per sample, with just a small fraction of
34 the dataset the RLS gathered during nominal operation on Mars (20 to 39 analysis) [182].

35 Through RAD-1 analysis, quartz (main peak at 464 cm^{-1}) was found to be the main
36 mineralogical phase in both drilled cores. In addition, peaks of medium intensity from calcite
37 (281 , 711 and 1086 cm^{-1}) and rutile (146 cm^{-1}) were also observed. The same samples were
38 further characterized at the site by means of the RLS-EQM2 system, which confirmed the
39 detection of quartz and calcite in both drilled cores (Figure 15) [35]. Thus, the in situ Raman
40 results fit very well with the mineralogical studies previously performed in this area, which
41 confirmed that these mineral compounds are among the main components of the soil in the
42 Tabernas Desert [183].



1

2 *Figure 15: Representative Raman spectra of quartz (a) and calcite (b) collected at the site by*
 3 *means of the EQM-2 system from the study of the TDC1 drilled core. The presented spectra*
 4 *were submitted to baseline correction by using the dedicated spectral tool of IDAT/SpectPro*
 5 *software (from Veneranda et al. [184]).*

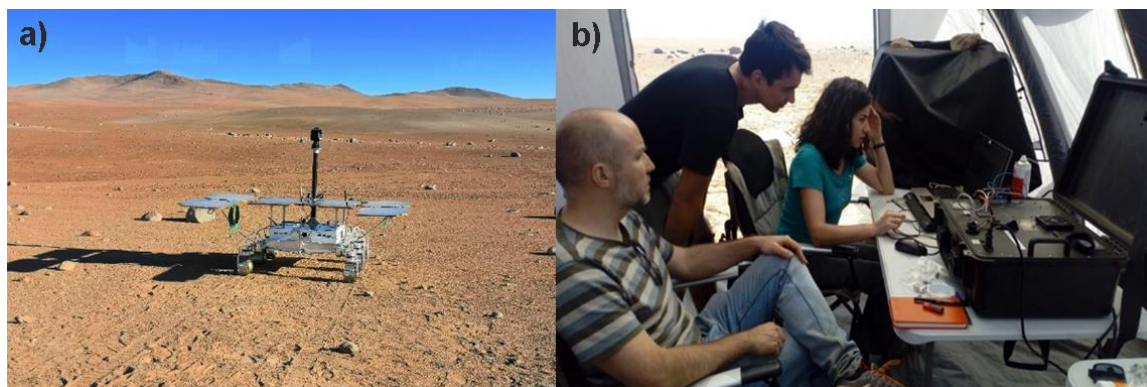
6 With regard to laboratory studies, powdered samples were placed on a replicate of the
 7 *ExoMars* refillable sample holder, and after flattening, point-by-point 39 spectra were
 8 automatically collected by the RLS-Sim. In addition to confirming the detection of the
 9 abovementioned minerals, the higher number of spectra per sample enabled the detection of
 10 additional minor compounds, such as muscovite (264, 402, 695 and 3625 cm^{-1}), anatase (240,
 11 445 and 610 cm^{-1}) and plagioclase (165, 285, 407, 478, 508, 769, 805 and 1100 cm^{-1}). The main
 12 Raman spectra collected in the laboratory are provided in a dedicated manuscript [184].
 13 Among them, the detection of muscovite is particularly interesting, as the detection (by RLS
 14 and MicrOmega) and further analysis (by MOMA) of phyllosilicate minerals has been
 15 established as the highest priority targets for fulfilment of the astrobiological goals of the
 16 *ExoMars 2022* mission. Overall, the Raman results fit very well with the X-ray diffractograms,
 17 which detected quartz, calcite and phyllosilicate (chlorite and muscovite) as the main mineral
 18 phases of both drilled cores [184].

19 In addition to the characterization of inorganic compounds, Raman analysis of subsoil samples
 20 enabled the identification of vibrational features potentially derived from organic functional
 21 groups (893, 1300, 1330, 1565, 2370, 2480 and 2570 cm^{-1}). Knowing that the Tabernas Desert
 22 has many mineralogical and environmental similarities with Oxia Planum, the detection of
 23 organics in both drilled cores is a very promising result, as it proves that the RLS system could
 24 be able to detect crucial analytical clues for the selection of potential biomarker-bearing
 25 mineralogical samples on Mars.

26

27 *3.3. ExoMars-like Field Testing, ExoFiT (Atacama Desert, Chile)*

1 To further train the ExoMars team in enhancing collaboration practices between instrument
 2 working groups, a second ExoFiT trial was organized in the Atacama Desert (Chile, February
 3 2019). As in the case of the previous ExoFiT simulation, the Charlie rover performed complex
 4 sequences of scientific operations by following the ExoMars Reference Surface Mission (RSM)
 5 [185]. As seen in Figure 16, the Martian landscape of this region (combined with the hyperarid
 6 climate) makes this the ideal location where to test rovers [186–188] and analytical systems
 7 [189–191] for Martian exploration.



8
 9 Figure 16: a) Panoramic view of the Rosalind Franklin rover's simulator (Charlie) operating in
 10 the Atacama Desert (Chile). b) The RAD-1 prototype obtaining Raman spectra from the
 11 powdered core samples.

12 The site selected for the ExoFiT trial is located in the region of Antofagasta, approximately 11
 13 km west of the ESO Paranal observatory. According to previous studies, the mineralogy of the
 14 selected area is characterized by granodiorites, andesite and gabbro rocks [192], while
 15 phyllosilicates, iron oxides and evaporitic minerals can be found as alteration products. This
 16 region displays strong levels of thermal excursion and surface ultraviolet (UV) irradiance
 17 ($>1100 \text{ W/m}^2$) [193], together with extremely low values of humidity (5–20%) and rainfall (an
 18 average of 10 mm per year) [194], which makes it one of the best terrestrial analogue sites to
 19 verify the capability of analytical instruments developed for astrobiological-related studies to
 20 detect organics. Indeed, it is well known that extremophile microorganisms proliferate in the
 21 subsurface of the Atacama Desert by relying on analogue metabolic mechanisms similar to
 22 those that may occur or may have occurred on Mars [195–197]. Therefore, Vitek and
 23 coworkers performed several in situ analyses to assess the capability of Raman spectroscopy
 24 to detect organic compounds in Atacama geological samples, obtaining encouraging results
 25 [198–200].

26 Taking a step forward in this field of study, during the second ExoFiT trial, the RLS science team
 27 was able to carry out Raman studies very closely following the real operation protocol
 28 established for the ExoMars mission. For that, the portable RAD-1 system used in Chile
 29 presented numerous hardware and software updates that allowed us to more faithfully
 30 replicate RLS-FM operations on Mars.

- 31
- Raman analysis of drilled cores

32 During the mission simulation, two cores were also drilled. In this case, each core (DC1 and
 33 DC2) was divided into two parts (upper UP and lower LP, respectively); therefore, the

1 multianalytical study was carried out on a total of 4 samples, which were previously crushed
 2 and sieved to replicate the granulometry produced by the ExoMars crusher. For the case of the
 3 Tabernas Desert, the strict time constraint imposed by the real mission simulation allowed
 4 only between 6 and 8 spots per sample to be analysed in situ.

5 As seen in Table 01, the in situ Raman analysis allowed us to identify feldspar in both ADC1
 6 samples, while a more complex mineralogy was detected in the ADC2 core. In detail, the
 7 characteristic peaks of quartz and calcite were identified in the ADC2-UP sample, whereas
 8 quartz, feldspar, amphibole, and phyllosilicate were observed in ADC2-LP. Regarding
 9 laboratory analysis, the 39 spectra per sample analysed by means of the RLS-Sims proved that
 10 by increasing the number of spots of analysis, a more detailed comprehension of the
 11 mineralogical composition of the material under study can be reached. Therefore, quartz,
 12 feldspar, anatase and phyllosilicate were detected in all samples [35]. Depending on the
 13 sample under analysis, amphibole and phyllosilicate were also detected together with
 14 evaporitic minerals (gypsum and calcite, see Table 01). On the whole, the mineralogical results
 15 obtained from the interpretation of Raman datasets fit very well the information extrapolated
 16 from X-ray diffractograms [35].

17 *Table 01: Comparison of Raman (RLS-Sim and RAD1) and XRD results obtained from the study*
 18 *of Atacama core samples.*

Sample	quartz	feldspar	anatase	amphibole	phyllosilicate	gypsum	anhydrite	calcite	hematite	organics
ADC2-UP (0-15cm)	x ◊ o	x o	x o	x o	x o	x o	o	x ◊ o		◊
ADC2LP (15-30cm)	x ◊ o	x ◊ o	x	◊	x ◊ o			x o		
ADC1-UP (0-15cm)	x o	x ◊ o	x	x o	x o			x		x
ADC1-LP (15-30cm)	x o	x ◊ o	x		x o				o	x

19

x = RLS ExoMars Simulator ◊ = Rad1 o = XRD

20

21 As seen in Table 01, spectroscopic analysis also detected vibrational peaks that can be assigned
 22 organic compounds. Specifically, peaks at 1340, 2190, 2250, 2800 and 2850 cm^{-1} (among
 23 others) were detected in the two ADC1 samples by RLS-Sim, while in the ADC2-UP sample,
 24 they were only detected by in situ analysis with the RAD-1 instrument [35]. Similar samples on
 25 Mars would be considered optimal candidates for MOMA analysis, as this instrument would be
 26 able to assess their biotic or abiotic origin.

27 On the one hand, the detection of organic features proves the capability of the RLS to support
 28 MOMA analysis by optimizing sample selection. On the other hand, considering that organics
 29 in sample ADC2-UP were only detected by RAD-1 proves that the 39 spots analysed by the RLS-
 30 Sim were not sufficient to ensure the detection of trace compounds potentially preserved
 31 within the mineralogical matrix. Therefore, this test was extremely useful for the RLS team, as
 32 it suggests that more than one cycle of analysis per sample should be considered when subsoil

1 materials of high scientific interest (e.g., rich in potential biomarker-bearing minerals, as is the
2 case with phyllosilicates) will be collected by the Rosalind Franklin rover on Mars.

3

4 **4. Discussion**

5 Placing Raman spectroscopy at the centre of this discussion, the first part of this section
6 evaluates the pros and cons expected by the application of this technique in planetary
7 missions. To do so, the potential scientific outcome of Raman systems is compared with that
8 provided by molecular and mineralogical techniques already operating on Mars. Starting with
9 Mössbauer spectroscopy, it is well known that the analytical systems onboard both Spirit and
10 Opportunity Mars Exploration Rovers enabled us to deeply probe the composition of Fe-
11 bearing materials found at the landing sites [7]. Mössbauer analysis of Martian rocks and soils
12 identified a large number of new mineral phases, thus providing information of key
13 importance to reconstruct the geological and mineralogical evolution of the planet. For
14 example, the detection of alunite and jarosite minerals shed light on the past occurrence of
15 superficial acidic waters at the surface of Mars, which is an extremely important discovery for
16 the field of astrobiology research [8]. Although Raman is sensitive to a great variety of iron
17 oxides, hydroxides and additional Fe-bearing phases, Mössbauer spectroscopy often provides
18 more detailed information about the electronic structure and geometry of the investigated
19 molecule. However, the ability of the Mössbauer technique to accurately analyse Fe-bearing
20 minerals is partially countered by the inability to detect Fe-free minerals. In this sense, the
21 main advantage of Raman spectroscopy is the ability to detect any mineral phase that
22 undergoes a change in molecular polarizability as it vibrates, regardless of its elemental
23 composition. The combined Mössbauer-Raman investigations carried out at the JHS, Rio Tinto
24 and Tenerife terrestrial analogue sites demonstrated the complementarity between the two
25 techniques. In light of current and future missions, the greater versatility of Raman
26 spectroscopy can be particularly useful when investigating heterogeneous geological
27 environments [64,99]. This is the case for the Mars2020 rover, which, after analysing Jezero
28 crater bedrocks and phyllosilicate-bearing deposits, will target the Mg-rich carbonate units
29 detected at the crater rim [16].

30 In addition to Mössbauer spectroscopy, much of the current knowledge about Martian
31 mineralogy at a micrometric scale is due to the CheMin XRF-XRD system onboard the Curiosity
32 rover, which has been operating at the Gale crater since 2012 [201]. As it allows the
33 identification of any kind of crystal structure, X-ray diffractometry is the primary method for
34 the mineralogical characterization of rocks and soils. Despite being particularly suitable for
35 planetary exploration missions, the detection limit of the technique allows minor and trace
36 compounds to often pass undetected. In the case of CheMin, the miniaturization of the
37 components, the simplified geometry and the low energy consumption requirements causes
38 the estimated detection limit of the instrument to be approximately 3% [130,202,203].

39 By investigating the selected target at a micrometric scale, Raman spectroscopy is capable of
40 punctually detecting minor compounds that are below the detection limit of XRD. The
41 numerous cases of study in which terrestrial analogue materials have been characterized by
42 both diffractometric and Raman instruments helped demonstrate that Raman spectroscopy is
43 often capable of identifying additional minor phases provided that the number of observed

1 spots on the sample is sufficient. The detection of minor compounds is relevant, as they can
2 supply very valuable information about the formation and/or alteration processes of the
3 geological sample under analysis. Knowing the RLS system onboard the Rosalind Franklin rover
4 will nominally perform between 20 and 39 point-by-point observations on the sample surface
5 [204], the Raman investigations to be carried out in the framework of the ExoMars mission
6 should allow the identification of both major and minor phases composing Martian rocks and
7 soils. In this sense, the mission simulations carried out in Almeria and Atacama (see Section 3)
8 proved that the higher the number of Raman analyses carried out on a powdered sample is,
9 the greater the probability of completely disclosing its mineralogical heterogeneities. For this
10 reason, when a sample of high scientific-astrobiological interest is processed by the ExoMars
11 analytical payload, running more than one cycle of analysis should be considered. Another
12 observed difference from XRD analysis is the difficulty of identifying amorphous systems with
13 this last technique [205]. Raman spectroscopy can handle these materials, although important
14 difficulties arise when fluorescence appears, which is very often present in clay minerals.

15 Furthermore, compared with Mössbauer spectroscopy and XRD, the greater advantage of
16 Raman spectroscopy is the ability to additionally detect organic compounds (e.g., biomarkers),
17 which makes it suitable for astrobiological studies. Indeed, we presented numerous cases in
18 which Raman prototypes simulating the scientific capability of RLS and SuperCam enabled the
19 detection of organic features from terrestrial analogue samples, as was the case in the
20 Barberton, Rio Tinto, Svalbard and Atacama samples. This characteristic makes Raman
21 spectroscopy particularly suitable for the fulfilment of Mars2020 and ExoMars missions, whose
22 main objective is to determine if life ever took hold on Mars [16,95].

23 As the analytical investigation of unknown mineralogical samples can benefit from the
24 combined use of multiple analytical techniques, the scientific outcome of Raman analysis can
25 be optimized by complementary molecular and/or elemental data. In this sense, both Mars
26 2020 and ExoMars missions will provide the opportunity to investigate the same target with
27 complementary analytical systems. As the subsoil samples collected by the ExoMars rover will
28 be characterized by both Raman and NIR spectrometers, many of the studies presented in
29 Section 2 had the purpose of determining the advantages provided by the combined use of
30 these two techniques. For example, the multianalytical investigation of terrestrial analogue
31 samples from Rio Tinto, LOC and CBIS proves the different sensitivity of the two spectroscopic
32 systems towards the detection of specific mineral phases, making the mineralogical results
33 obtained from the interpretation of both Raman and NIR data more complete than those
34 achieved by using only one of the two instruments. In the case of the future ExoMars mission,
35 it should be highlighted that the MicrOmega system will map areas of $5 \times 5 \text{ mm}^2$ of the
36 powdered samples with a spatial sampling of $20 \text{ }\mu\text{m}$ per pixel [13]. This offers a great
37 advantage for Raman investigations since the raster of spots analysed by the RLS can be
38 selected by taking into account NIR results [206].

39 Looking at the Mars 2020 mission, remote (SuperCam [18]) and proximity (Sherloc [21]) Raman
40 analyses the Perseverance rover is performing on Mars are supported by the elemental
41 information provided by LIBS and XRF analysis, respectively. In the case of the SuperCam
42 analytical suite, additional spectroscopic information can be gathered in VISIR and
43 fluorescence modes. As the ERICA research group took part in the development of the
44 SuperCam instrument [17], several terrestrial analogue materials were investigated by hybrid
45 Raman-LIBS remote systems. Technically, the analysis of terrestrial analogues proved that

1 combined spectroscopic instrumentations provide great advantages in terms of mass and
2 volume requirements, which are key parameters to consider in the development of space
3 exploration instruments. Analytically, hybrid Raman-LIBS systems afford advantages, as both
4 molecular and elemental data can be gathered from the same spot of interest. As described in
5 the examples provided in Section 2, remote Raman-LIBS analysis helps to optimize the
6 geochemical and mineralogical characterization of the samples under analysis. Therefore, the
7 combination of the two spectroscopic methods will help gather key information for the
8 selection of soil and rock samples to be returned to Earth [207].

9 From a broader perspective, this review highlights that the analysis of terrestrial analogue
10 materials represents a cornerstone tool to constrain and predict the potential scientific
11 outcome of analytical instruments for planetary exploration. In this sense, the ERICA research
12 group is collaborating with an international consortium in the development of the Planetary
13 Terrestrial Analogue Library (PTAL). Funded by the European Union's Horizon 2020 research
14 and innovation programme, the PTAL project aims at supporting forthcoming space missions
15 to Mars and other extraterrestrial bodies by providing the scientific community with XRD, LIBS,
16 Raman and NIR data collected by over 100 different terrestrial analogue materials [208–211].
17 In addition to PTAL, the research group is also building a novel database of pure mineral
18 phases that are relevant for Mars exploration. Called Analytical Database of Martian Minerals
19 (ADaMM), a collection of more than 300 different mineral phases is being analysed by
20 combining the use of diffractometric and spectroscopic instruments providing results
21 qualitatively comparable to the analytical systems (soon) operating on Mars [212]. In addition
22 to analogue/mineral databases, the ERICA research group aims to additionally support rover
23 missions through the development of tailored software that is meant to facilitate the analysis
24 and interpretation of the spectroscopic data gathered on Mars. For example, through the PTAL
25 and ADaMM platforms, a downloadable version of IDAT/SpectPro software will be provided to
26 the scientific community [36,213]. Developed in the framework of the ExoMars mission to
27 receive, decodify, calibrate and verify the telemetries generated by the RLS on Mars, further
28 details about this novel analytical tool will be provided in a dedicated manuscript.

29

30 **5. Perspectives**

31 In light of the forthcoming deployment of novel spectroscopic techniques on Mars, the
32 analytical study of terrestrial analogue sites and materials gains importance. As summarized in
33 Section 2, the spectroscopic-based characterization of representative terrestrial analogues of
34 Martian geological contexts helps to shed light on the potential scientific outcome that could
35 derive from the operation of Raman systems on Mars. In detail, the mentioned studies confirm
36 the capability of this spectroscopic technique to gather mineralogical data qualitatively
37 comparable to those provided by further analytical techniques that have been successfully
38 employed on Mars in previous rover missions (e.g., Mössbauer and X-ray diffractometry).
39 Compared with these, Raman spectrometers proved to effectively detect organics within
40 analogue geological samples, thus confirming the potential key role this technique could play
41 in the fulfilment of the main objective of both ExoMars and Mars 2020 missions: to detect
42 clues of past or present life on Mars. Furthermore, the multianalytical investigation of
43 terrestrial analogue materials confirmed the complementarity of Raman spectroscopy with NIR
44 and LIBS systems, thus providing crucial information for the proper interpretation of the data

1 returned by the Perseverance and Rosalind Franklin rovers. In addition to analysing the
 2 scientific capabilities of spectroscopic instruments, mission simulations described in Section 3
 3 offered the opportunity to optimize the synergistic collaboration between instrument working
 4 groups and to practice with real mission issues. While confirming the complementarity
 5 between spectroscopic techniques, the experience gained by participating in mission
 6 simulations helped refine the analytical protocols to follow during nominal operations on
 7 Mars.

8

9 **Acknowledgments:**

10 This work is financed through the Ministry of Economy and Competitiveness (MINECO, grant
 11 PID2019-107442RB-C31 and the European Research Council in the H2020- COMPET-2015
 12 programme (grant 687302). The authors gratefully acknowledge the support of the SIGUE-
 13 Mars consortium (MINECO, grant RDE2018-102600-T). The authors are grateful to all
 14 researchers that took part in the presented investigations, in particular Fernando Gazquez,
 15 Gloria Venegas, Antonio Sansano (in-memoriam), Jose Maria Calaforra, Stephanie C. Werner,
 16 Francois Poulet and Goestar Klingelhofer (in-memoriam).

17

18 **References:**

- 19 [1] T. Economou, Chemical analyses of martian soil and rocks obtained by the Pathfinder
 20 Alpha Proton X-ray spectrometer, *Radiat. Phys. Chem.* 61 (2001) 191–197.
 21 [https://doi.org/10.1016/S0969-806X\(01\)00240-7](https://doi.org/10.1016/S0969-806X(01)00240-7).
- 22 [2] R. Gellert, R. Rieder, J. Brückner, B.C. Clark, G. Dreibus, G. Klingelhöfer, G. Lugmair,
 23 D.W. Ming, H. Wänke, A. Yen, J. Zipfel, S.W. Squyres, Alpha Particle X-Ray Spectrometer
 24 (APXS): Results from Gusev crater and calibration report, *J. Geophys. Res. E Planets.* 111
 25 (2006). <https://doi.org/10.1029/2005JE002555>.
- 26 [3] L.A. Soderblom, R.C. Anderson, R.E. Arvidson, J.F. Bell, N.A. Cabrol, W. Calvin, P.R.
 27 Christensen, B.C. Clark, T. Economou, B.L. Ehlmann, W.H. Farrand, D. Fike, R. Gellert,
 28 T.D. Glotch, M.P. Golombek, R. Greeley, J.P. Grotzinger, K.E. Herkenhoff, D.J. Jerolmack,
 29 J.R. Johnson, B. Jolliff, C. Klingelhöfer, A.H. Knoll, Z.A. Learner, R. Li, M.C. Malin, S.M.
 30 McLennan, H.Y. McSween, D.W. Ming, R. V. Morris, J.W. Rice, L. Richter, R. Rieder, D.
 31 Rodionov, C. Schröder, F.P. Seelos IV, J.M. Soderblom, S.W. Squyres, R. Sullivan, W.A.
 32 Watters, C.M. Weitz, M.B. Wyatt, A. Yen, J. Zipfel, Soils of eagle crater and Meridiani
 33 Planum at the opportunity Rover landing site, *Science* (80-.). 306 (2004) 1723–1726.
 34 <https://doi.org/10.1126/science.1105127>.
- 35 [4] L.M. Thompson, M.E. Schmidt, J.G. Spray, J.A. Berger, A.G. Fairén, J.L. Campbell, G.M.
 36 Perrett, N. Boyd, R. Gellert, I. Pradler, S.J. VanBommel, Potassium-rich sandstones
 37 within the Gale impact crater, Mars: The APXS perspective, *J. Geophys. Res. Planets.*
 38 121 (2016) 1981–2003. <https://doi.org/10.1002/2016JE005055>.
- 39 [5] S. Maurice, R.C. Wiens, M. Saccoccio, B. Barraclough, O. Gasnault, O. Forni, N. Mangold,
 40 D. Baratoux, S. Bender, G. Berger, J. Bernardin, M. Berthé, N. Bridges, D. Blaney, M.
 41 Bouyé, P. Cais, B. Clark, S. Clegg, A. Cousin, D. Cremers, A. Cros, L. Deflores, C. Derycke,
 42 B. Dingler, G. Dromart, B. Dubois, M. Dupieux, E. Durand, L. D’Uston, C. Fabre, B. Faure,
 43 A. Gaboriaud, T. Gharsa, K. Herkenhoff, E. Kan, L. Kirkland, D. Kouach, J.L. Lacour, Y.
 44 Langevin, J. Lasue, S. Le Mouélic, M. Lescure, E. Lewin, D. Limonadi, G. Manhès, P.
 45 Mauchien, C. McKay, P.Y. Meslin, Y. Michel, E. Miller, H.E. Newsom, G. Orttner, A.

- 1 Paillet, L. Parès, Y. Parot, R. Pérez, P. Pinet, F. Poitrasson, B. Quertier, B. Sallé, C. Sotin,
2 V. Sautter, H. Séran, J.J. Simmonds, J.B. Sirven, R. Stiglich, N. Striebig, J.J. Thocaven, M.J.
3 Toplis, D. Vaniman, The ChemCam instrument suite on the Mars Science Laboratory
4 (MSL) rover: Science objectives and mast unit description, *Space Sci. Rev.* 170 (2012)
5 95–166. <https://doi.org/10.1007/s11214-012-9912-2>.
- 6 [6] E.B. Rampe, M.G.A. Lapotre, T.F. Bristow, R.E. Arvidson, R. V. Morris, C.N. Achilles, C.
7 Weitz, D.F. Blake, D.W. Ming, S.M. Morrison, D.T. Vaniman, S.J. Chipera, R.T. Downs,
8 J.P. Grotzinger, R.M. Hazen, T.S. Peretyazhko, B. Sutter, V. Tu, A.S. Yen, B. Horgan, N.
9 Castle, P.I. Craig, D.J. Des Marais, J. Farmer, R. Gellert, A.C. McAdam, J.M. Morookian,
10 P.C. Sarrazin, A.H. Treiman, Sand Mineralogy Within the Bagnold Dunes, Gale Crater, as
11 Observed In Situ and From Orbit, *Geophys. Res. Lett.* 45 (2018) 9488–9497.
12 <https://doi.org/10.1029/2018GL079073>.
- 13 [7] R. V. Morris, G. Klingelhöfer, B. Bernhardt, C. Schröder, D.S. Rodionov, P.A. De Souza, A.
14 Yen, R. Gellert, E.N. Evlanov, J. Foh, E. Kankleit, P. Gütlich, D.W. Ming, F. Renz, T.
15 Wdowiak, S.W. Squyres, R.E. Arvidson, Mineralogy at Gusev crater from the Mössbauer
16 spectrometer on the Spirit rover, *Science* (80-.). 305 (2004) 833–836.
17 <https://doi.org/10.1126/science.1100020>.
- 18 [8] R. V. Morris, G. Klingelhöfer, C. Schröder, D.S. Rodionov, A.S. Yen, D.W. Ming, J.A. de
19 Souza, T. Wdowiak, I. Fleischer, R. Gellert, B. Bernhardt, U. Bonnes, B.A. Cohen, E.N.
20 Evlanov, J. Foh, P. Gütlich, E. Kankleit, T. McCoy, D.W. Mittlefehldt, F. Renz, M.E.
21 Schmidt, B. Zubkov, S.W. Squyres, R.E. Arvidson, Mössbauer mineralogy of rock, soil,
22 and dust at Meridiani Planum, Mars: Opportunity's journey across sulfate-rich outcrop,
23 basaltic sand and dust, and hematite lag deposits, *J. Geophys. Res. E Planets.* 111 (2006)
24 E12S15.
- 25 [9] V. Ciarletti, S. Clifford, D. Plettemeier, A. Le Gall, Y. Hervé, S. Dorizon, C. Quantin-Nataf,
26 W.S. Benedix, S. Schwenzer, E. Pettinelli, E. Heggy, A. Herique, J.J. Berthelier, W.
27 Kofman, J.L. Vago, S.E. Hamran, The WISDOM Radar: Unveiling the Subsurface Beneath
28 the ExoMars Rover and Identifying the Best Locations for Drilling, *Astrobiology.* 17
29 (2017) 565–584. <https://doi.org/10.1089/ast.2016.1532>.
- 30 [10] R. Paul, D. Redlich, T. Tattusch, L. Richter, M. Thiel, F. Musso, S. Durrant, Sample flow
31 and implications on design and testing for the SPDS mechanism chain on the Exomars
32 2020 rover, 14th Symp. Adv. Sp. Technol. Robot. Autom. (2017).
- 33 [11] F. Rull, S. Maurice, I. Hutchinson, A. Moral, C. Perez, C. Diaz, M. Colombo, T. Belenguer,
34 G. Lopez-Reyes, A. Sansano, O. Forni, Y. Parot, N. Striebig, S. Woodward, C. Howe, N.
35 Tarcea, P. Rodriguez, L. Seoane, A. Santiago, J.A. Rodriguez-Prieto, J. Medina, P. Gallego,
36 R. Canchal, P. Santamaría, G. Ramos, J.L. Vago, The Raman Laser Spectrometer for the
37 ExoMars Rover Mission to Mars, *Astrobiology.* 17 (2017) 627–654.
38 <https://doi.org/10.1089/ast.2016.1567>.
- 39 [12] A.G. Moral, F. Rull, S. Maurice, I.B. Hutchinson, C.P. Canora, L. Seoane, G. López-Reyes,
40 J.A. Rodriguez Prieto, P. Rodríguez, G. Ramos, Y. Parot, O. Forni, Design, development,
41 and scientific performance of the Raman Laser Spectrometer EQM on the 2020
42 ExoMars (ESA) Mission, *J. Raman Spectrosc.* (2019) 1–11.
43 <https://doi.org/10.1002/jrs.5711>.
- 44 [13] J.P. Bibring, V. Hamm, C. Pilorget, J.L. Vago, M. Team, The MicrOmega Investigation
45 Onboard ExoMars, *Astrobiology.* 17 (2017) 621–626.
46 <https://doi.org/10.1089/ast.2016.1642>.
- 47 [14] F. Goesmann, W.B. Brinckerhoff, F. Raulin, W. Goetz, R.M. Danell, S.A. Getty, S.
48 Siljeström, H. Mißbach, H. Steininger, R.D. Arevalo, A. Buch, C. Freissinet, A. Grubisic,

- 1 U.J. Meierhenrich, V.T. Pinnick, F. Stalport, C. Szopa, J.L. Vago, R. Lindner, M.D. Schulte,
2 J.R. Brucato, D.P. Glavin, N. Grand, X. Li, F.H.W. Van Amerom, The Mars Organic
3 Molecule Analyzer (MOMA) Instrument: Characterization of Organic Material in
4 Martian Sediments, *Astrobiology*. 17 (2017) 655–685.
5 <https://doi.org/10.1089/ast.2016.1551>.
- 6 [15] B.K. Muirhead, A.K. Nicholas, J. Umland, O. Sutherland, S. Vijendran, Mars Sample
7 Return Campaign Concept Status, *Acta Astronaut.* 176 (2020) 131–138.
8 <https://doi.org/10.1016/j.actaastro.2020.06.026>.
- 9 [16] K.A. Farley, K.H. Williford, K.M. Stack, R. Bhartia, A. Chen, M. de la Torre, K. Hand, Y.
10 Goreva, C.D.K. Herd, R. Hueso, Y. Liu, J.N. Maki, G. Martinez, R.C. Moeller, A. Nelessen,
11 C.E. Newman, D. Nunes, A. Ponce, N. Spanovich, P.A. Willis, L.W. Beegle, J.F. Bell, A.J.
12 Brown, S.E. Hamran, J.A. Hurowitz, S. Maurice, D.A. Paige, J.A. Rodriguez-Manfredi, M.
13 Schulte, R.C. Wiens, Mars 2020 Mission Overview, *Space Sci. Rev.* 216 (2020) 142.
- 14 [17] J.A. Manrique, G. Lopez-Reyes, A. Cousin, F. Rull, S. Maurice, R.C. Wiens, M.B. Madsen,
15 J.M. Madariaga, O. Gasnault, J. Aramendia, G. Arana, P. Beck, S. Bernard, P. Bernardi,
16 M.H. Bernt, A. Berrocal, O. Beyssac, P. Caïs, C. Castro, K. Castro, S.M. Clegg, E. Cloutis,
17 G. Dromart, C. Drouet, B. Dubois, D. Escribano, C. Fabre, A. Fernandez, O. Forni, V.
18 Garcia-Baonza, I. Gontijo, J. Johnson, J. Laserna, J. Lasue, S. Madsen, E. Mateo-Marti, J.
19 Medina, P.Y. Meslin, G. Montagnac, A. Moral, J. Moros, A.M. Ollila, C. Ortega, O. Prieto-
20 Ballesteros, J.M. Reess, S. Robinson, J. Rodriguez, J. Saiz, J.A. Sanz-Arranz, I. Sard, V.
21 Sautter, P. Sobron, M. Toplis, M. Veneranda, SuperCam Calibration Targets: Design and
22 Development, *Space Sci. Rev.* 216 (2020) 1–27. <https://doi.org/10.1007/s11214-020-00764-w>.
- 24 [18] R.C. Wiens, S. Maurice, S.H. Robinson, A.E. Nelson, P. Cais, P. Bernardi, R.T. Newell, S.
25 Clegg, S.K. Sharma, S. Storms, J. Deming, D. Beckman, A.M. Ollila, O. Gasnault, R.B.
26 Anderson, Y. André, S.M. Angel, G. Arana, E. Auden, P. Beck, J. Becker, K. Benzerara, S.
27 Bernard, O. Beyssac, L. Borges, B. Bousquet, K. Boyd, M. Caffrey, J. Carlson, K. Castro, J.
28 Celis, B. Chide, K. Clark, E. Cloutis, E.C. Cordoba, A. Cousin, M. Dale, L. Deflores, D.
29 Delapp, M. Deleuze, M. Dirmyer, C. Donny, G. Dromart, M.G. Duran, M. Egan, J. Ervin,
30 C. Fabre, A. Fau, W. Fischer, O. Forni, I. Gontijo, J. Grotzinger, X. Jacob, S. Jacquino, J.
31 Laserna, J. Lasue, S. Le, M. Carey, L. Iv, R. Leveille, E. Lewin, G.L. Ralph, E. Lorigny, S.P.
32 Love, B. Lucero, J. Manuel, The SuperCam Instrument Suite on the NASA Mars 2020
33 Rover : Body Unit and Combined System Tests, The Author(s), 2021.
34 <https://doi.org/10.1007/s11214-020-00777-5>.
- 35 [19] S. Maurice, R.C. Wiens, P. Bernardi, P. Caïs, S. Robinson, T. Nelson, O. Gasnault, J.-M.
36 Reess, M. Deleuze, F. Rull, J.-A. Manrique, S. Abbaki, R.B. Anderson, Y. André, S.M.
37 Angel, G. Arana, T. Battault, P. Beck, K. Benzerara, S. Bernard, J.-P. Berthias, O. Beyssac,
38 M. Bonafous, B. Bousquet, M. Boutillier, A. Cadu, K. Castro, F. Chapron, B. Chide, K.
39 Clark, E. Clavé, S. Clegg, E. Cloutis, C. Collin, E.C. Cordoba, A. Cousin, J.-C. Dameury, W.
40 D’Anna, Y. Daydou, A. Debus, L. Deflores, E. Dehouck, D. Delapp, G. De Los Santos, C.
41 Donny, A. Doressoundiram, G. Dromart, B. Dubois, A. Dufour, M. Dupieux, M. Egan, J.
42 Ervin, C. Fabre, A. Fau, W. Fischer, O. Forni, T. Fouchet, J. Frydenvang, S. Gauffre, M.
43 Gauthier, V. Gharakanian, O. Gilard, I. Gontijo, R. Gonzalez, D. Granena, J. Grotzinger, R.
44 Hassen-Khodja, M. Heim, Y. Hello, G. Hervet, O. Humeau, X. Jacob, S. Jacquino, J.R.
45 Johnson, D. Kouach, G. Lacombe, N. Lanza, L. Lapauw, J. Laserna, J. Lasue, L. Le Deit, S.
46 Le Mouélic, E. Le Comte, Q.-M. Lee, C. Leggett, R. Leveille, E. Lewin, C. Leyrat, G. Lopez-
47 Reyes, R. Lorenz, B. Lucero, J.M. Madariaga, S. Madsen, M. Madsen, N. Mangold, F.
48 Manni, J.-F. Mariscal, J. Martinez-Frias, K. Mathieu, R. Mathon, K.P. McCabe, T.
49 McConnochie, S.M. McLennan, J. Mekki, N. Melikechi, P.-Y. Meslin, Y. Micheau, Y.

- 1 Michel, J.M. Michel, D. Mimoun, A. Misra, G. Montagnac, C. Montaron, F. Montmessin,
 2 J. Moros, V. Mousset, Y. Morizet, N. Murdoch, R.T. Newell, H. Newsom, N. Nguyen
 3 Tuong, A.M. Ollila, G. Orttner, L. Oudda, L. Pares, J. Parisot, Y. Parot, R. Pérez, D. Pheav,
 4 L. Picot, P. Pilleri, C. Pilorget, P. Pinet, G. Pont, F. Poulet, C. Quantin-Nataf, B. Quartier,
 5 D. Rambaud, W. Rapin, P. Romano, L. Roucayrol, C. Royer, M. Ruellan, B.F. Sandoval, V.
 6 Sautter, M.J. Schoppers, S. Schröder, H.-C. Seran, S.K. Sharma, P. Sobron, M. Sodki, A.
 7 Sournac, V. Sridhar, D. Standarovsky, S. Storms, N. Striebig, M. Tatat, M. Toplis, I. Torre-
 8 Fdez, N. Toulemont, C. Velasco, M. Veneranda, D. Venhaus, C. Virmontois, M. Viso, P.
 9 Willis, K.W. Wong, The SuperCam Instrument Suite on the Mars 2020 Rover: Science
 10 Objectives and Mast-Unit Description, *Space Sci. Rev.* 217 (2021) 47.
- 11 [20] A.C. Allwood, L.A. Wade, M.C. Foote, W.T. Elam, J.A. Hurowitz, S. Battel, D.E. Dawson,
 12 R.W. Denise, E.M. Ek, M.S. Gilbert, M.E. King, C.C. Liebe, T. Parker, D.A.K. Pedersen, D.P.
 13 Randall, R.F. Sharrow, M.E. Sondheim, G. Allen, K. Arnett, M.H. Au, C. Basset, M. Benn,
 14 J.C. Bousman, D. Braun, R.J. Calvet, B. Clark, L. Cinquini, S. Conaby, H.A. Conley, S.
 15 Davidoff, J. Delaney, T. Denver, E. Diaz, G.B. Doran, J. Ervin, M. Evans, D.O. Flannery, N.
 16 Gao, J. Gross, J. Grotzinger, B. Hannah, J.T. Harris, C.M. Harris, Y. He, C.M. Heirwegh, C.
 17 Hernandez, E. Hertzberg, R.P. Hodyss, J.R. Holden, C. Hummel, M.A. Jadusingh, J.L.
 18 Jørgensen, J.H. Kawamura, A. Kitiyakara, K. Kozaczek, J.L. Lambert, P.R. Lawson, Y. Liu,
 19 T.S. Luchik, K.M. Macneal, S.N. Madsen, S.M. McLennan, P. McNally, P.L. Meras, R.E.
 20 Muller, J. Napoli, B.J. Naylor, P. Nemere, I. Ponomarev, R.M. Perez, N. Pootrakul, R.A.
 21 Romero, R. Rosas, J. Sachs, R.T. Schaefer, M.E. Schein, T.P. Setterfield, V. Singh, E. Song,
 22 M.M. Soria, P.C. Stek, N.R. Tallarida, D.R. Thompson, M.M. Tice, L. Timmermann, V.
 23 Torossian, A. Treiman, S. Tsai, K. Uckert, J. Villalvazo, M. Wang, D.W. Wilson, S.C. Worel,
 24 P. Zamani, M. Zappe, F. Zhong, R. Zimmerman, PIXL: Planetary Instrument for X-Ray
 25 Lithochemistry, *Space Sci. Rev.* 216 (2020) 134.
- 26 [21] L. Beegle, R. Bhartia, M. White, L. Deflores, W. Abbey, Y.H. Wu, B. Cameron, J. Moore,
 27 M. Fries, A. Burton, K.S. Edgett, M.A. Ravine, W. Hug, R. Reid, T. Nelson, S. Clegg, R.
 28 Wiens, S. Asher, P. Sobron, SHERLOC: Scanning habitable environments with Raman &
 29 luminescence for organics & chemicals, in: *IEEE Aerosp. Conf. Proc.*, 2015: pp. 1–11.
 30 <https://doi.org/10.1109/AERO.2015.7119105>.
- 31 [22] S. Schröder, T. Belenguer, U. Böttger, M. Buder, Y. Cho, E. Dietz, M. Gensch, T.
 32 Hagelschuer, F. Hanke, H.-W. Hübers, S. Kameda, E. Kopp, S. Kubitza, A. Moral, C.
 33 Paproth, M. Pertenais, G. Peter, K. Rammelkamp, P. Rodriguez, F. Rull, C. Ryan, T.
 34 Säuberlich, F. Schrandt, S. Ulamec, T. Usui, R. Vance, In-situ Raman spectroscopy on
 35 Phobos: RAX on the MMX rover, in: *51st Lunar Planet. Sci. Conf.*, The Woodlands
 36 (Texas), 2020: p. 2019. <https://doi.org/10.5840/dspl20203218>.
- 37 [23] S. Ulamec, N.M. Patrick Michel, Matthias Grott, Ute Böttger, Heinz-Wilhelm Hübers,
 38 F.R. Pierre Vernazza, Özgür Karatekin, Jörg Knollenberg, Konrad Willner, Markus
 39 Grebenstein, Stephane Mary, Pascale Chazalnoël, Jens Biele, Christian Krause, Tra-Mi
 40 Ho, Caroline Lange, Jan Thimo Grundmann, Kaname Sasaki, Michael Maibaum, Oliver
 41 Küchemann, Jose, A rover for the JAXA MMX Mission to Phobos, in: *70th Int. Astronaut.*
 42 *Congr.*, 2019: pp. 1–8.
- 43 [24] T. Usui, K. ichi Bajo, W. Fujiya, Y. Furukawa, M. Koike, Y.N. Miura, H. Sugahara, S.
 44 Tachibana, Y. Takano, K. Kuramoto, The Importance of Phobos Sample Return for
 45 Understanding the Mars-Moon System, *Space Sci. Rev.* 216 (2020) 49.
- 46 [25] C.B. Phillips, K.P. Hand, M.L. Cable, A.E. Hofmann, K.L. Craft, Updates on the Europa
 47 Lander Mission Concept, in: *50th Lunar Planet. Sci. Conf.*, The Woodlands (Texas), 2019:
 48 p. 2685. <https://doi.org/10.1130/abs/2018am-324050>.
- 49 [26] S.K. Sharma, J.N. Porter, A.K. Misra, T.E. Acosta-Maeda, S.M. Angel, C.P. McKay,

- 1 Standoff Raman spectroscopy for future Europa Lander missions, *J. Raman Spectrosc.*
2 51 (2020) 1782–1793. <https://doi.org/10.1002/jrs.5814>.
- 3 [27] N. Tallarida, J. Lambert, A. Wang, Fluorescence mitigation using the Compact Integrated
4 Raman Spectrometer (CIRS) for in situ analysis of minerals and organics, in: 49th Lunar
5 Planet. Sci. Conf. 2018, 2018: p. 2779.pdf.
- 6 [28] M. Veneranda, J.A. Manrique-Martinez, G. Lopez-Reyes, J. Medina, I. Torre-Fdez, K.
7 Castro, J.M. Madariaga, C. Lantz, F. Poulet, A.M. Krzesińska, H. Hellevang, S.C. Werner,
8 F. Rull, Spectroscopic study of olivine-bearing rocks and its relevance to the ExoMars
9 rover mission, *Spectrochim. Acta - Part A Mol. Biomol. Spectrosc.* 223 (2019) 117360.
10 <https://doi.org/10.1016/j.saa.2019.117360>.
- 11 [29] M. Veneranda, G. Lopez-Reyes, J.A. Manrique, J. Medina, P. Ruiz-Galende, I. Torre-Fdez,
12 K. Castro, C. Lantz, F. Poulet, H. Dypvik, S.C. Werner, F. Rull, ExoMars raman laser
13 spectrometer: A tool for the potential recognition of wet-target craters on mars,
14 *Astrobiology.* 20 (2020) 349–363. <https://doi.org/10.1089/ast.2019.2095>.
- 15 [30] M. Veneranda, G. Lopez-Reyes, E.P. Sanchez, A.M. Krzesińska, J.A. Manrique-Martinez,
16 A. Sanz-Arran, C. Lantz, E. Lalla, A. Moral, J. Medina, F. Poulet, H. Dypvik, S.C. Werner,
17 J.L. Vago, F. Rull, ExoMars Raman Laser Spectrometer (RLS): a tool to semi-quantify the
18 serpentinization degree of olivine-rich rocks on Mars, *Astrobiology.* (2020) (under
19 press).
- 20 [31] K.A. Warren-Rhodes, K.C. Lee, S.D.J. Archer, N. Cabrol, L. Ng-Boyle, D. Wettergreen, K.
21 Zacny, S.B. Pointing, Subsurface microbial habitats in an extreme desert Mars-analog
22 environment, *Front. Microbiol.* 10 (2019) 1–11.
23 <https://doi.org/10.3389/fmicb.2019.00069>.
- 24 [32] A.G. Fairén, A.F. Davila, D. Lim, N. Bramall, R. Bonaccorsi, J. Zavaleta, E.R. Uceda, C.
25 Stoker, J. Wierzbos, J.M. Dohm, R. Amils, D. Andersen, C.P. McKay, *Astrobiology*
26 through the ages of Mars: The study of terrestrial analogues to understand the
27 habitability of Mars, *Astrobiology.* 10 (2010) 821–843.
28 <https://doi.org/10.1089/ast.2009.0440>.
- 29 [33] G. Lopez-Reyes, F. Rull, G. Venegas, F. Westall, F. Foucher, N. Bost, A. Sanz, A. Catalá-
30 Espí, A. Vegas, I. Hermosilla, A. Sansano, J. Medina, Analysis of the scientific capabilities
31 of the ExoMars Raman laser spectrometer instrument, *Eur. J. Mineral.* 25 (2013) 721–
32 733. <https://doi.org/10.1127/0935-1221/2013/0025-2317>.
- 33 [34] G. Lopez-Reyes, M. Veneranda, A.G. Martín, J.A. Manrique, A. Moral, C. Perez-Canora,
34 J.A.R. Prieto, A. Sanz-Arranz, J. Saiz, E. Lalla, M. Konstantinidis, O.P. Ballesteros, J.
35 Medina, L.M.N. Calzada, F. Rull, RLS Sim: a heavy-duty Raman tool for ground testing on
36 ExoMars, *J. Raman Spectrosc.* This issue (2021).
- 37 [35] M. Veneranda, G. Lopez-Reyes, J. Saiz, J.A. Manrique-Martinez, A. Sanz-Arranz, J.
38 Medina, A. Moral, L. Seoane, S. Ibarria, F. Rull, ExoFiT trial at the Atacama Desert
39 (Chile): Raman detection of biomarkers by representative prototypes of the
40 ExoMars/Raman Laser Spectrometer, *Sci. Rep.* 11 (2021) 1461.
41 <https://doi.org/10.1038/s41598-021-81014-z>.
- 42 [36] M. Veneranda, J. Saiz, G. Lopez-reyes, J.A. Manrique, A. Sanz, C. Garcia-prieto, S.C.
43 Werner, A. Moral, J.M. Madariaga, F. Rull, PTAL , ADAMM and SpectPro : novel tools to
44 support ExoMars and Mars 2020 science operations, in: *Eur. Sci. Congr., Virtual, 2020*.
- 45 [37] J.L. Bishop, Hydrothermal alteration products as key to formation of duricrust and rock
46 coating on Mars, in: *Lunar Planet. Sci.* XXX, 1999: p. 1887.pdf.

- 1 [38] B.M. Jakosky, Martian exobiology: Introduction, *J. Geophys. Res. Planets.* 102 (1997)
2 23673–23674. <https://doi.org/10.1029/97je01997>.
- 3 [39] M.L. Urquhart, V. Gulick, Lander detection and identification of hydrothermal deposits,
4 in: *First Land. Site Work. MER 2003, 2003*: p. 9031.pdf.
- 5 [40] J.D. Farmer, Hydrothermal systems: Doorways to early biosphere evolution, *GSA Today.*
6 10 (2000) 1–9.
- 7 [41] J. Martinez-Frias, R. Lunar, J.A. Rodriguez-Losada, A. Delgado, F. Rull, The volcanism-
8 related multistage hydrothermal system of El Jaroso (SE Spain), *Earth, Planets Sp.* 56
9 (2004) v--viii.
- 10 [42] J. Martinez Frias, Sulphide and sulphosalt mineralogy and paragenesis from the Sierra
11 Almagrera veins, Betic Cordillera (SE Spain), *Estud. Geol.* 47 (1991) 271–279.
12 <https://doi.org/10.3989/egeol.91475-6423>.
- 13 [43] A.M. Negrodo, P. Bird, C. Sanz de Galdeano, E. Buforn, Neotectonic modeling of the
14 Ibero-Maghrebian region, *J. Geophys. Res. Solid Earth.* 107 (2002) ETG 10-1-ETG 10-15.
15 <https://doi.org/10.1029/2001jb000743>.
- 16 [44] J. Martínez-Frías, An ancient Ba-Sb-Ag-Fe-Hg-bearing hydrothermal system in SE Spain,
17 *Episodes.* 21 (1998) 248–251. <https://doi.org/10.18814/epiugs/1998/v21i4/006>.
- 18 [45] G. Klingelhöfer, R. V. Morris, B. Bernhardt, C. Schröder, D.S. Rodionov, P.A. De Souza, A.
19 Yen, R. Gellert, E.N. Evlanov, B. Zubkov, J. Foh, U. Bonnes, E. Kankleit, P. Gütlich, D.W.
20 Ming, F. Renz, T. Wdowiak, S.W. Squyres, R.E. Arvidson, Jarosite and hematite at
21 Meridiani Planum from opportunity's Mössbauer spectrometer, *Science (80-)*. 306
22 (2004) 1740–1745. <https://doi.org/10.1126/science.1104653>.
- 23 [46] G. Klingelhöfer, R. V. Morris, B. Bernhardt, D. Rodionov, P.A. de Souza, S.W. Squyres, J.
24 Foh, E. Kankleit, U. Bonnes, R. Gellert, C. Schröder, S. Linkin, E. Evlanov, B. Zubkov, O.
25 Prilutski, Athena MIMOS II Mössbauer spectrometer investigation, *J. Geophys. Res. E*
26 *Planets.* 108 (2003). <https://doi.org/10.1029/2003je002138>.
- 27 [47] F. Rull, I. Fleischer, J. Martinez-Frias, A. Sanz, C. Upadhyay, G. Klingelhöfer, Raman and
28 Mössbauer Spectroscopic Characterisation of Sulfate Minerals From the Mars Analogue
29 Sites At Rio Tinto and Jaroso Ravine, Spain., *Lunar Planet. Sci.* XXXIX. (2008) 4–5.
- 30 [48] F. Rull, G. Klingelhöfer, J. Martinez-Frias, I. Fleischer, J. Medina, A. Sansano, IN-SITU
31 RAMAN, LIBS AND MÖSSBAUER SPECTROSCOPY OF SURFACE MINERALS AT JAROSO
32 RAVINE AND RELATED AREAS IN SIERRA ALMAGRERA (ALMERIA-SPAIN), in: *41st Lunar*
33 *Planet. Sci. Conf.*, 2010: p. 2736.pdf.
- 34 [49] F. Rull, G. Klingelhöfer, RAMAN-LIBS and Mössbauer spectroscopic study of alteration
35 minerals from the Mars analogue Jaroso Ravine (Spain), in: *Eur. Planet. Sci. Congr.*
36 2010, 2010: p. 845.
- 37 [50] M.Y. Zolotov, E.L. Shock, Formation of jarosite-bearing deposits through aqueous
38 oxidation of pyrite at Meridiani Planum, Mars, *Geophys. Res. Lett.* 32 (2005) 1–5.
39 <https://doi.org/10.1029/2005GL024253>.
- 40 [51] H. Wang, J.M. Bigham, O.H. Tuovinen, Formation of schwertmannite and its
41 transformation to jarosite in the presence of acidophilic iron-oxidizing microorganisms,
42 *Mater. Sci. Eng. C.* 26 (2006) 588–592. <https://doi.org/10.1016/j.msec.2005.04.009>.
- 43 [52] G. Amaral, J. Martinez-Frias, L. Vazquez, Astrobiological significance of minerals on
44 Mars surface environment: UV-shielding properties of Fe (jarosite) vs. Ca (gypsum)
45 sulphates, *Rev. Environ. Sci. Biotechnol.* 5 (2006) 219–231.

- 1 <http://arxiv.org/abs/physics/0512140>.
- 2 [53] G. Venegas del Valle, J. Martínez-Frías, J. Medina, A. Sansano, A. Sanz-Arranz, R.
3 Navarro-Azor, F. Rull, Caracterización Mineralógica de la Alteración Supergénica de El
4 Jaroso Mediante Espectroscopía Raman, *Rev. La Soc. Española Mineral.* 13 (2010) 223–
5 224.
- 6 [54] R.L. Frost, M. Weier, J. Martinez-Frias, F. Rull, B. Jagannadha Reddy, Sulphate
7 efflorescent minerals from El Jaroso Ravine, Sierra Almagrera-An SEM and Raman
8 spectroscopic study, *Spectrochim. Acta - Part A Mol. Biomol. Spectrosc.* 66 (2007) 177–
9 183. <https://doi.org/10.1016/j.saa.2006.01.054>.
- 10 [55] F. Rull, Raman-LIBS: un Espectrómetro Combinado para el Estudio Mineralógico y
11 Geoquímico de Marte dentro de la Misión ExoMars, *Rev. La Soc. Española Mineral.* 9
12 (2008) 225–226.
- 13 [56] S. Maurice, S.M. Clegg, R.C. Wiens, O. Gasnault, W. Rapin, O. Forni, A. Cousin, V.
14 Sautter, N. Mangold, L. Le Deit, M. Nachon, R.B. Anderson, N.L. Lanza, C. Fabre, V.
15 Payré, J. Lasue, P.Y. Meslin, R.J. Léveillé, B.L. Barraclough, P. Beck, S.C. Bender, G.
16 Berger, J.C. Bridges, N.T. Bridges, G. Dromart, M.D. Dyar, R. Francis, J. Frydenvang, B.
17 Gondet, B.L. Ehlmann, K.E. Herkenhoff, J.R. Johnson, Y. Langevin, M.B. Madsen, N.
18 Melikechi, J.L. Lacour, S. Le Mouélic, E. Lewin, H.E. Newsom, A.M. Ollila, P. Pinet, S.
19 Schröder, J.B. Sirven, R.L. Tokar, M.J. Toplis, C. D'Uston, D.T. Vaniman, A.R. Vasavada,
20 ChemCam activities and discoveries during the nominal mission of the Mars Science
21 Laboratory in Gale crater, Mars, *J. Anal. At. Spectrom.* 31 (2016) 863–889.
22 <https://doi.org/10.1039/c5ja00417a>.
- 23 [57] R.L. Frost, D.L. Wain, B.J. Reddy, W. Martens, J. Martinez-Frias, F. Rull, Sulphate
24 efflorescent minerals from the El Jaroso ravine, Sierra Almagrera, Spain - A scanning
25 electron microscopic and infrared spectroscopic study, *J. Near Infrared Spectrosc.* 14
26 (2006) 167–178. <https://doi.org/10.1255/jnirs.612>.
- 27 [58] R.L. Frost, D. Wain, W.N. Martens, A.C. Locke, J. Martinez-Frias, F. Rull, Thermal
28 decomposition and X-ray diffraction of sulphate efflorescent minerals from El Jaroso
29 Ravine, Sierra Almagrera, Spain, *Thermochim. Acta.* 460 (2007) 9–14.
30 <https://doi.org/10.1016/j.tca.2007.05.011>.
- 31 [59] J. Martínez-Frías, A. Delgado-Huertas, F. García-Moreno, E. Reyes, R. Lunar, F. Rull,
32 Isotopic signatures of extinct low-temperature hydrothermal chimneys in the Jaroso
33 Mars analog, *Planet. Space Sci.* 55 (2007) 441–448.
34 <https://doi.org/10.1016/j.pss.2006.09.004>.
- 35 [60] R. Amils, E. González-Toril, D. Fernández-Remolar, F. Gómez, Á. Aguilera, N. Rodríguez,
36 M. Malki, A. García-Moyano, A.G. Fairén, V. de la Fuente, J. Luis Sanz, Extreme
37 environments as Mars terrestrial analogs: The Rio Tinto case, *Planet. Space Sci.* 55
38 (2007) 370–381. <https://doi.org/10.1016/j.pss.2006.02.006>.
- 39 [61] R. Amils, D. Fernández-Remolar, V. Parro, J.A. Rodríguez-Manfredi, M. Oggerin, M.
40 Sánchez-Román, F.J. López, J.P. Fernández-Rodríguez, F. Puente-Sánchez, C. Briones, O.
41 Prieto-Ballesteros, F. Tornos, F. Gómez, M. García-Villadangos, N. Rodríguez, E.
42 Omoregie, K. Timmis, A. Arce, J.L. Sanz, D. Gómez-Ortiz, Río Tinto: A geochemical and
43 mineralogical terrestrial analogue of Mars, *Life.* 4 (2014) 511–534.
44 <https://doi.org/10.3390/life4030511>.
- 45 [62] A.I. López-Archilla, I. Marin, R. Amils, Microbial community composition and ecology of
46 an acidic aquatic environment: The Tinto River, Spain, *Microb. Ecol.* 41 (2001) 20–35.
47 <https://doi.org/10.1007/s002480000044>.

- 1 [63] I. Sánchez-Andrea, N. Rodríguez, R. Amils, J.L. Sanz, Microbial diversity in anaerobic
2 sediments at Río Tinto, a naturally acidic environment with a high heavy metal content,
3 *Appl. Environ. Microbiol.* 77 (2011) 6085–6093. [https://doi.org/10.1128/AEM.00654-](https://doi.org/10.1128/AEM.00654-11)
4 11.
- 5 [64] I. Fleischer, G. Klingelhöfer, F. Rull, S. Wehrheim, S. Ebert, M. Panthöfer, M. Blumers, D.
6 Schmanke, J. Maul, C. Schröder, In-situ Mössbauer spectroscopy with MIMOS II at Río
7 Tinto, Spain, *J. Phys. Conf. Ser.* 217 (2010). [https://doi.org/10.1088/1742-](https://doi.org/10.1088/1742-6596/217/1/012062)
8 6596/217/1/012062.
- 9 [65] P. Sobron, A. Sanz, T. Acosta, F. Rull, A Raman spectral study of stream waters and
10 efflorescent salts in Río Tinto, Spain, *Spectrochim. Acta - Part A Mol. Biomol. Spectrosc.*
11 71 (2009) 1678–1682. <https://doi.org/10.1016/j.saa.2008.06.035>.
- 12 [66] F. Rull, J. Martínez-Frías, J. Medina, Surface mineral analysis from two possible Martian
13 analogs (Río Tinto and Jaroso Ravine , Spain) using micro- , macro- , and remote laser
14 Raman spectroscopy, *Geophys. Res. Abstr.* 7 (2005) 09114.
- 15 [67] P. Sobron, J.L. Bishop, D.F. Blake, B. Chen, F. Rull, Natural Fe-bearing oxides and sulfates
16 from the Río Tinto Mars analog site: Critical assessment of VNIR reflectance
17 spectroscopy, laser Raman spectroscopy, and XRD as mineral identification tools, *Am.*
18 *Mineral.* 99 (2014) 1199–1205. <https://doi.org/10.2138/am.2014.4595>.
- 19 [68] J. Guerrero-Fernández, R. Navarro-Azor, J. Medina, A. Sansano, A. Sanz-Arranz, J.
20 Martínez-Frías, F. Rull, Caracterización mediante Espectroscopía Raman y LIBS de la
21 Composición Geoquímica del Nacimiento del Río Tinto, *Rev. La Soc. Española Mineral.*
22 13 (2010) 119–120.
- 23 [69] F. Rull, J. Guerrero, G. Venegas, F. Gázquez, J. Medina, Spectroscopic Raman study of
24 sulphate precipitation sequence in Río Tinto mining district (SW Spain), *Environ. Sci.*
25 *Pollut. Res.* 21 (2014) 6783–6792. <https://doi.org/10.1007/s11356-013-1927-z>.
- 26 [70] G. Venegas, J. Guerrero, A. Sansato, A. Sanz, F. Rull, Raman study of mineralogical
27 precipitation sequence of Río Tinto “Mars analog,” *Eur. Planet. Sci. Congr.* 2012. 7
28 (2012).
- 29 [71] F. Rull, F. Sobrón, J. Guerrero, J. Medina, G. Venegas, F. Gázquez, J. Martínez-Frías, In-
30 situ raman analysis of the precipitation sequence of sulphate minerals using small
31 droplets: Application to Río Tinto (Spain), *Lect. Notes Earth Syst. Sci.* (2014) 801–805.
32 https://doi.org/10.1007/978-3-642-32408-6_173.
- 33 [72] H.G.M. Edwards, P. Vandenabeele, S.E. Jorge-Villar, E.A. Carter, F.R. Perez, M.D.
34 Hargreaves, The Río Tinto Mars Analogue site: An extremophilic Raman spectroscopic
35 study, *Spectrochim. Acta - Part A Mol. Biomol. Spectrosc.* 68 (2007) 1133–1137.
36 <https://doi.org/10.1016/j.saa.2006.12.080>.
- 37 [73] M. López-Martínez, D. York, J.A. Hanes, A $4^{\circ} \text{Ar} / 39\text{Ar}$ geochronological study of
38 komatiites and komatiitic basalts from the Lower Onverwacht Volcanics : Barberton
39 Mountain Land, South Africa, *Precambrian Res.* 57 (1992) 91–119.
- 40 [74] C.E.J. de Ronde, M.J. de Wit, Tectonic history of the Barberton greenstone belt, South
41 Africa: 490 million years of Archean crustal evolution, *Tectonics.* 13 (1994) 983–1005.
42 <https://doi.org/10.1029/94TC00353>.
- 43 [75] H. Furnes, M. de Wit, B. Robins, A review of new interpretations of the
44 tectonostratigraphy, geochemistry and evolution of the Onverwacht Suite, Barberton
45 Greenstone Belt, South Africa, *Gondwana Res.* 23 (2013) 403–428.
46 <https://doi.org/10.1016/j.gr.2012.05.007>.

- 1 [76] D. Nna-Mvondo, J. Martinez-Frias, Review komatiites: From Earth's geological settings
2 to planetary and astrobiological contexts, *Earth, Moon Planets.* 100 (2007) 157–179.
3 <https://doi.org/10.1007/s11038-007-9135-9>.
- 4 [77] A. Maturilli, J. Helbert, J.M. St. John, J.W. Head, W.M. Vaughan, M. D'Amore, M.
5 Gottschalk, S. Ferrari, Komatiites as Mercury surface analogues: Spectral measurements
6 at PEL, *Earth Planet. Sci. Lett.* 398 (2014) 58–65.
7 <https://doi.org/10.1016/j.epsl.2014.04.035>.
- 8 [78] N. Bost, F. Westall, F. Gaillard, C. Ramboz, F. Foucher, Synthesis of a spinifex-textured
9 basalt as an analog to Gusev crater basalts, Mars, *Meteorit. Planet. Sci.* 47 (2012) 820–
10 831. <https://doi.org/10.1111/j.1945-5100.2012.01355.x>.
- 11 [79] M. Shore, A.D. Fowler, The origin of spinifex texture in komatiites, *Nature.* 397 (1999)
12 691–694. <https://doi.org/10.1038/17794>.
- 13 [80] S.W. Parman, T.L. Grove, J.C. Dann, The production of Barberton komatiites in an
14 Archean subduction zone, *Geophys. Res. Lett.* 28 (2001) 2513–2516.
15 <https://doi.org/10.1029/2000GL012713>.
- 16 [81] I.S. Puchtel, J. Blichert-Toft, M. Touboul, R.J. Walker, G.R. Byerly, E.G. Nisbet, C.R.
17 Anhaeusser, Insights into early Earth from Barberton komatiites: Evidence from
18 lithophile isotope and trace element systematics, *Geochim. Cosmochim. Acta.* 108
19 (2013) 63–90. <https://doi.org/10.1016/j.gca.2013.01.016>.
- 20 [82] N. Bost, C. Ramboz, N. Le Breton, G. Lopez Reyes, C. Pilorget, S. De Angelis, F. Foucher,
21 F. Westall, A Blind Test to test the future ExoMars instruments, *Eur. Planet. Sci. Congr.*
22 2013, Held 8-13 Sept. London, UK. Online [Http//Meetings. Copernicus. Org/Epsc2013](http://Meetings.Copernicus.Org/Epsc2013),
23 Id. EPSC2013-662. 8 (2013) 3–4.
- 24 [83] M. Veneranda, G. Lopez-Reyes, E. Pascual Sanchez, A.M. Krzesińska, J.A. Manrique-
25 Martinez, A. Sanz-Arranz, C. Lantz, E. Lalla, A. Moral, J. Medina, F. Poulet, H. Dypvik, S.C.
26 Werner, J.L. Vago, F. Rull, ExoMars Raman Laser Spectrometer: A Tool to Semiquantify
27 the Serpentinization Degree of Olivine-Rich Rocks on Mars, *Astrobiology.* 21 (2021)
28 307–322. <https://doi.org/10.1089/ast.2020.2265>.
- 29 [84] O. Müntener, Serpentine and serpentinization: A link between planet formation and
30 life, *Geology.* 38 (2010) 959–960. <https://doi.org/10.1130/focus102010.1>.
- 31 [85] M. Ledevin, N. Arndt, C. Chauvel, E. Jaillard, A. Simionovici, The sedimentary origin of
32 black and white banded cherts of the Buck Reef, Barberton, South Africa, *Geosciences.*
33 9 (2019) 424. <https://doi.org/10.3390/geosciences9100424>.
- 34 [86] F. Westall, D. Gerneke, <title>Electron microscope methods in the search for the
35 earliest life forms on Earth (in 3.5-3.3 Ga cherts from the Barberton greenstone belt,
36 South Africa): applications for extraterrestrial life studies</title>, *Instruments,*
37 *Methods, Mission. Astrobiol.* 3441 (1998) 158–169. <https://doi.org/10.1117/12.319833>.
- 38 [87] F. Westall, M.J. De Wit, J. Dann, S. Van der Gaast, C.E.J. De Ronde, D. Gerneke, Early
39 archean fossil bacteria and biofilms in hydrothermally-influenced sediments from the
40 Barberton greenstone belt, South Africa, *Precambrian Res.* 106 (2001) 93–116.
41 [https://doi.org/10.1016/S0301-9268\(00\)00127-3](https://doi.org/10.1016/S0301-9268(00)00127-3).
- 42 [88] F. Westall, B. Hofmann, A. Brack, The search for life on mars using macroscopically
43 visible microbial mats (stromatolites) in 3.5-3.3 Ga cherts from the Pilbara in Australia
44 and Barberton in South Africa as analogues., *Lunar Planet. Sci.* XXXV. (2004) Abstract
45 1077.
- 46 [89] F. Westall, C.E.J. De Ronde, G. Southam, N. Grassineau, M. Colas, C. Cockell, H. Lammer,

- 1 Implications of a 3.472-3.333 Gyr-old subaerial microbial mat from the Barberton
 2 greenstone belt, South Africa for the UV environmental conditions on the early Earth,
 3 *Philos. Trans. R. Soc. B Biol. Sci.* 361 (2006) 1857–1875.
 4 <https://doi.org/10.1098/rstb.2006.1896>.
- 5 [90] F. Westall, B. Cavalazzi, L. Lemelle, Y. Marrocchi, J.N. Rouzaud, A. Simionovici, M.
 6 Salomé, S. Mostefaoui, C. Andreazza, F. Foucher, J. Toporski, A. Jauss, V. Thiel, G.
 7 Southam, L. MacLean, S. Wirick, A. Hofmann, A. Meibom, F. Robert, C. Défarge,
 8 Implications of in situ calcification for photosynthesis in a ~3.3Ga-old microbial biofilm
 9 from the Barberton greenstone belt, South Africa, *Earth Planet. Sci. Lett.* 310 (2011)
 10 468–479. <https://doi.org/10.1016/j.epsl.2011.08.029>.
- 11 [91] D. Gourier, L. Binet, T. Calligaro, S. Cappelli, H. Vezin, J. Bréhéret, K. Hickman-Lewis, P.
 12 Gautret, F. Foucher, K. Campbell, F. Westall, Extraterrestrial organic matter preserved
 13 in 3.33 Ga sediments from Barberton, South Africa, *Geochim. Cosmochim. Acta.* 258
 14 (2019) 207–225. <https://doi.org/10.1016/j.gca.2019.05.009>.
- 15 [92] F. Rull, J. Medina, G. Benegas, E. Lalla, R. Navarro, A. Sanz, A mineralogical
 16 characterization of materials from Pongola Supergroup and Barberton Greenstone Belt
 17 using XRD, IR and microRaman techniques, in: *Geobiol. Sp. Explor.*, 2011.
- 18 [93] F. Rull, G. Venegas, O. Montero, J. Medina, Study of Carbonaceous Material in cherts
 19 from Barberton Greenstone Belt and the Astrobiological Implications ., in: *Geophys.*
 20 *Res. Abstr.*, 2012: p. 7002.
- 21 [94] F. Foucher, G. Lopez-Reyes, N. Bost, F. Rull-Perez, P. Rößmann, F. Westall, Effect of
 22 grain size distribution on Raman analyses and the consequences for in situ planetary
 23 missions, *J. Raman Spectrosc.* 44 (2013) 916–925. <https://doi.org/10.1002/jrs.4307>.
- 24 [95] J.L. Vago, F. Westall, A.J. Coates, R. Jaumann, O. Korablev, V. Ciarletti, I. Mitrofanov, J.L.
 25 Josset, M.C. De Sanctis, J.P. Bibring, F. Rull, F. Goesmann, H. Steininger, W. Goetz, W.
 26 Brinckerhoff, C. Szopa, F. Raulin, H.G.M. Edwards, L.G. Whyte, A.G. Fairén, J. Bridges, E.
 27 Hauber, G.G. Ori, S. Werner, D. Loizeau, R.O. Kuzmin, R.M.E. Williams, J. Flahaut, F.
 28 Forget, D. Rodionov, H. Svedhem, E. Sefton-Nash, G. Kminek, L. Lorenzoni, L. Joudrier,
 29 V. Mikhailov, A. Zashchirinskiy, S. Alexashkin, F. Calantropio, A. Merlo, P. Poulakis, O.
 30 Witasse, O. Bayle, S. Bayón, U. Meierhenrich, J. Carter, J.M. García-Ruiz, P. Baglioni, A.
 31 Haldemann, A.J. Ball, A. Debus, R. Lindner, F. Haessig, D. Monteiro, R. Trautner, C.
 32 Volland, P. Rebeyre, D. Gouly, F. Didot, S. Durrant, E. Zekri, D. Koschny, A. Toni, G.
 33 Visentin, M. Zwick, M. Van Winnendael, M. Azkarate, C. Carreau, Habitability on Early
 34 Mars and the Search for Biosignatures with the ExoMars Rover, *Astrobiology.* 17 (2017)
 35 471–510. <https://doi.org/10.1089/ast.2016.1533>.
- 36 [96] L. Xiao, J. Huang, P.R. Christensen, R. Greeley, D.A. Williams, J. Zhao, Q. He, Ancient
 37 volcanism and its implication for thermal evolution of Mars, *Earth Planet. Sci. Lett.* 323–
 38 324 (2012) 9–18. <https://doi.org/10.1016/j.epsl.2012.01.027>.
- 39 [97] L.D. Graham, R. V. Morris, T.G. Graff, R.A. Yingst, I.L. Ten Kate, D.P. Glavin, M. Hedlund,
 40 C.A. Malespin, E. Mumm, Moon and mars analog mission activities for mauna kea 2012,
 41 in: *IEEE Aerosp. Conf. Proc.*, 2013. <https://doi.org/10.1109/AERO.2013.6497195>.
- 42 [98] E.A. Lalla, A. Sanz-Arranz, G. Lopez-Reyes, A. Sansano, J. Medina, D. Schmanke, G.
 43 Klingelhofer, J.A. Rodríguez-Losada, J. Martínez-Frías, F. Rull, Raman-Mössbauer-XRD
 44 studies of selected samples from “los Azulejos” outcrop: A possible analogue for
 45 assessing the alteration processes on Mars, *Adv. Sp. Res.* 57 (2016) 2385–2395.
 46 <https://doi.org/10.1016/j.asr.2016.03.014>.
- 47 [99] E.A. Lalla, A. Sanz-Arranz, G. Lopez-Reyes, A. Sansano, J. Medina, D. Schmanke, G.

- 1 Klingelhofer, J.A. Rodríguez-Losada, J. Martínez-Frías, F. Rull, Raman-Mössbauer-XRD
2 studies of selected samples from “los Azulejos” outcrop: A possible analogue for
3 assessing the alteration processes on Mars, *Adv. Sp. Res.* 57 (2016) 2385–2395.
4 <https://doi.org/10.1016/j.asr.2016.03.014>.
- 5 [100] E. Lalla, A. Sansano, A. Sanz-Arranz, P. Alonso-Alonso, J. Medina, J. Martínez-Frías, F.
6 Rull, Espectroscopía Raman de Basaltos Correspondientes al Volcán de Las Arenas,
7 Tenerife, *Rev. La Soc. Española Mineral.* 13 (2010) 129–130.
- 8 [101] F.R. Rull, G. Klingelhofer, J. Martinez Frias, J.A. Rodriguez, J. Medina, E. Lalla, A
9 Combined Raman and Mössbauer Analysis of Atered Basalts in Tenerife Island:
10 Analogies with Mars, *Publ. 43rd Lunar Planet. Sci. Conf. Held March 19--23, 2012*
11 *Woodlands, Texas. LPI Contrib. No. 1659, Id.2882.* (2012).
- 12 [102] J.R. Michalski, E.Z.N. Dobreá, P.B. Niles, J. Cuadros, Ancient hydrothermal seafloor
13 deposits in Eridania basin on Mars, *Nat. Commun.* 8 (2017) 1–10.
14 <https://doi.org/10.1038/ncomms15978>.
- 15 [103] R. Greeley, Release of Juvenile Water on Mars : Estimated Amounts and Timing
16 Associated Volcanism, *Reports.* (1987) 1653–1654.
- 17 [104] E.A. Lalla, G. López-Reyes, A. Sansano, A. Sanz-Arranz, D. Schmanke, G. Klingelhofer, J.
18 Medina-García, J. Martínez-Frías, F. Rull-Pérez, Estudio espectroscópico y DRX de
19 afloramientos terrestres volcánicos en la isla de Tenerife como posibles análogos de la
20 geología marciana, *Estud. Geol.* 71 (2015). <https://doi.org/10.3989/egeol.41927.354>.
- 21 [105] K.H. Williford, K.A. Farley, K.M. Stack, A.C. Allwood, D. Beaty, L.W. Beegle, R. Bhartia,
22 A.J. Brown, M. de la Torre Juarez, S.-E. Hamran, M.H. Hecht, J.A. Hurowitz, J.A.
23 Rodríguez-Manfredi, S. Maurice, S. Milkovich, R.C. Wiens, *The NASA Mars 2020 Rover*
24 *Mission and the Search for Extraterrestrial Life*, 1 st, Elsevier Inc., Amsterdam, 2018.
25 <https://doi.org/10.1016/b978-0-12-809935-3.00010-4>.
- 26 [106] E.A. Lalla, A. Sanz-Arranz, G. Lopez-Reyes, M. Konstantinidis, M. Veneranda, R.
27 Aquilano, F. Rull, M. Aznar, J. Medina, J. Martínez-Frías, Estudio Mineralógico Mediante
28 Técnicas Espectroscópicas (Raman-Ftir-Drx-Frx) De Muestras Volcánicas De La Zona De
29 Chamorga (Tenerife, España), *Rev. La Soc. Geológica España.* 33 (2020) 71–93.
- 30 [107] B.L. Ehlmann, J.F. Mustard, R.N. Clark, G.A. Swayze, S.L. Murchie, Evidence for low-
31 grade metamorphism, hydrothermal alteration, and diagenesis on mars from
32 phyllosilicate mineral assemblages, *Clays Clay Miner.* 59 (2011) 359–377.
33 <https://doi.org/10.1346/CCMN.2011.0590402>.
- 34 [108] E.A. Lalla, G. Lopez-Reyes, A.D. Lozano-Gorrín, F. Rull, Combined vibrational, structural,
35 elemental and Mössbauer spectroscopic analysis of natural phillipsite (zeolite) from
36 historical eruptions in Tenerife, Canary Islands: Implication for Mars, *Vib. Spectrosc.* 101
37 (2019) 10–19. <https://doi.org/10.1016/j.vibspec.2018.12.003>.
- 38 [109] J.F. Mustard, F. Poulet, A. Gendrin, J.P. Bibring, Y. Langevin, B. Gondet, N. Mangold, G.
39 Bellucci, F. Altieri, Olivine and pyroxene diversity in the crust of Mars, *Science* (80-.).
40 307 (2005) 1594–1597. <https://doi.org/10.1126/science.1109098>.
- 41 [110] S.M. Pelkey, J.F. Mustard, S. Murchie, R.T. Clancy, M. Wolff, M. Smith, R.E. Milliken, J.P.
42 Bibring, A. Gendrin, F. Poulet, Y. Langevin, B. Gondet, CRISM multispectral summary
43 products: Parameterizing mineral diversity on Mars from reflectance, *J. Geophys. Res. E*
44 *Planets.* 112 (2007) 1–18. <https://doi.org/10.1029/2006JE002831>.
- 45 [111] E.S. Amador, J.L. Bandfield, N.H. Thomas, A search for minerals associated with
46 serpentinization across Mars using CRISM spectral data, *Icarus.* 311 (2018) 113–134.

- 1 <https://doi.org/10.1016/j.icarus.2018.03.021>.
- 2 [112] L. Riu, F. Poulet, J.P. Bibring, B. Gondet, The M3 project: 2 - Global distributions of mafic
3 mineral abundances on Mars, *Icarus*. 322 (2019) 31–53.
4 <https://doi.org/10.1016/j.icarus.2019.01.002>.
- 5 [113] R.E. Arvidson, S.W. Squyres, R.C. Anderson, J.F. Bell, D. Blaney, J. Brückner, N.A. Cabrol,
6 W.M. Calvin, M.H. Carr, P.R. Christensen, B.C. Clark, L. Crumpler, D.J. Des Marais, J.A. de
7 Souza, C. d’Uston, T. Economou, J. Farmer, W.H. Farrand, W. Folkner, M.P. Golombek,
8 S. Gorevan, J.A. Grant, R. Greeley, J. Grotzinger, E. Guinness, B.C. Hahn, L. Haskin, K.E.
9 Herkenhoff, J.A. Hurowitz, S. Hviid, J.R. Johnson, G. Klingelhöfer, A.H. Knoll, G. Landis, C.
10 Leff, M. Lemmon, R. Li, M.B. Madsen, M.C. Malin, S.M. McLennan, H.Y. McSween, D.W.
11 Ming, J. Moersch, R. V. Morris, T. Parker, J.W. Rice, L. Richter, R. Rieder, D.S. Rodionov,
12 C. Schröder, M. Sims, M. Smith, P. Smith, L.A. Soderblom, R. Sullivan, S.D. Thompson,
13 N.J. Tosca, A. Wang, H. Wänke, J. Ward, T. Wdowiak, M. Wolff, A. Yen, Overview of the
14 Spirit Mars Exploration Rover Mission to Gusev Crater: Landing site to Backstay Rock in
15 the Columbia Hills, *J. Geophys. Res. E Planets*. 111 (2006) 1–22.
16 <https://doi.org/10.1029/2005JE002499>.
- 17 [114] D.F. Blake, R. V. Morris, G. Kocurek, S.M. Morrison, R.T. Downs, D. Bish, D.W. Ming, K.S.
18 Edgett, D. Rubin, W. Goetz, M.B. Madsen, R. Sullivan, R. Gellert, I. Campbell, A.H.
19 Treiman, S.M. McLennan, A.S. Yen, J. Grotzinger, D.T. Vaniman, S.J. Chipera, C.N.
20 Achilles, E.B. Rampe, D. Sumner, P.Y. Meslin, S. Maurice, O. Forni, O. Gasnault, M. Fisk,
21 M. Schmidt, P. Mahaffy, L.A. Leshin, D. Glavin, A. Steele, C. Freissinet, R. Navarro-
22 González, R.A. Yingst, L.C. Kah, N. Bridges, K.W. Lewis, T.F. Bristow, J.D. Farmer, J.A.
23 Crisp, E.M. Stolper, D.J. Des Marais, P. Sarrazin, Curiosity at Gale Crater, Mars:
24 Characterization and analysis of the rocknest sand shadow, *Science* (80-.). 341 (2013)
25 1–6. <https://doi.org/10.1126/science.1239505>.
- 26 [115] B.L. Ehlmann, K.S. Edgett, B. Sutter, C.N. Achilles, M.L. Litvak, M.G.A. Lapotre, R.
27 Sullivan, A.A. Fraeman, R.E. Arvidson, D.F. Blake, N.T. Bridges, P.G. Conrad, A. Cousin,
28 R.T. Downs, T.S.J. Gabriel, R. Gellert, V.E. Hamilton, C. Hardgrove, J.R. Johnson, S. Kuhn,
29 P.R. Mahaffy, S. Maurice, M. McHenry, P.Y. Meslin, D.W. Ming, M.E. Minitti, J.M.
30 Morookian, R. V. Morris, C.D. O’Connell-Cooper, P.C. Pinet, S.K. Rowland, S. Schröder,
31 K.L. Siebach, N.T. Stein, L.M. Thompson, D.T. Vaniman, A.R. Vasavada, D.F. Wellington,
32 R.C. Wiens, A.S. Yen, Chemistry, mineralogy, and grain properties at Namib and High
33 dunes, Bagnold dune field, Gale crater, Mars: A synthesis of Curiosity rover
34 observations, *J. Geophys. Res. Planets*. 122 (2017) 2510–2543.
35 <https://doi.org/10.1002/2017JE005267>.
- 36 [116] J.G. Blank, S.J. Green, D. Blake, J.W. Valley, N.T. Kita, A. Treiman, P.F. Dobson, An
37 alkaline spring system within the Del Puerto Ophiolite (California, USA): A Mars analog
38 site, *Planet. Space Sci.* 57 (2009) 533–540. <https://doi.org/10.1016/j.pss.2008.11.018>.
- 39 [117] N. Szponar, W.J. Brazelton, M.O. Schrenk, D.M. Bower, A. Steele, P.L. Morrill,
40 Geochemistry of a continental site of serpentinization, the Tablelands Ophiolite, Gros
41 Morne National Park: A Mars analogue, *Icarus*. 224 (2013) 286–296.
42 <https://doi.org/10.1016/j.icarus.2012.07.004>.
- 43 [118] R.N. Greenberger, J.F. Mustard, E.A. Cloutis, L.M. Pratt, P.E. Sauer, P. Mann, K. Turner,
44 M.D. Dyar, D.L. Bish, Serpentinization, iron oxidation, and aqueous conditions in an
45 ophiolite: Implications for hydrogen production and habitability on Mars, *Earth Planet.
46 Sci. Lett.* 416 (2015) 21–34. <https://doi.org/10.1016/j.epsl.2015.02.002>.
- 47 [119] M. Crespo-Medina, K.I. Twing, R. Sánchez-Murillo, W.J. Brazelton, T.M. McCollom, M.O.
48 Schrenk, Methane dynamics in a tropical serpentinizing environment: The Santa Elena

- 1 Ophiolite, Costa Rica, *Front. Microbiol.* 8 (2017) 1–14.
2 <https://doi.org/10.3389/fmicb.2017.00916>.
- 3 [120] B.L. Ehlmann, J.F. Mustard, S.L. Murchie, Geologic setting of serpentine deposits on
4 Mars, *Geophys. Res. Lett.* 37 (2010) L06201. <https://doi.org/10.1029/2010gl042596>.
- 5 [121] G.R. Dunning, R.B. Pedersen, U/Pb ages of ophiolites and arc-related plutons of the
6 Norwegian Caledonides: implications for the development of Iapetus, *Contrib. to*
7 *Mineral. Petrol.* 98 (1988) 13–23. <https://doi.org/10.1007/BF00371904>.
- 8 [122] S. Maaløe, The dunite bodies, websterite and orthopyroxenite dikes of the Leka
9 ophiolite complex, Norway, *Mineral. Petrol.* 85 (2005) 163–204.
10 <https://doi.org/10.1007/s00710-005-0085-5>.
- 11 [123] O. Plümpner, S. Piazzolo, H. Austrheim, Olivine pseudomorphs after serpentinized
12 orthopyroxene record transient oceanic lithospheric mantle dehydration (Leka
13 Ophiolite complex, Norway), *J. Petrol.* 53 (2012) 1943–1968.
14 <https://doi.org/10.1093/petrology/egs039>.
- 15 [124] B. O’Driscoll, R.J. Walker, J.M.D. Day, R.D. Ash, J.S. Daly, Generations of melt extraction,
16 melt-rock interaction and high-temperature metasomatism preserved in peridotites of
17 the ~497 Ma Leka Ophiolite Complex, Norway, *J. Petrol.* 56 (2015) 1797–1828.
18 <https://doi.org/10.1093/petrology/egv055>.
- 19 [125] A. Bjerga, J. Konopásek, R.B. Pedersen, Talc-carbonate alteration of ultramafic rocks
20 within the Leka Ophiolite Complex, Central Norway, *Lithos.* 227 (2015) 21–36.
21 <https://doi.org/10.1016/j.lithos.2015.03.016>.
- 22 [126] I. Torre-Fdez, J. Aramendia, L. Gomez-Nubla, K. Castro, J.M. Madariaga, Geochemical
23 study of the Northwest Africa 6148 Martian meteorite and its terrestrial weathering
24 processes, *J. Raman Spectrosc.* 48 (2017) 1536–1543. <https://doi.org/10.1002/jrs.5148>.
- 25 [127] S.P. Wright, P.R. Christensen, T.G. Sharp, Laboratory thermal emission spectroscopy of
26 shocked basalt from Lonar Crater, India, and implications for Mars orbital and sample
27 data, *J. Geophys. Res. E Planets.* 116 (2011) 1–18.
28 <https://doi.org/10.1029/2010JE003785>.
- 29 [128] T. Rhind, J. Ronholm, B. Berg, P. Mann, D. Applin, J. Stromberg, R. Sharma, L.G. Whyte,
30 E.A. Cloutis, Gypsum-hosted endolithic communities of the Lake St. Martin impact
31 structure, Manitoba, Canada: Spectroscopic detectability and implications for Mars, *Int.*
32 *J. Astrobiol.* 31 (2014) 366–377. <https://doi.org/10.1017/S1473550414000378>.
- 33 [129] C. Brolly, J. Parnell, S. Bowden, Raman spectroscopy of shocked gypsum from a
34 meteorite impact crater, *Int. J. Astrobiol.* 16 (2017) 286–292.
35 <https://doi.org/10.1017/S1473550416000367>.
- 36 [130] R. Li, B.A. Archinal, R.E. Arvidson, J. Bell, P. Christensen, L. Crumpler, D.J. Des Marais, K.
37 Di, T. Duxbury, M.P. Golombek, J.A. Grant, R. Greeley, J. Guinn, A. Johnson, R.L. Kirk, M.
38 Maimone, L.H. Matthies, M. Malin, T. Parker, M. Sims, S. Thompson, S.W. Squyres, L.A.
39 Soderblom, Spirit rover localization and topographic mapping at the landing site of
40 Gusev crater, Mars, *J. Geophys. Res. E Planets.* 111 (2006) 1–13.
41 <https://doi.org/10.1029/2005JE002483>.
- 42 [131] J.J. Wray, Gale crater: The Mars Science Laboratory/Curiosity rover landing site, *Int. J.*
43 *Astrobiol.* 12 (2013) 25–38. <https://doi.org/10.1017/S1473550412000328>.
- 44 [132] N. Mangold, G. Dromart, V. Ansan, F. Salese, M.G. Kleinhan, M. Massé, C. Quantin-
45 Nataf, K.M. Stack, Fluvial Regimes, Morphometry, and Age of Jezero Crater Paleolake
46 Inlet Valleys and Their Exobiological Significance for the 2020 Rover Mission Landing

- 1 Site, *Astrobiology*. 20 (2020) 994–1013. <https://doi.org/10.1089/ast.2019.2132>.
- 2 [133] J.W. Horton, J. Ormö, D.S. Powars, G.S. Gohn, Chesapeake Bay impact structure:
3 Morphology, crater fill, and relevance for impact structures on Mars, *Meteorit. Planet.*
4 *Sci.* 41 (2006) 1613–1624. <https://doi.org/10.1111/j.1945-5100.2006.tb00439.x>.
- 5 [134] W.E. Sanford, A simulation of the hydrothermal response to the Chesapeake Bay bolide
6 impact, *Geofluids*. 5 (2005) 185–201. [https://doi.org/10.1111/j.1468-](https://doi.org/10.1111/j.1468-8123.2005.00110.x)
7 [8123.2005.00110.x](https://doi.org/10.1111/j.1468-8123.2005.00110.x).
- 8 [135] M.S. Dodd, D. Papineau, T. Grenne, J.F. Slack, M. Rittner, F. Pirajno, J. O’Neil, C.T.S.
9 Little, Evidence for early life in Earth’s oldest hydrothermal vent precipitates, *Nature*.
10 543 (2017) 60–64. <https://doi.org/10.1038/nature21377>.
- 11 [136] J.A.P. Rodriguez, S. Sasaki, R.O. Kuzmin, J.M. Dohm, K.L. Tanaka, H. Miyamoto, K. Kurita,
12 G. Komatsu, A.G. Fairén, J.C. Ferris, Outflow channel sources, reactivation, and chaos
13 formation, *Xanthe Terra, Mars, Icarus*. 175 (2005) 36–57.
14 <https://doi.org/10.1016/j.icarus.2004.10.025>.
- 15 [137] J.W. Horton, M.J. Kunk, H.E. Belkin, J.N. Aleinikoff, J.C. Jackson, I.M. Chou, Evolution of
16 crystalline target rocks and impactites in the chesapeake bay impact structure, ICDP-
17 USGS eyreville B core, *Spec. Pap. Geol. Soc. Am.* 458 (2009) 277–316.
18 [https://doi.org/10.1130/2009.2458\(14\)](https://doi.org/10.1130/2009.2458(14)).
- 19 [138] P.F. McMillan, G.H. Wolf, P. Lambert, A Raman spectroscopic study of shocked single
20 crystalline quartz, *Phys. Chem. Miner.* 19 (1992) 71–79.
21 <https://doi.org/10.1007/BF00198604>.
- 22 [139] A.H. Treiman, H.E.F. Amundsen, D.F. Blake, T. Bunch, Hydrothermal origin for carbonate
23 globules in Martian meteorite ALH84001: A terrestrial analogue from Spitsbergen
24 (Norway), *Earth Planet. Sci. Lett.* 204 (2002) 323–332. [https://doi.org/10.1016/S0012-](https://doi.org/10.1016/S0012-821X(02)00998-6)
25 [821X\(02\)00998-6](https://doi.org/10.1016/S0012-821X(02)00998-6).
- 26 [140] E.S. Varnes, B.M. Jakosky, T.M. McCollom, Biological potential of martian hydrothermal
27 systems, *Astrobiology*. 3 (2003) 407–414.
28 <https://doi.org/10.1089/153110703769016479>.
- 29 [141] G.E. Cushing, T.N. Titus, J.J. Wynne, P.R. Christensen, THEMIS observes possible cave
30 skylights on Mars, *Geophys. Res. Lett.* 34 (2007) 4–8.
31 <https://doi.org/10.1029/2007GL030709>.
- 32 [142] R.J. L veill , S. Datta, Lava tubes and basaltic caves as astrobiological targets on Earth
33 and Mars: A review, *Planet. Space Sci.* 58 (2010) 592–598.
34 <https://doi.org/10.1016/j.pss.2009.06.004>.
- 35 [143] T.N. Titus, G.E. Cushing, C. Okubo, R.G. Vaughan, Wood valley pit crater cave
36 microclimate: a possible analogue for Mars, in: 2nd Int. Planet. Caves Conf., 2015: p.
37 9017.
- 38 [144] R. Popa, A.R. Smith, R. Popa, J. Boone, M. Fisk, Olivine-respiring bacteria isolated from
39 the rock-ice interface in a lava-tube cave, a mars analog environment, *Astrobiology*. 12
40 (2012) 9–18. <https://doi.org/10.1089/ast.2011.0639>.
- 41 [145] F. G zquez, J.M. Calaforra, P. Forti, Black Mn-Fe crusts as markers of abrupt
42 palaeoenvironmental changes in El Soplao Cave (Cantabria, Spain), *Int. J. Speleol.* 40
43 (2011) 163–169. <https://doi.org/10.5038/1827-806X.40.2.8>.
- 44 [146] F. G zquez, J.M. Calaforra, F. Rull, P. Forti, A. Garc a-Casco, Organic matter of fossil
45 origin in the amberine speleothems from El Soplao Cave (Cantabria, Northern Spain),

- 1 Int. J. Speleol. 41 (2012) 113–123. <https://doi.org/10.5038/1827-806X.41.1.12>.
- 2 [147] F. Gázquez, F. Rull, J.M. Calaforra, G. Venegas, J.A. Manrique, A. Sanz, J. Medina, A.
3 Catalá-Espí, A. Sansano, R. Navarro, P. Forti, J. De Waele, J. Martínez-Frías,
4 Caracterización mineralógica y geoquímica de minerales hidratados de ambientes
5 subterráneos: implicaciones para la exploración planetaria, *Estud. Geol.* 70 (2014).
6 <https://doi.org/10.3989/egeol.41688.314>.
- 7 [148] C. Rossi, R.P. Lozano, N. Isanta, J. Hellstrom, Manganese stromatolites in caves: El
8 Soplao (Cantabria, Spain), *Geology*. 38 (2010) 1119–1122.
9 <https://doi.org/10.1130/G31283.1>.
- 10 [149] A.P. Nutman, V.C. Bennett, C.R.L. Friend, M.J. Van Kranendonk, A.R. Chivas, Rapid
11 emergence of life shown by discovery of 3,700-million-year-old microbial structures,
12 *Nature*. 537 (2016) 535–538. <https://doi.org/10.1038/nature19355>.
- 13 [150] A.C. Allwood, M.R. Walter, I.W. Burch, B.S. Kamber, 3.43 billion-year-old stromatolite
14 reef from the Pilbara Craton of Western Australia: Ecosystem-scale insights to early life
15 on Earth, *Precambrian Res.* 158 (2007) 198–227.
16 <https://doi.org/10.1016/j.precamres.2007.04.013>.
- 17 [151] A. Olcott Marshall, C.P. Marshall, Field-based raman spectroscopic analyses of an
18 ordovician stromatolite, *Astrobiology*. 13 (2013) 814–820.
19 <https://doi.org/10.1089/ast.2013.1026>.
- 20 [152] S.H. Kose, S.C. George, I.C. Lau, Distinguishing in situ stromatolite biosignatures from
21 silicification and dolomitisation using short wave, visible-near and thermal infrared
22 spectroscopy: A Mars analogue study, *Vib. Spectrosc.* 87 (2016) 67–80.
23 <https://doi.org/10.1016/j.vibspec.2016.09.007>.
- 24 [153] M.D. West, J.D.A. Clarke, M. Thomas, C.F. Pain, M.R. Walter, The geology of Australian
25 Mars analogue sites, *Planet. Space Sci.* 58 (2010) 447–458.
26 <https://doi.org/10.1016/j.pss.2009.06.012>.
- 27 [154] J.D.A. Clarke, C.R. Stoker, Searching for stromatolites: The 3.4Ga Strelley Pool
28 Formation (Pilbara region, Western Australia) as a Mars analogue, *Icarus*. 224 (2013)
29 413–423. <https://doi.org/10.1016/j.icarus.2013.02.006>.
- 30 [155] M. Veneranda, G. Lopez-Reyes, J.A. Manrique, F. Guazquez, J.M. Calaforra, J. Medina,
31 Rull F., Raman characterization of speleothems from El Soplao Cave (Cantabria, Spain):
32 implications for Mars exploration, in: *Georaman 2018*, 2018: p. 176.
- 33 [156] R.P. Lozano, C. Rossi, Exceptional preservation of Mn-oxidizing microbes in cave
34 stromatolites (El Soplao, Spain), *Sediment. Geol.* 255–256 (2012) 42–55.
35 <https://doi.org/10.1016/j.sedgeo.2012.02.003>.
- 36 [157] F. Gázquez, F. Rull, A. Sanz-Arranz, J. Medina, J.M. Calaforra, C. de las Heras, J.A.
37 Lasheras, In situ Raman characterization of minerals and degradation processes in a
38 variety of cultural and geological heritage sites, *Spectrochim. Acta - Part A Mol. Biomol.*
39 *Spectrosc.* 172 (2017) 48–57. <https://doi.org/10.1016/j.saa.2016.04.035>.
- 40 [158] F. Gázquez, F. Rull, J.-M. Calaforra, E. Guirado, A. Sanz, J. Medina, C. De la Heras, A.
41 Prada, J. Antonio Lasheras, Análisis no destructivo e in situ de minerales y pigmentos en
42 cuevas mediante espectroscopia Raman José María Calaforra y Juan José Durán (
43 Editores) Aracena , 2014, in: *Iberoamérica Subterránea*, 2014: p. 297.
- 44 [159] C. Julien, M. Massot, R. Baddour-Hadjean, S. Franger, S. Bach, J.P. Pereira-Ramos,
45 Raman spectra of birnessite manganese dioxides, *Solid State Ionics*. 159 (2003) 345–
46 356. [https://doi.org/10.1016/S0167-2738\(03\)00035-3](https://doi.org/10.1016/S0167-2738(03)00035-3).

- 1 [160] S. Bernardini, F. Bellatreccia, G. Della Ventura, P. Ballirano, A. Sodo, Raman
2 spectroscopy and laser-induced degradation of groutellite and ramsdellite, two cathode
3 materials of technological interest, *RSC Adv.* 10 (2019) 923–929.
4 <https://doi.org/10.1039/c9ra08662e>.
- 5 [161] Z.M. Chan, D.A. Kitchev, J.N. Weker, C. Schnedermann, K. Lim, G. Ceder, W. Tumas,
6 M.F. Toney, D.G. Nocera, Electrochemical trapping of metastable Mn³⁺ ions for
7 activation of MnO₂ oxygen evolution catalysts, *Proc. Natl. Acad. Sci. U. S. A.* 115 (2018)
8 E5261–E5268. <https://doi.org/10.1073/pnas.1722235115>.
- 9 [162] E. Hauber, M. Ulrich, F. Preusker, F. Trauthan, D. Reiss, A.E. Carlsson, H. Hiesinger,
10 Svalbard (Norway) as a terrestrial analogue for Martian landforms : Results on alluvial
11 fans, *Science* (80-.). 4 (2009) 4–5. <https://doi.org/10.1029/2008GL034954>.
- 12 [163] J. Toporski, H. Amundsen, a Steele, J. Maule, M. Fogel, M. Schweizer, a Treiman, L.
13 Benning, The Arctic Mars Analog Svalbard Expedition (AMASE) project References :,
14 *Earth.* (2004) 84001–84001.
- 15 [164] H.E.F. Amundsen, F. Westall, A. Steele, J. Vago, N. Schmitz, A. Bauer, C.R. Cousins, F.
16 Rull, A. Sansano, I. Midtkandal, Integrated ExoMars PanCam, Raman, and close-up
17 imaging field tests on AMASE 2009, *EGU Gen. Assem.* 12 (2010) 8757.
18 <http://meetingorganizer.copernicus.org/EGU2010/EGU2010-8757.pdf>.
- 19 [165] N. Schmitz, D. Barnes, A. Coates, A. Griffiths, E. Hauber, R. Jaumann, H. Michaelis, Field
20 Test of the ExoMars Panoramic Camera in the High Arctic - First Results and Lessons
21 Learned, *Assembly.* 11 (2009) 10621.
- 22 [166] R. Léveillé, Validation of astrobiology technologies and instrument operations in
23 terrestrial analogue environments, *Comptes Rendus - Palevol.* 8 (2009) 637–648.
24 <https://doi.org/10.1016/j.crpv.2009.03.005>.
- 25 [167] A. Steele, H. Amundsen, L. Benning, M. Fogel, N. Schmitz, The Arctic Mars Analogue
26 Svalbard Expedition 2010 ., *Geophys. Res. Abstr.* 13 (2011) 9607–9607.
- 27 [168] F. Rull, A. Vegas, F. Barreiro, In-situ Raman-LIBS combined spectroscopy for surface
28 mineral analysis at stand-off distances, *Lunar Planet. Inst.* (2011) 4–5.
- 29 [169] S.M. Angel, N.R. Gomer, S.K. Sharma, C. McKay, N. Ames, Remote Raman spectroscopy
30 for planetary exploration: A review, *Appl. Spectrosc.* 66 (2012) 137–150.
31 <https://doi.org/10.1366/11-06535>.
- 32 [170] R.C. Wiens, S. Maurice, F.R. Perez, The SuperCam remote sensing instrument suite for
33 the mars 2020 rover: A preview, *Spectrosc. (Santa Monica).* 32 (2017) 50–55.
- 34 [171] A.H. Treiman, Eruption age of the Sverrefjellet volcano, Spitsbergen Island, Norway,
35 *Polar Res.* 31 (2012) 1–7. <https://doi.org/10.3402/polar.v31i0.17320>.
- 36 [172] D.W. Deamer, C.D. Georgiou, Hydrothermal Conditions and the Origin of Cellular Life,
37 *Astrobiology.* 15 (2015) 1091–1095. <https://doi.org/10.1089/ast.2015.1338>.
- 38 [173] R. V. Morris, S.W. Ruff, R. Gellert, D.W. Ming, R.E. Arvidson, B.C. Clark, D.C. Golden, K.
39 Siebach, G. Klingelhöfer, C. Schröder, I. Fleischer, A.S. Yen, S.W. Squyres, Identification
40 of carbonate-rich outcrops on Mars by the spirit rover, *Science* (80-.). 329 (2010) 421–
41 424. <https://doi.org/10.1126/science.1189667>.
- 42 [174] R.V. Morris, D.F. Blake, D. Bish, D.W. Ming, D.G. Agresti, A.H. Treiman, A. Steele, H.E.F.
43 Amundsen, A. Team, A terrestrial analogue from Spitsbergen (Svalbard, Norway) for the
44 Comanche carbonate at Gusev Crater, Mars, *Lunar Planet. Sci.* 42 (2011) 1699–1700.
- 45 [175] F. Rull, A. Vegas, A. Sansano, P. Sobron, Analysis of Arctic ices by Remote Raman

- 1 Spectroscopy, *Spectrochim. Acta - Part A Mol. Biomol. Spectrosc.* 80 (2011) 148–155.
2 <https://doi.org/10.1016/j.saa.2011.04.007>.
- 3 [176] M. Balme, Team Exofit, The ExoFit Rover field trial - simulating ExoMars Rover
4 operations, in: 19th EANA Astrobiol. Conf., Orléans (France), 2019.
- 5 [177] J.-L. Josset, V. Cessa, S. Beauvivre, P. Martin, Development of the science instrument
6 CLUPI: the close-up imager on board the ExoMars rover, 10566 (2017) 93.
7 <https://doi.org/10.1117/12.2308276>.
- 8 [178] X.Y. Li, A. González, A. Solé-Benet, Laboratory methods for the estimation of infiltration
9 rate of soil crusts in the Tabernas Desert badlands, *Catena*. 60 (2005) 255–266.
10 <https://doi.org/10.1016/j.catena.2004.12.004>.
- 11 [179] I. Miralles, F. Domingo, E. García-Campos, C. Trasar-Cepeda, M.C. Leirós, F. Gil-Sotres,
12 Biological and microbial activity in biological soil crusts from the Tabernas desert, a sub-
13 arid zone in SE Spain, *Soil Biol. Biochem.* 55 (2012) 113–121.
14 <https://doi.org/10.1016/j.soilbio.2012.06.017>.
- 15 [180] Y. Cantón, A. Solé-Benet, R. Lázaro, Soil-geomorphology relations in gypsiferous
16 materials of the tabernas desert (almería, se spain), *Geoderma*. 115 (2003) 193–222.
17 [https://doi.org/10.1016/S0016-7061\(03\)00012-0](https://doi.org/10.1016/S0016-7061(03)00012-0).
- 18 [181] D.A. Burkett, I.T. Graham, C.R. Ward, The application of portable X-ray diffraction to
19 quantitative mineralogical analysis of hydrothermal systems, *Can. Mineral.* 53 (2015)
20 429–454. <https://doi.org/10.3749/canmin.1400099>.
- 21 [182] G. Lopez-Reyes, F. Rull Pérez, A method for the automated Raman spectra acquisition,
22 *J. Raman Spectrosc.* 48 (2017) 1654–1664. <https://doi.org/10.1002/jrs.5185>.
- 23 [183] Y. Cantón, A. Solé-Benet, I. Queralt, R. Pini, Weathering of a gypsum-calcareous
24 mudstone under semi-arid environment at Tabernas, SE Spain: Laboratory and field-
25 based experimental approaches, *Catena*. 44 (2001) 111–132.
26 [https://doi.org/10.1016/S0341-8162\(00\)00153-3](https://doi.org/10.1016/S0341-8162(00)00153-3).
- 27 [184] M. Veneranda, G. Lopez-Reyes, J. Antonio Manrique-Martinez, A. Sanz-Arranz, J.
28 Medina, C. Pérez, C. Quintana, A. Moral, J.A. Rodríguez, J. Zafra, L.M. Nieto Calzada, F.
29 Rull, Raman spectroscopy and planetary exploration: testing the ExoMars/RLS system at
30 the Tabernas Desert (Spain), *Microchem. J.* 165 (2021) 106149.
31 <https://doi.org/10.1016/j.microc.2021.106149>.
- 32 [185] European Space Agency webpage, (n.d.). [https://exploration.esa.int/web/mars/-](https://exploration.esa.int/web/mars/-/45082-rover-scientific-objectives)
33 [/45082-rover-scientific-objectives](https://exploration.esa.int/web/mars/-/45082-rover-scientific-objectives).
- 34 [186] N.A. Cabrol, G. Chong-Díaz, C.R. Stoker, V.C. Gulick, R. Landheim, P. Lee, T.L. Roush, A.P.
35 Zent, C.H. Lameli, A.J. Iglesia, M.P. Arrerondo, J.M. Dohm, R. Keaten, D. Wettergreen,
36 M.H. Sims, K. Schwher, M.G. Bualat, H.J. Thomas, E. Zbinden, D. Christian, L. Pedersen,
37 A. Bettis, G. Thomas, B. Witzke, Nomad Rover field experiment, Atacama Desert, Chile
38 1. Science results overview, *J. Geophys. Res. E Planets*. 106 (2001) 7785–7806.
39 <https://doi.org/10.1029/1999JE001166>.
- 40 [187] D.S. Wettergreen, M.D. Wagner, D. Jonak, V. Baskaran, M.C. Deans, S. Heys, D. Pane, T.
41 Smith, J. Teza, D.R. Thompson, P. Tompkins, C. Williams, Long-Distance Autonomous
42 Survey and Mapping in the Robotic Investigation of Life in the Atacama Desert, *Int.*
43 *Symp. Artif. Intell. Robot. Autom. Sp.* (2008).
- 44 [188] M. Woods, A. Shaw, I. Wallace, M. Malinowski, P. Rendell, Demonstrating autonomous
45 Mars Rover Science Operations in the Atacama Desert, (n.d.).

- 1 [189] V. Parro, G. De Diego-Castilla, J.A. Rodríguez-Manfredi, L.A. Rivas, Y. Blanco-López, E.
2 Sebastián, J. Romeral, C. Compostizo, P.L. Herrero, A. García-Marín, M. Moreno-Paz, M.
3 García-Villadangos, P. Cruz-Gil, V. Peinado, J. Martín-Soler, J. Pérez-Mercader, J. Gómez-
4 Elvira, SOLID3: A multiplex antibody microarray-based optical sensor instrument for in
5 situ life detection in planetary exploration, *Astrobiology*. 11 (2011) 15–28.
6 <https://doi.org/10.1089/ast.2010.0501>.
- 7 [190] R.C. Quinn, A.P. Zent, F.J. Grunthaner, P. Ehrenfreund, C.L. Taylor, J.R.C. Garry,
8 Detection and characterization of oxidizing acids in the Atacama Desert using the Mars
9 Oxidation Instrument, *Planet. Space Sci.* 53 (2005) 1376–1388.
10 <https://doi.org/10.1016/j.pss.2005.07.004>.
- 11 [191] J. Wei, A. Wang, J.L. Lambert, D. Wettergreen, N. Cabrol, K. Warren-Rhodes, K. Zacny,
12 Autonomous soil analysis by the Mars Micro-beam Raman Spectrometer (MMRS) on-
13 board a rover in the Atacama Desert: A terrestrial test for planetary exploration, *J.*
14 *Raman Spectrosc.* 46 (2015) 810–821. <https://doi.org/10.1002/jrs.4656>.
- 15 [192] F. Bournon, A Geological Description of Cerro Paranal or Another Insight Into the "
16 Perfect Site for Astronomy ", (1992).
- 17 [193] R.R. Cordero, A. Damiani, G. Seckmeyer, J. Jorquera, M. Caballero, P. Rowe, J. Ferrer, R.
18 Mubarak, J. Carrasco, R. Rondanelli, M. Matus, D. Laroze, The Solar Spectrum in the
19 Atacama Desert, *Sci. Rep.* 6 (2016) 1–15. <https://doi.org/10.1038/srep22457>.
- 20 [194] ESO, European Southern Observatory, (2020).
21 <https://www.eso.org/sci/facilities/paranal/astroclimate/site.html>.
- 22 [195] A. Crits-Christoph, C.K. Robinson, T. Barnum, W.F. Fricke, A.F. Davila, B. Jedynek, C.P.
23 McKay, J. DiRuggiero, Colonization patterns of soil microbial communities in the
24 Atacama Desert, *Microbiome*. 1 (2013) 1–13. <https://doi.org/10.1186/2049-2618-1-28>.
- 25 [196] V. Parro, G. De Diego-Castilla, M. Moreno-Paz, Y. Blanco, P. Cruz-Gil, J.A. Rodríguez-
26 Manfredi, D. Fernández-Remolar, F. Gómez, M.J. Gómez, L.A. Rivas, C. Demergasso, A.
27 Echeverría, V.N. Urtuvia, M. Ruiz-Bermejo, M. García-Villadangos, M. Postigo, M.
28 Sánchez-Román, G. Chong-Díaz, J. Gómez-Elvira, A microbial oasis in the hypersaline
29 atacama subsurface discovered by a life detector chip: Implications for the search for
30 life on mars, *Astrobiology*. 11 (2011) 969–996. <https://doi.org/10.1089/ast.2011.0654>.
- 31 [197] J. DiRuggiero, J. Wierzchos, C.K. Robinson, T. Souterre, J. Ravel, O. Artieda, V. Souza-
32 Egipsy, C. Ascaso, Microbial colonisation of chasmoendolithic habitats in the hyper-arid
33 zone of the Atacama Desert, *Biogeosciences*. 10 (2013) 2439–2450.
34 <https://doi.org/10.5194/bg-10-2439-2013>.
- 35 [198] P. Vitek, J. Jehlicka, H.G.M. Edwards, I. Hutchinson, C. Ascaso, J. Wierzchos,
36 Miniaturized Raman instrumentation detects carotenoids in Mars-analogue rocks from
37 the Mojave and Atacama deserts, *Philos. Trans. R. Soc. A Math. Phys. Eng. Sci.* 372
38 (2014). <https://doi.org/10.1098/rsta.2014.0196>.
- 39 [199] P. Vitek, J. Jehlička, H.G.M. Edwards, I. Hutchinson, C. Ascaso, J. Wierzchos, The
40 miniaturized Raman system and detection of traces of life in halite from the Atacama
41 desert: Some considerations for the search for life signatures on Mars, *Astrobiology*. 12
42 (2012) 1095–1099. <https://doi.org/10.1089/ast.2012.0879>.
- 43 [200] P. Vitek, C. Ascaso, O. Artieda, J. Wierzchos, Raman imaging in geomicrobiology:
44 endolithic phototrophic microorganisms in gypsum from the extreme sun irradiation
45 area in the Atacama Desert, *Anal. Bioanal. Chem.* 408 (2016) 4083–4092.
46 <https://doi.org/10.1007/s00216-016-9497-9>.

- 1 [201] R.T. Downs, Determining mineralogy on mars with the CheMin X-ray diffractometer,
2 Elements. 11 (2015) 45–50. <https://doi.org/10.2113/gselements.11.1.45>.
- 3 [202] J. Grant, a R. Vasavada, M. Watkins, L. Lorenzoni, J. Griffes, CHEMIN: A definitive
4 mineralogy instrument on the Mars Science Laboratory (MSL '09) Rover, in: Seventh Int.
5 Conf. Mars, 2009: pp. 2–5.
- 6 [203] D. Bish, D. Blake, D. Vaniman, P. Sarrazin, T. Bristow, C. Achilles, P. Dera, S. Chipera, J.
7 Crisp, R.T. Downs, J. Farmer, M. Gailhanou, D. Ming, J.M. Morookian, R. Morris, S.
8 Morrison, E. Rampe, A. Treiman, A. Yen, The first X-ray diffraction measurements on
9 Mars, IUCrJ. 1 (2014) 514–522. <https://doi.org/10.1107/S2052252514021150>.
- 10 [204] F. Rull, S. Maurice, I. Hutchinson, A. Moral, C. Perez, C. Diaz, M. Colombo, T. Belenguer,
11 G. Lopez-Reyes, A. Sansano, O. Forni, Y. Parot, N. Striebig, S. Woodward, C. Howe, N.
12 Tarcea, P. Rodriguez, L. Seoane, A. Santiago, J.A. Rodriguez-Prieto, J. Medina, P. Gallego,
13 R. Canchal, P. Santamaría, G. Ramos, J.L. Vago, The Raman Laser Spectrometer for the
14 ExoMars Rover Mission to Mars, Astrobiology. 17 (2017).
15 <https://doi.org/10.1089/ast.2016.1567>.
- 16 [205] E.B. Rampe, D.F. Blake, T.F. Bristow, D.W. Ming, D.T. Vaniman, R. V. Morris, C.N.
17 Achilles, S.J. Chipera, S.M. Morrison, V.M. Tu, A.S. Yen, N. Castle, G.W. Downs, R.T.
18 Downs, J.P. Grotzinger, R.M. Hazen, A.H. Treiman, T.S. Peretyazhko, D.J. Des Marais,
19 R.C. Walroth, P.I. Craig, J.A. Crisp, B. Lafuente, J.M. Morookian, P.C. Sarrazin, M.T.
20 Thorpe, J.C. Bridges, L.A. Edgar, C.M. Fedo, C. Freissinet, R. Gellert, P.R. Mahaffy, H.E.
21 Newsom, J.R. Johnson, L.C. Kah, K.L. Siebach, J. Schieber, V.Z. Sun, A.R. Vasavada, D.
22 Wellington, R.C. Wiens, Mineralogy and geochemistry of sedimentary rocks and eolian
23 sediments in Gale crater, Mars: A review after six Earth years of exploration with
24 Curiosity, Chemie Der Erde. 80 (2020). <https://doi.org/10.1016/j.chemer.2020.125605>.
- 25 [206] N. Bost, C. Ramboz, N. LeBreton, F. Foucher, G. Lopez-Reyes, S. De Angelis, M. Josset, G.
26 Venegas, A. Sanz-Arranz, F. Rull, J. Medina, J.L. Josset, A. Souchon, E. Ammannito, M.C.
27 De Sanctis, T. Di Iorio, C. Carli, J.L. Vago, F. Westall, Testing the ability of the ExoMars
28 2018 payload to document geological context and potential habitability on Mars,
29 Planet. Space Sci. 108 (2015) 87–97. <https://doi.org/10.1016/j.pss.2015.01.006>.
- 30 [207] L. Sopegno, K.P. Valavanis, M.J. Rutherford, L. Casalino, Mars Sample Return Mission:
31 Mars Ascent Vehicle Propulsion Design, IEEE Aerosp. Conf. Proc. (2020) 1–9.
32 <https://doi.org/10.1109/AERO47225.2020.9172367>.
- 33 [208] C. Lantz, F. Poulet, D. Loizeau, L. Riu, C. Pilorget, J. Carter, H. Dypvik, F. Rull, S.C.
34 Werner, Planetary Terrestrial Analogues Library project: 1. characterization of samples
35 by near-infrared point spectrometer, Planet. Space Sci. 189 (2020) 104989.
36 <https://doi.org/10.1016/j.pss.2020.104989>.
- 37 [209] D. Loizeau, G. Lequertier, F. Poulet, V. Hamm, C. Pilorget, L. Meslier-Lourit, C. Lantz, S.C.
38 Werner, F. Rull, J.P. Bibring, Planetary Terrestrial Analogues Library project: 2. building
39 a laboratory facility for MicrOmega characterization, Planet. Space Sci. 193 (2020)
40 105087. <https://doi.org/10.1016/j.pss.2020.105087>.
- 41 [210] M. Veneranda, J. Sáiz, A. Sanz-Arranz, J.A. Manrique, G. Lopez-Reyes, J. Medina, H.
42 Dypvik, S.C. Werner, F. Rull, Planetary Terrestrial Analogues Library (PTAL) project:
43 Raman data overview, J. Raman Spectrosc. (2019) 1–19.
44 <https://doi.org/10.1002/jrs.5652>.
- 45 [211] H. Dypvik, H. Hellevang, A. Krzesinska, C. Sætre, J.-C. Viennet, B. Bultel, D. Ray, F.
46 Poulet, D. Loizeau, M. Veneranda, F. Rull, A. Cousin, S.C. Werner, The Planetary
47 Terrestrial Analogues Library (PTAL) - An Exclusive Lithological Selection of Possible

- 1 Martian Earth Analogues, Planet. Space Sci. (2021) (under press).
- 2 [212] M. Veneranda, G. Lopez-Reyes, A.S. Arranz, J.A. Manrique, J. Saiz, C. Gracia-Prieto, J.
3 Medina, M. Konstantinidis, E. Lalla, A. Moral, L.M.N. Calzada, F. Rull, Analytical
4 Database of Martian Minerals (ADaMM): Project synopsis and Raman data overview, J.
5 Ram. (2021) (under press).
- 6 [213] J. Saiz, G. Lopez-reyes, M. Veneranda, J.A. Manrique, A. Guzmán, D. Moreno-
7 dominguez, S. Werner, F. Poulet, J. Medina, Automated sample identification with
8 SpectPro and PTAL database for the analysis of spectra from planetary missions, in: EGU
9 Gen. Assem. 2019, Vienna (Austria), 2019: p. 17904.
- 10

Journal Pre-proof

Sample	quartz	feldspar	anatase	amphibole	phyllosilicate	gypsum	anhydrite	calcite	hematite	organics
ADC2-UP (0-15cm)	x ◊ o	x o	x o	x o	x o	x o	o	x ◊ o		◊
ADC2LP (15-30cm)	x ◊ o	x ◊ o	x	◊	x ◊ o			x o		
ADC1-UP (0-15cm)	x o	x ◊ o	x	x o	x o			x		x
ADC1-LP (15-30cm)	x o	x ◊ o	x		x o				o	x

x = RLS ExoMars Simulator

◊ = Rad1

o = XRD



Elena Charro

She obtained her Ph.D. in Physical Chemistry from the University of Valladolid (UVa, Spain) in 1993 in the field of microwave spectroscopy and was appointed Postdoctoral Fellow in the Department of Applied Mathematics of Queen`s University of Belfast (UK) in 1998 working in the field of photoionization process in species of astrophysical interest and fusion plasmas. In 2018 she became Full Professor at UVa. Her main research topics are: Microwave spectroscopy, Atomic Spectra Calculations in Fusion Plasma of Astrophysical Interest (30 publications), Determination of Natural Radionuclides in Soils and Soil Organic Carbon studies.

Journal Pre-proof

Emmanuel Lalla

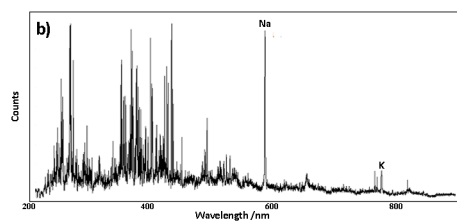
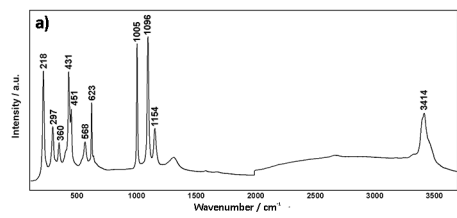
Emmanuel Lalla is a Research Associate at York University, where he leads and collaborates on science and technology development projects for space exploration. In 2021 he became co-PI of several projects funded by the Canadian Space Agency, where he engages in knowledge transfer activities among research institutions and industry at all technology readiness levels. He received his Ph.D. in Physics from the University of Valladolid, Spain, and worked as a researcher at several institutions in Europe before coming to Canada. He is a research collaborator of the Raman Laser Spectrometer at ExoMars Mission, currently scheduled for flight in 2022.

Journal Pre-proof

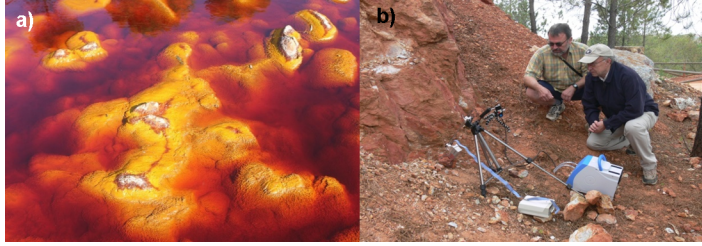
Fernando Rull

He is the founder and coordinator of Erica Research Group. Since 1989 Fernando Rull is Chair Professor of Crystallography and Mineralogy in the University of Valladolid. He has over 20 years of experience in the development of spectroscopic instruments and in their application to the study of terrestrial analogue materials. He co-authored over 240 papers in SCI journals and more than 150 conference abstracts. Currently Fernando Rull is PI of the Raman Laser Spectrometer (RLS) of the ExoMars mission, and co-PI of SuperCam and RAX instruments for the Mars2020 and MMX missions (to Mars and Phobos, respectively).

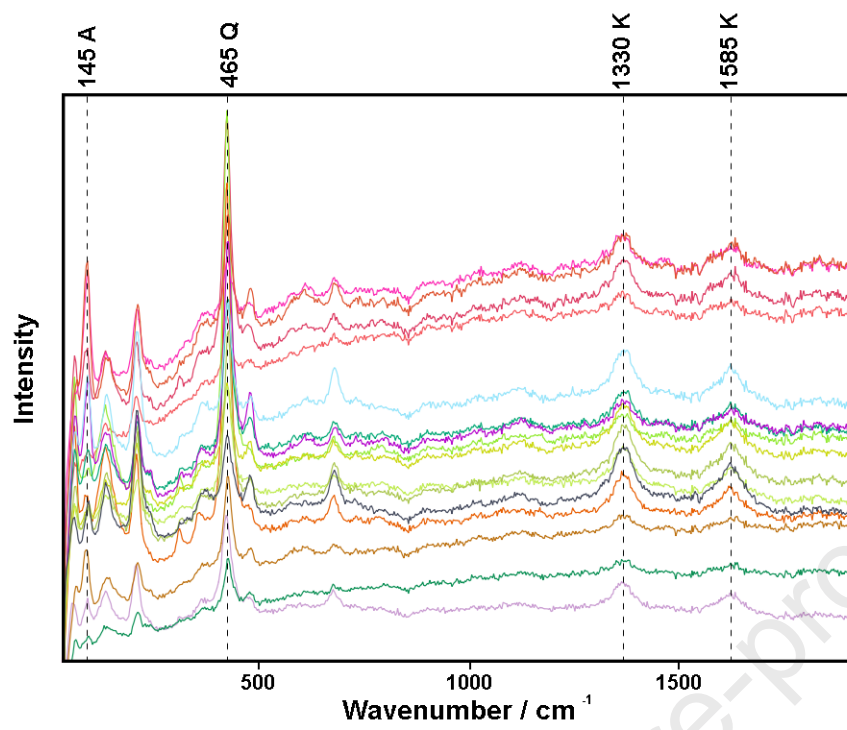
Journal Pre-proof

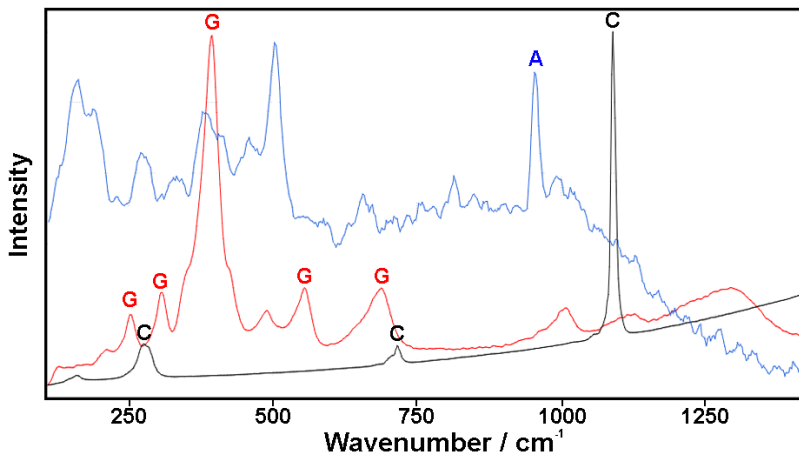


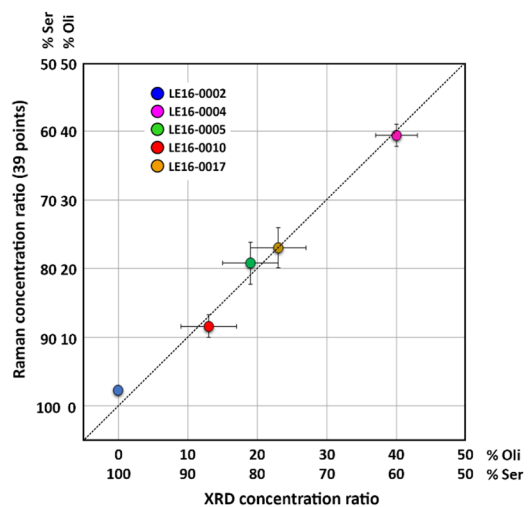
Journal Pre-proof



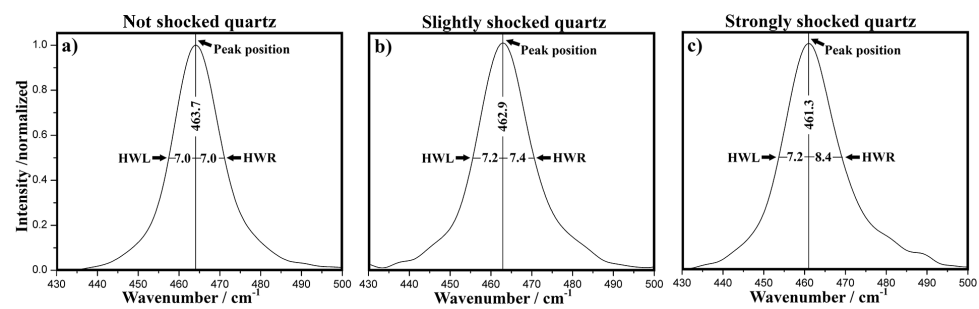
Journal Pre-proof

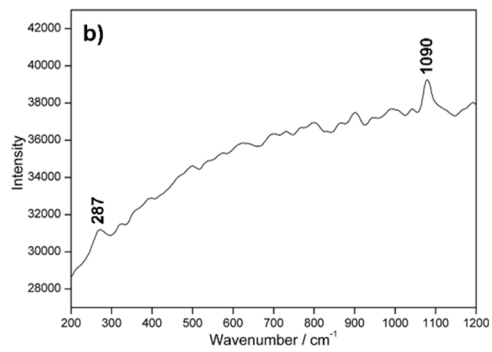
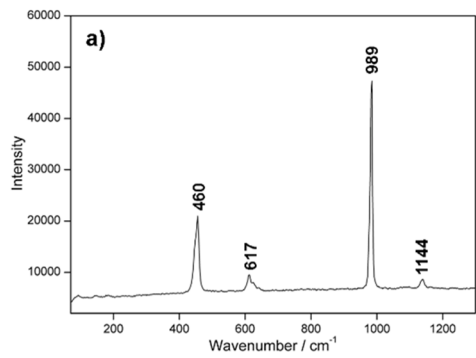






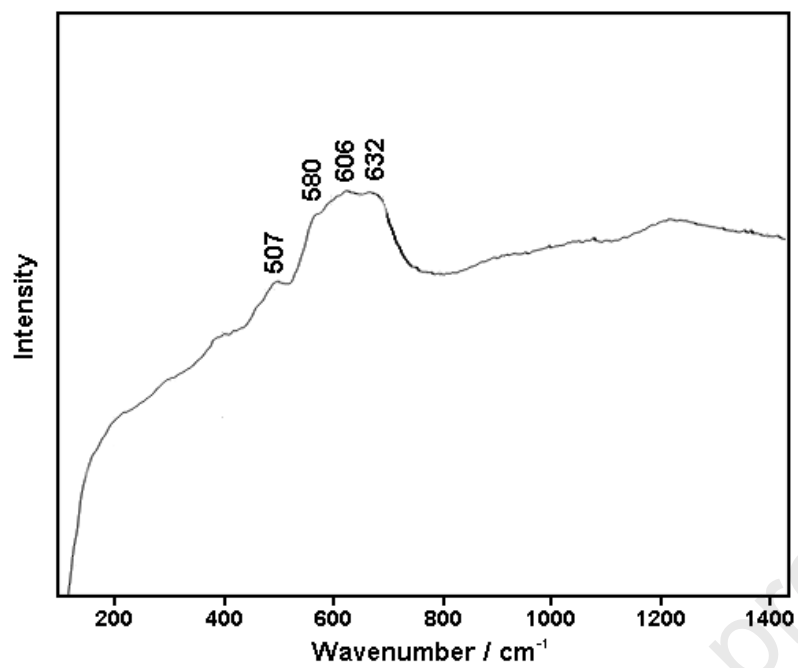
Journal Pre-proof

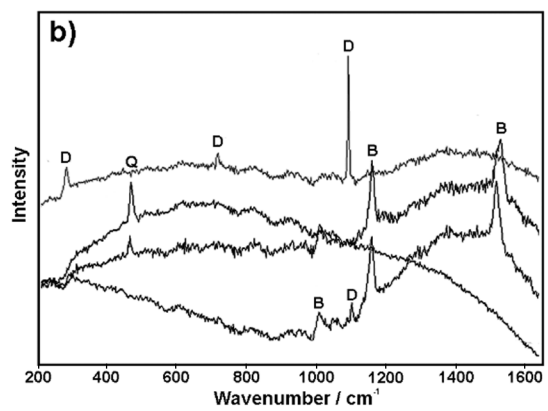
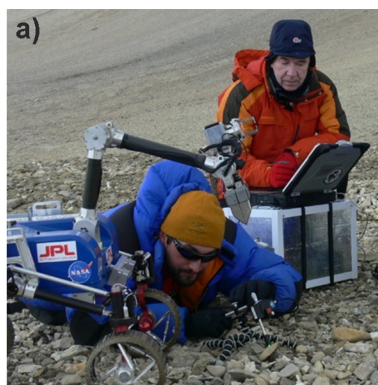




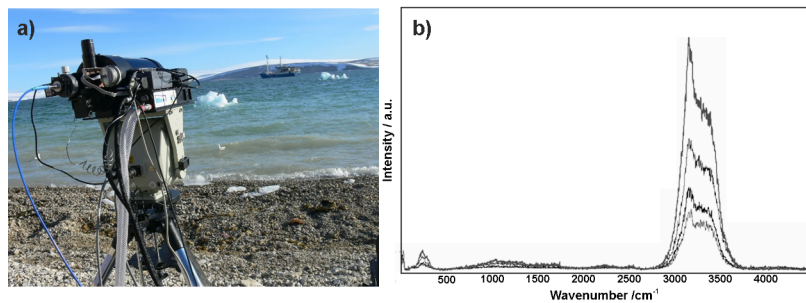


Journal Pre-proof

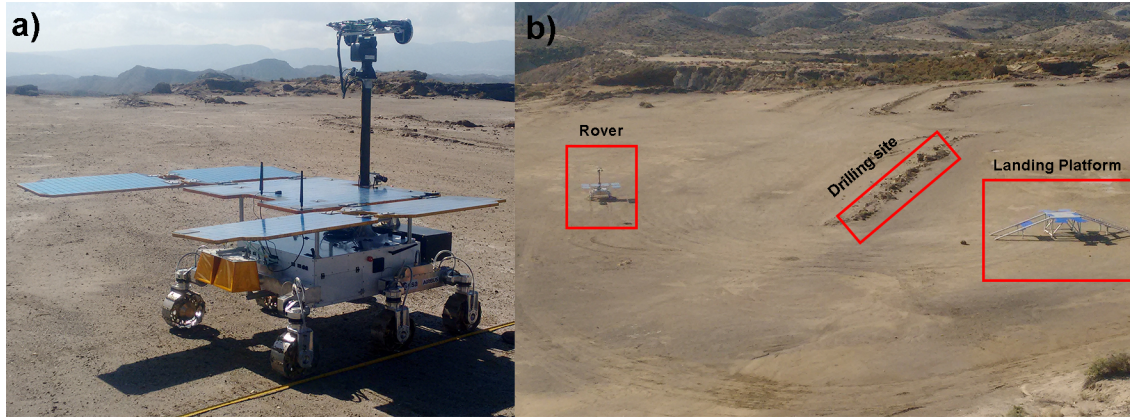




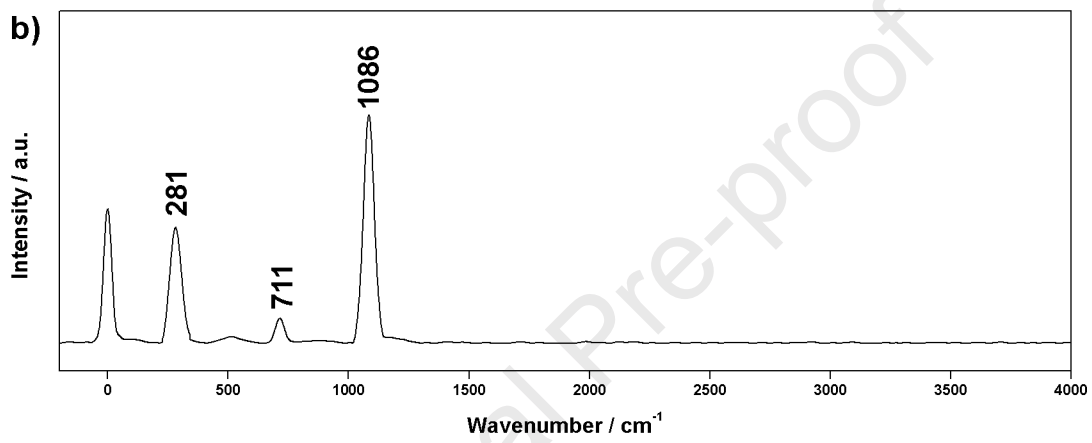
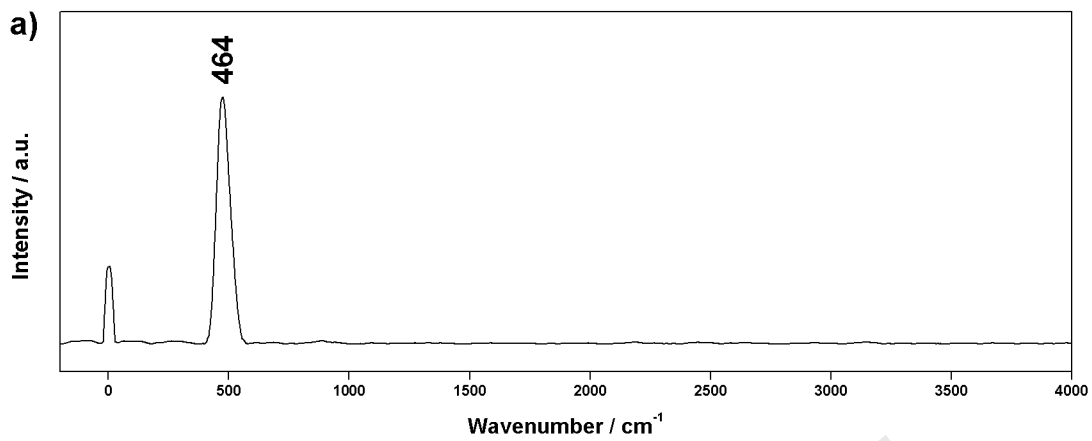
Journal Pre-proof

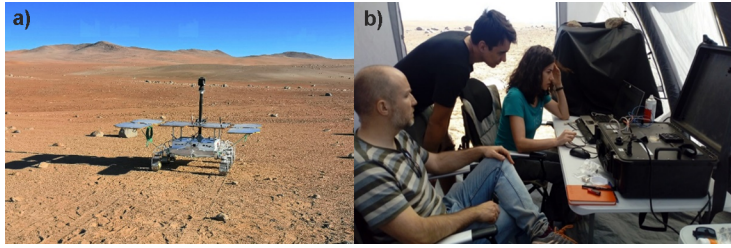


Journal Pre-proof

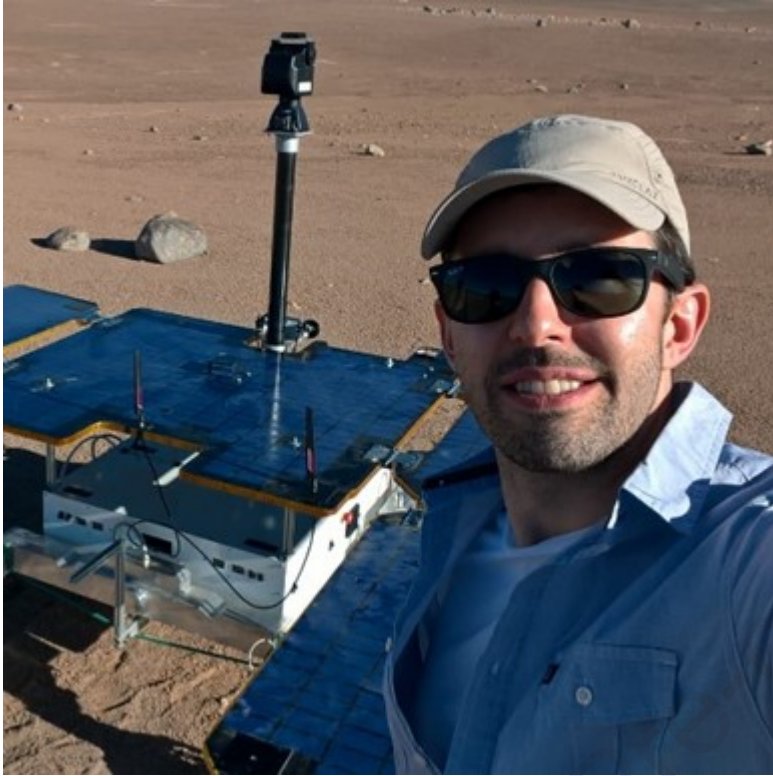


Journal Pre-proof





Journal Pre-proof



Jesus Medina

PhD. in Chemistry, and Professor of the Condensed Matter Physics, Crystallography and Mineralogy Department of the University of Valladolid. His major research areas are mineralogy and planetary science. He has been collaborating in the development of spectroscopic instrumentation for planetary exploration and in the analytical characterization of terrestrial analogue sites. Member of the ERICA research group, he co-authored over 50 articles in SCI journals and more than 100 conference abstracts.

Journal Pre-proof

Jesus Saiz

Jesus Saiz is a telecommunications systems technician currently working for the ERICA group from the University of Valladolid. He is the ground software developer of the RLS (Raman Laser Spectrometer) instrument of the ExoMars2022 mission, as well as developer of the PTAL(Planetary Terrestrial Analogues Library) platform of the European Commission project within Horizon 2020 program. He co-authored more than 20 and participated as a speaker at several international conferences and social dissemination activities.

Journal Pre-proof

Laura Seoane

She is a space systems engineer at INTA with more than 15 years of experience in satellites and space instruments development. She has been deeply involved in the INTA Small Satellites Program, performing a wide range of activities, from System Engineering to Operations, HW/SW development, and AIV at board, unit and satellite level. During the last six years, she has been mainly focused on the development of the RLS (Raman Laser Spectrometer) instrument for the ExoMars 2022 mission, in charge of the on-board SW and Operations. She co-authored more than 20 publications in peer-reviewed journals and conferences.

Journal Pre-proof

Luis Miguel Nieto

He is professor of Theoretical Physics at the University of Valladolid, developing lines of research in Mathematical Physics, such as “Mathematical modeling of graphene and other metamaterials”, “Safe quantum communications” or “Integrability, symmetries and non-linear dynamics of classical and quantum systems”.

He has published 125 articles in indexed journals, having participated in 50 research projects. In 2018 he received the Award from the Social Council of the University of Valladolid for all his activity. He is referee of 15 scientific journals and coordinates predoctoral and postdoctoral research activities. He has been Vice Chancellor and currently heads the Department of Theoretical Physics.

Journal Pre-proof

Marco Veneranda

With a PhD in analytical chemistry, he works as postdoctoral researcher at the University of Valladolid (UVa). He is directly involved in many research projects related to Mars exploration. As an official member of Operations and Science Support teams of both ESA/ExoMars (RLS) and NASA/Mars 2020 (SuperCam) missions, his current research interests include the spectroscopic analysis of Martian-relevant rocks and the development of novel Raman semi-quantification strategies and Raman-LIBS chemometric tools for Mars exploration. He co-authored over 35 articles in SCI journals and more than 40 conference abstracts.

Journal Pre-proof

Highlights:

- We present a review of the terrestrial analogue studies performed by the ERICA group.
- Details about planetary mission simulations are also provided.
- The main results gathered from the use of multiple analytical systems are compared.
- Pros and cons expected by the use of Raman spectrometers on Mars are presented.
- The work aims to support the interpretation of data returned from Mars2020 and ExoMars rovers.

Journal Pre-proof

Emmanuel Lalla

Emmanuel Lalla is a Research Associate at York University, where he leads and collaborates on science and technology development projects for space exploration. In 2021 he became co-PI of several projects funded by the Canadian Space Agency, where he engages in knowledge transfer activities among research institutions and industry at all technology readiness levels. He received his Ph.D. in Physics from the University of Valladolid, Spain, and worked as a researcher at several institutions in Europe before coming to Canada. He is a research collaborator of the Raman Laser Spectrometer at ExoMars Mission, currently scheduled for flight in 2022.

Journal Pre-proof

Andoni Gaizka Moral

He currently works at Instituto Nacional de Técnica Aeroespacial (Spain). Main research in Astrobiology, Aerospace Engineering and Optics Engineering. Project Manager of the 'Raman Laser Spectrometer' (RLS) Instrument for ESA's ExoMars 2020 Rover'. Project Manager of the 'Raman Laser Assembly' (RLA) of the Raman Instrument of the JAXA-DLR MMX mission. Project Manager of the 'Signs Of Life Detection' (SOLID) instrument for the NASA Icebreaker Mission Proposal. He co-authored 16 articles in SCI journals and more than 20 conference abstracts and book chapters.

Journal Pre-proof

Andoni Gaizka Moral

He currently works at Instituto Nacional de Técnica Aeroespacial (Spain). Main research in Astrobiology, Aerospace Engineering and Optics Engineering. Project Manager of the 'Raman Laser Spectrometer' (RLS) Instrument for ESA's ExoMars 2020 Rover'. Project Manager of the 'Raman Laser Assembly' (RLA) of the Raman Instrument of the JAXA-DLR MMX mission. Project Manager of the 'Signs Of Life Detection' (SOLID) instrument for the NASA Icebreaker Mission Proposal. He co-authored 16 articles in SCI journals and more than 20 conference abstracts and book chapters.

Journal Pre-proof

J. Aurelio Sanz-Arranz

He is a member of the ERICA research group from the University of Valladolid.

He is collaborating in multiple projects related to planetary exploration and provides analytical support to research lines developed in the framework of the ESA/ExoMars and NASA/Mars 2020 missions.

As "Raman craftsman" specialist his professional activity is principally devoted to Raman analysis of many kind of organic and inorganic compounds, including minerals, terrestrial analogues and materials of cultural interest.

He co-authored 34 SCI papers, 6 papers in no-SCI journals, 5 book chapters, and 102 conference abstracts.

Journal Pre-proof

Elena Charro

She obtained her Ph.D. in Physical Chemistry from the University of Valladolid (UVa, Spain) in 1993 in the field of microwave spectroscopy and was appointed Postdoctoral Fellow in the Department of Applied Mathematics of Queen`s University of Belfast (UK) in 1998 working in the field of photoionization process in species of astrophysical interest and fusion plasmas. In 2018 she became Full Professor at UVa. Her main research topics are: Microwave spectroscopy, Atomic Spectra Calculations in Fusion Plasma of Astrophysical Interest (30 publications), Determination of Natural Radionuclides in Soils and Soil Organic Carbon studies.

Journal Pre-proof

Fernando Rull

He is the founder and coordinator of Erica Research Group. Since 1989 Fernando Rull is Chair Professor of Crystallography and Mineralogy in the University of Valladolid. He has over 20 years of experience in the development of spectroscopic instruments and in their application to the study of terrestrial analogue materials. He co-authored over 240 papers in SCI journals and more than 150 conference abstracts. Currently Fernando Rull is PI of the Raman Laser Spectrometer (RLS) of the ExoMars mission, and co-PI of SuperCam and RAX instruments for the Mars2020 and MMX missions (to Mars and Phobos, respectively).

Journal Pre-proof

Guillermo Lopez-Reyes

Postdoctoral researcher at the University of Valladolid, he works on the development of spectroscopic instruments and data analysis techniques for planetary exploration missions. He is the Science Operations responsible of the RLS Raman spectrometer onboard the ESA ExoMars rover. He is also collaborator of the SuperCam Raman/LIBS spectrometer on NASA Mars 2020 and member of the Raman spectrometer RAX Scientific Team on JAXA MMX. He has 39 indexed publications, 120+ contributions to International conferences; 200+ documents and technical reports for the more than 15 projects in which he has participated.

Journal Pre-proof

Jesus Medina

PhD. in Chemistry, and Professor of the Condensed Matter Physics, Crystallography and Mineralogy Department of the University of Valladolid. His major research areas are mineralogy and planetary science. He has been collaborating in the development of spectroscopic instrumentation for planetary exploration and in the analytical characterization of terrestrial analogue sites. Member of the ERICA research group, he co-authored over 50 articles in SCI journals and more than 100 conference abstracts.

Journal Pre-proof

Jesus Saiz

Jesus Saiz is a telecommunications systems technician currently working for the ERICA group from the University of Valladolid. He is the ground software developer of the RLS (Raman Laser Spectrometer) instrument of the ExoMars2022 mission, as well as developer of the PTAL(Planetary Terrestrial Analogues Library) platform of the European Commission project within Horizon 2020 program. He co-authored more than 20 and participated as a speaker at several international conferences and social dissemination activities.

Journal Pre-proof

Laura Seoane

She is a space systems engineer at INTA with more than 15 years of experience in satellites and space instruments development. She has been deeply involved in the INTA Small Satellites Program, performing a wide range of activities, from System Engineering to Operations, HW/SW development, and AIV at board, unit and satellite level. During the last six years, she has been mainly focused on the development of the RLS (Raman Laser Spectrometer) instrument for the ExoMars 2022 mission, in charge of the on-board SW and Operations. She co-authored more than 20 publications in peer-reviewed journals and conferences.

Journal Pre-proof

Luis Miguel Nieto

He is professor of Theoretical Physics at the University of Valladolid, developing lines of research in Mathematical Physics, such as “Mathematical modeling of graphene and other metamaterials”, “Safe quantum communications” or “Integrability, symmetries and non-linear dynamics of classical and quantum systems”.

He has published 125 articles in indexed journals, having participated in 50 research projects. In 2018 he received the Award from the Social Council of the University of Valladolid for all his activity. He is referee of 15 scientific journals and coordinates predoctoral and postdoctoral research activities. He has been Vice Chancellor and currently heads the Department of Theoretical Physics.

Journal Pre-proof

Marco Veneranda

With a PhD in analytical chemistry, he works as postdoctoral researcher at the University of Valladolid (UVa). He is directly involved in many research projects related to Mars exploration. As an official member of Operations and Science Support teams of both ESA/ExoMars (RLS) and NASA/Mars 2020 (SuperCam) missions, his current research interests include the spectroscopic analysis of Martian-relevant rocks and the development of novel Raman semi-quantification strategies and Raman-LIBS chemometric tools for Mars exploration. He co-authored over 35 articles in SCI journals and more than 40 conference abstracts.

Journal Pre-proof

Carlos Pérez Canora

He currently works at Instituto Nacional de Técnica Aeroespacial (Spain) with more than 15 years of experience in space instruments development. Main research in Astrobiology, Aerospace Engineering and Optics Engineering. System Engineering of the 'Raman Laser Spectrometer' (RLS) Instrument for ESA's ExoMars 2020 Rover'. System Engineering of the 'Raman Laser Assembly' (RLA) of the Raman Instrument of the JAXA-DLR MMX mission. He co-authored 12 articles in SCI journals and more than 20 conference abstracts and book chapters.

Journal Pre-proof

Declaration of interests

The authors declare that they have no known competing financial interests or personal relationships that could have appeared to influence the work reported in this paper.

The authors declare the following financial interests/personal relationships which may be considered as potential competing interests:

Journal Pre-proof